Structural Modeling And Hierarchical Control Of Large-Scale Electric Power Systems

by

Xiaojun Zhang Liu

M.S., Massachusetts Institute of Technology
(1988)

B.S., Tsinghua University, Beijing, China
(1983)

Submitted to the Department of Mechanical Engineering
in Partial Fulfillment of the Requirements for the Degree of

Doctor of Philosophy

at the

Massachusetts Institute of Technology

April 1994

Signature of Author _____
Department of Mechanical Engineering
April 27, 1994

Certified by _____
Marija D. Ilic
Thesis Supervisor

Accepted by _____
Ain A. Sonin
Chairman, Department Graduate Committee

Structural Modeling And Hierarchical Control Of Large-Scale Electric Power Systems

by

Xiaojun Z. Liu

Submitted to the Department of Mechanical Engineering on April 27, 1994 in partial fulfillment of the requirements for the degree of Doctor of Philosophy in Mechanical Engineering.

Abstract

A new, structural modeling and hierarchical control approach to large-scale electric power systems is presented in this thesis. Structural models of power systems explicitly in terms of tie-line flows are derived. Simple, yet fundamental aggregate models of very low dimensions are proposed to represent interactions among the subsystems. In contrast to most existing methods, the new approach does not require the assumption of weak interconnections among the subsystems, and the new interaction variables preserve their physical meanings. The new modeling approach provides a solid basis and simple information structure for monitoring and control of power systems. A new control design on different time scales is proposed to improve the stability and performance of the interconnected system.

The general theoretical framework is applied to two important control tasks of electric power systems – the frequency control and voltage control. The emphasis of the approach proposed in this thesis is on the inherent structural properties of the system. It is proven that the interaction variables are simply the inter-regional tie-line power flows. It is further shown that the decoupled frequency dynamics are structurally singular, while the voltage dynamics do not possess the structural singularity, although numerical singularities are possible. A new, direct tie-line flow control method to remove the structural singularity of the frequency dynamics using FACTS technologies is introduced for the first time. Control designs on different hierarchical levels based on the new structural models are presented. Extensive simulations are done for both small power systems and the large-scale French Power Network. Simulations show that the proposed approach leads to an improved systemwide performance.

Thesis Supervisor: Dr. Marija D. Ilic
Title: Senior Research Scientist

Acknowledgments

My deep gratitudes go to Marija, who, as the thesis supervisor, has made my Ph.D. work both challenging and fun. First of all, I would like to thank Marija for getting me into the area of power systems. I have enjoyed the work in this area since our first meeting back in September 1991. All the way along, Marija has been extremely helpful in motivating the progress of the research. Whenever we got stuck on something, she always had some new ideas. And we moved on again. Personally, her informal and approachable style makes our work together easy and fun.

Prof. Micheal Athans has provided crucial help in this project. His strong experience and expertise in the control and related fields always help me go in the right direction. I really learned a great deal from him from our regular meetings and his control courses MCS I and II at MIT (plus his Bode Lecture at CDC'93!). My deep appreciations go also to Prof. Anuradha Annaswamy for serving as my thesis committee chairperson. I greatly appreciate her time for my committee meetings and her essential advices all along. My many thanks are also due to Dr. Christine Vialas of Electricité de France for the helpful discussions and arguments during her stay at MIT.

I would like also to thank Prof. Jeff Lang for initially getting me involved. His first letter to me while I was in China was "technically" the beginning of this thesis. Without his initial help, this thesis would not have been written. Other LEES members also provided valuable help along the way. Among them, Prof. George Verghese's expertise in dynamics and systems, and later in power systems has cleared many questions for me. Thanks also go to Prof. Chris DeMarco of the University of Wisconsin for his crucial lectures during his sabbatical stay at MIT. My fellow LEES students, Joaquin, Jeff, Brian, Kathy, Neil and Assef all gave me valuable help in our daily talks.

Finally, I would like to acknowledge the essential support given by my dearest wife, Mee, whose continuing encouragements and supports have always made me inspired and forced to move forward. I still cannot forget the countless Saturdays and Sundays when she accompanied me to school and sat with me on an Athena workstation for many hours, while what she really wanted to do was to go to movies, shopping, or yard sales. I always feel guilty in my heart; to me she always deserves more. I'm really happy that it's about to be all over!

Funding for the research in this thesis was provided by the Electricité de France. Their financial support is greatly acknowledged.

Contents

List of Figures

List of Tables

Part I

Theoretical Background

Chapter 1

Introduction

1.1 Thesis Motivation

This thesis is directly motivated by the need for a systematic coordination of controllers in administratively separated regions in large-scale electric power systems and it represents a new, systematic, structurally-based modeling and control approach to power systems. The approach provides solutions beyond the coordination problem that directly motivates the thesis.

In the past, power system monitoring and control has been based on a hierarchical structure under which the monitoring and control tasks are shared by different hierarchical levels. Local (primary) controllers on individual generating units are presently decentralized in the sense that they respond to deviations of local outputs from the steady state values, or set values, assigned from the higher levels. The steady state set values of primary controllers are regulated at a regional level (secondary), assuming weak interconnections among the regions. The regional controllers are, however, not systematically coordinated at present, leading to deviations from optimal systemwide

performance and a possibility of potential global system instability.

This lack of systematic coordination exists in two most important control problems of the power system – the frequency regulation and the voltage regulation. In the case of frequency control of the power system, a simple coordination scheme, commonly referred to as the Automatic Generation Control (AGC), has been automated throughout the United States, as well as in some other parts of the world. This scheme is based on a reduced information structure which allows for simple automation. Although it has been successful in practice in relatively static operating environment, hidden problems that may lead to potential loss of global frequency regulation have been identified in the literature [1]. They are becoming more likely to occur under the newly evolving regulatory changes which create truly dynamic operation of large-scale systems by encouraging unusual energy generation and transmission over far electrical distances. Significant research effort is needed to provide a theoretically sound basis for generalizing control concepts that are amenable to the new operating modes of power systems.

In the case of voltage control, a systemwide coordination level is not automated at present time. Each administratively separated region regulates its own voltages, with interconnections to the neighboring regions neglected, and relies on the operator's expertise, as well as some off-line optimization algorithms such as Optimal Power Flow (OPF) techniques, to provide coordinating signals with other regions. However, as the system experiences unusual reactive power deficiency due to large disturbances, the need for a systematic, on-line coordination is emerging to insure the global security of the interconnected system. This voltage coordination problem is a direct motivation

for the work in this thesis.

A motivation for the thesis beyond solving the specific coordination problem is a recognition of the need for systematic, structurally-based modeling approach and control design to provide a theoretically sound basis for power system planning and operations, particularly in the present and future energy management environment created by the new regulatory changes. Under the new operating rules, presently working monitoring and control principles upon which high quality and efficient energy delivery is based will not hold entirely. The power system operation has been for the utilities to schedule real power generation to meet their load demands and to maintain the negotiated tie-line flow schedules, at the same time, maintaining voltages within the prespecified limits to support the scheduled real power delivery. Under the new operation regulations, the traditional "scheduling" of the loads becomes relatively meaningless, because any load can be conceptually served at its own choice by any power producers in the network, including Independent Power Producers (IPP). The new regulatory rules greatly increase the trend towards the non-participation of IPP's in AGC. As a result, significantly large number of these uncontrolled IPP's may very well cause the potential loss of systemwide frequency regulation. Also, the open access among all subsystems leads to stronger interconnections among them. This rules out one of the traditionally made assumptions in operation of power systems, the assumption of weak interconnections.

In summary, the new regulation rules and the need for better understanding of power systems call for a fundamental study of power system dynamics and control. The prime goal is to develop a structurally-based modeling and control approach which

yields a systematic coordination scheme for regional frequency and voltage regulations to enhance the global stability and security of the interconnected system.

1.2 Contributions

The contributions of this thesis can be classified into two major categories: (1) general theoretical development for large-scale electric power systems, and (2) its applications to specific sub-areas of power system operation.

In the general theoretical setting, this thesis introduces a structurally-based modeling and control approach for large-scale electric power systems whose interactions among the subsystems are characterized by the inter-regional flows[1]. An interconnected system is first decomposed into administratively divided regions. This natural division makes practical sense because each region has independent controls and makes its own decisions. Next dynamics of each region are obtained by combining local dynamics of individual generator units with the algebraic power balance constraints imposed by the transmission network. Throughout this thesis, loads are assumed to be disturbances, rather than measurable, known quantities. Control design principles studied in this thesis have the main purpose of suppressing the effects of load demand fluctuations in normal operating conditions over the variety of time scales, ranging from seconds through hours. Standard dynamical model in the form of ordinary differential equations (ODE) is obtained in the extended state space from the usual form of differential-algebraic equations (DAE) by differentiating the power balance algebraic

[1] Area and region are used interchangeably throughout this thesis. The approach proposed in this thesis is general enough so that the area or region can be arbitrarily chosen. For practical purposes, an area or region is chosen as an independent administrative region in this thesis.

constraints with respect to time. This structural model, first of all, reveals new fundamental structural properties of power system dynamics and offers clear physical insights on the not well understood phenomenon of inter-area dynamics. Second, this model provides a theoretically solid basis for hierarchical control design of power systems taking into account the effect of neighboring regions through new simple aggregate models proposed in the thesis.

Introduction of the structurally-based aggregation is another major contribution of this thesis. Structural interaction variables on different control levels are defined and the corresponding interaction dynamical models are obtained to account for interactions on different time scales among the interconnected regions. A particular important feature of the interaction variables is that they are interpreted in terms of physically meaningful quantities such as inter-regional power flows. The preservation of physical meanings of the interaction variables, in contrast to all other aggregation methods presently known in the area of power systems, is critically important for systematic control designs aimed at responding to changes in neighboring regions. The derived aggregate models provide a basis for coordinated on-line automatic control of large-scale power systems, because they extract information only relevant for each specific control level and are of very low dimensions relative to the detailed models of typical electric power systems.

A distinct advantage offered by the results of this thesis is that no assumptions with regard to the strength of interconnections are needed, in contrast to the present state-of-the-art methods which typically require the weak interconnection assumption. Since the system is decomposed according to its structural properties, instead of numerical

ones, the approach is entirely independent of the strength of interconnections. Avoiding the weak interconnection assumption is important, because strong interconnections are needed for inter-regional wheelings imposed in the open access operating mode.

On the application side, this thesis studies in detail two most important problems of power systems, the real power/frequency control and reactive power/voltage control, using the new structurally-based modeling and control approach proposed in the thesis. In the case of real power/frequency control, a simple extended state space model in terms of generator power outputs is introduced. The model reflects the most important property that the inter-area frequency dynamics are caused by the net real power mismatches among the interconnected regions. Moreover, the notion of a single frequency for each region used in the present AGC formulations is generalized using the proposed structural modeling approach to include individual frequencies of all generators participating in frequency regulation. This simple model also provides a straightforward mechanism for proving the need for centralized controls in order to directly regulate the inter-area dynamics. The direct control of the inter-area dynamics using Flexible AC Transmission Systems (FACTS) technology to remove the structural singularity under the present local control structure is shown to be the most natural way of controlling the inter-area frequency dynamics. The proposed scheme introduces for the first time a systematic utilization of FACTS devices for the purpose of directly controlling inter-area dynamics on large-scale power systems [2].

In the case of reactive power/voltage control, it is shown that it is possible to introduce a fully automated systemwide voltage control in the same spirit as the automated real power/frequency control. A completely decentralized improved regional voltage

control is proposed to take into account the effect of neighboring re, ions. Coordination of the decentralized regional controllers is formulated as an optimal control problem on the tertiary level. Explicit solutions for the optimal control are derived. With the structural approach developed, it is proven that the reactive power/voltage problem remains a qualitatively different one from the real power/frequency dynamics, in that voltage dynamics are structurally nonsingular. Extensive simulations are performed both on small examples and on the French network to demonstrate the feasibility of the new structural approach. Part III of the thesis addresses the reactive power/voltage control.

1.3 Thesis Organization

This thesis is organized in the following way: Part I presents a theoretical development of the structurally-based modeling and control approach in general setting. It includes an introduction to cover the motivations, contributions and organization of the thesis, as well as background material of power systems and underlying assumptions made in the thesis.

In Part II, the general approach is applied to the real power/frequency control of power systems, under the assumption of decoupled real power/frequency and reactive power/voltage dynamics. Detailed modeling approach using new state variables and control designs is presented. The new direct flow control design using FACTS devices to suppress inter-area oscillations is proposed. Perspectives for higher level control designs using the proposed approach are discussed.

Part III of the thesis is devoted to the reactive power/voltage control of power

systems. The general structural modeling approach and hierarchical control design are applied to the voltage control design. Particularly, new concepts needed for automatic voltage regulation over mid- or long-term time horizons are introduced. A new improved voltage control at the regional level and coordination scheme of regional controllers at the tertiary level are proposed. Extensive simulations are given for small examples and the large-scale French electric power network.

1.4 Literature Survey

Power system dynamics are a combination of the real power/frequency and reactive power/voltage dynamics. A review of basic concepts of real and reactive power modeling, analysis and control can be found in [3]. Most of modeling and analysis work is available for studies of primary frequency dynamics, which regulates closed-loop dynamics in response to fast disturbances. This work can be identified as small-signal dynamical and transient stability studies, primarily concerned with the problem of frequency response over the short period of time. The primary controllers for this purpose are governors on the generators. Most of this work views the interconnected system as one. The exception to this was the work by several researchers following the infamous New York blackout in 1968 concerned with model aggregation; the purpose of this work was to identify coherent electrical areas which respond as one single generator to fast disturbances, eventually resulting in a lower order aggregate model of direct interest to a particular region of the interconnected system. All of the coherent area eigenmodes of the linearized dynamic model of the electric power system, and are not easily interpreted in terms of system structure. Particularly, the states contributing to the modes

relevant for the inter-area dynamics are generally a linear combination of states across the administrative regions. These aggregate models do not lend themselves naturally to the control design necessary to directly regulate inter-area dynamics. As a result, at present there are no solutions for straightforward regulation of the inter-area dynamics on the short-term domain. This is despite the fact that persistent inter-area oscillations in the range of 0.7 Hz to 1 Hz have been reported and need to be controlled [4] [5]. More centralized controls than present entirely localized controls of the existing controllers on generators, such as governors, as well as the control concepts for new hardware capable of directly regulating power-line flows (recognized under the FACTS technology), that would guarantee certain degree of inter-area dynamical performance are basically an open question at present. This area takes on an even higher relevance since there has been a significant technological breakthrough in the area of fast communications across selected points of the power systems. With centralized, reliable communications available, new developments are needed in the area of supporting control concepts to meet specifications on the inter-area dynamics.

On the other hand, the supplementary inter-regional frequency control of large electric power systems needed to regulate set points for the primary frequency controllers has been one of the nice examples of successful automation on the complex large-scale systems. This supplementary control is recognized under the term of AGC. The ingenuity of the engineering concept behind AGC can be seen through the use of truly minimum information structure across an otherwise very complex system. This concept has served as a strong motivation to the developments in this thesis. They could be summarized as generalizations of AGC for controlling fast inter-area dynamics, as well as for improved AGC-like control schemes at the higher control levels which

do not meet the assumptions under which the AGC was originally conceived. AGC was designed based on the area control principle, that the goal of the controls in each region is to maintain its own frequency and the scheduled tie-line flows [6][7]. The basic assumption of AGC is that each area has a single frequency and that different areas can have different frequencies. In its actual implementation, AGC employs the area control error, a linear combination of the errors in frequency and the net tie-line exchange. One of the major problems with AGC is that the overall stability of the system is not guaranteed, although the actual implementation of AGC has been quite successful [8].

It is important to recognize that AGC concepts hold only in the normal quasi-static operating mode [9] [10]. They are designed primarily to compensate small and slow load variations around nominal conditions. Generalization of the AGC concepts to a general competitive multi-utility environment to yield desired system operations has been an open research question and it is therefore conceptually solved in this thesis.

For reactive power/voltage control, majority of the literature has been focused on the local dynamics of generator-excitation systems, with [11] [12] [13] as a few examples. Little has been given to formulating voltage problem as a dynamical process on the system level, except in France and Italy [14] [15]. Based on the assumption that tie-line interconnections are so weak that they can be neglected, regional dynamical models for voltage has been derived in the past [16]. The need to neglect the tie-line interconnections in this formulation was a direct consequence of the fact that the modeling approach adopted was not general enough to include interconnections. An isolated region must be singled out first before the sensitivity matrix could be

calculated. As such, interconnections could not be appropriately modeled.

Systematic coordination of regional voltage controllers to enhance the global security and performance of the interconnected system does not appear to have been extensively addressed. As the system becomes more dynamical under active wheelings by IPP's, coordination of reactive generations in different regions has emerged as necessary to ensure satisfactory operation of the global system. The need for systematic formulation and analysis of the systemwide coordination for regional controllers has served as a direct motivation for the work in this thesis.

Chapter 2

Structural Modeling and Structural Singularity

2.1 Introduction

This chapter introduces a new structurally-based modeling approach to large-scale electric power systems. While the approach recognizes the decomposition of the system into interconnected, but administratively divided regions, it does not make any a priori assumptions with respect to strength of their interconnections. The administrative regions within the interconnected system are tied together through the tie-lines, and the regional dynamics are coupled through the tie-line power flows. To maintain the traditional decentralized control structure, we always choose an administrative region as the base for study, and derive the dynamical models for this particular region explicitly in terms of the tie-line flows. It will be shown that this framework of modeling captures fundamental properties of power system dynamics and facilitates the physical understanding of the inter-area dynamics.

Each administrative region consists of a certain number of generating and control

units, and a transmission network that connects these generating and control units together. Typically these units are located over different locations, and each individual generator has its own local control, in the sense that the control regulates output variables associated with this particular generator only. The schematic representation of the structure is shown in Fig. 2.1.

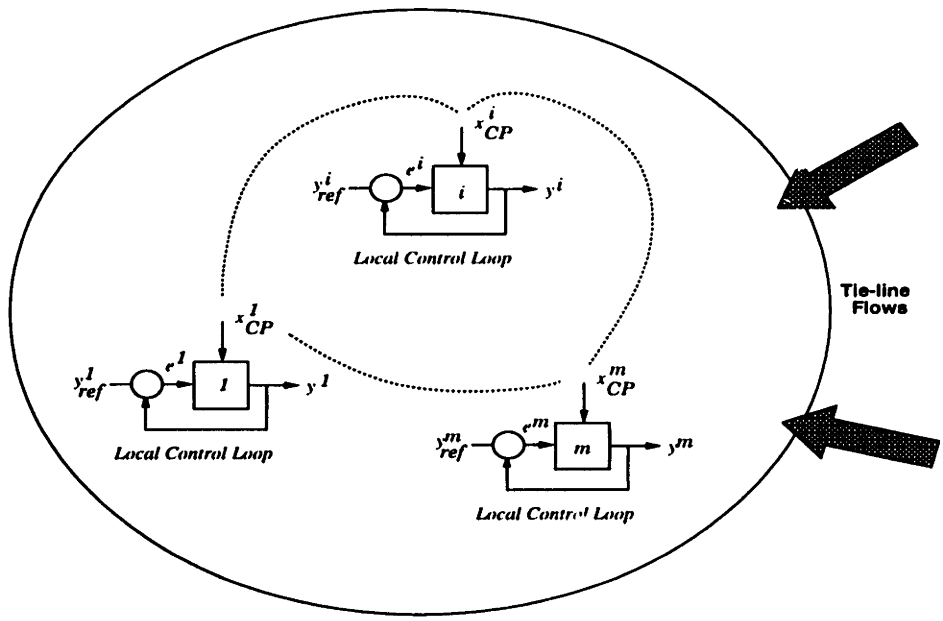

Figure 2.1: An Administrative Region with Local Controls

Dynamics of each individual unit, referred to in this thesis as the *local dynamics*, are derived in terms of local state variables of each unit. If the transmission network, which connects all the generating units together, were not present, the local dynamics of these generating units would be completely decoupled. The role of the transmission network is to constrain outputs of individual equipment by imposing power balance conditions on subset of local variables of all the generators and loads connected through the transmission network. The subset of local variables directly constrained by the system interconnections is named in this thesis as the *coupling variables*, because they

couple local dynamics of individual units. The local dynamics of individual units, in the form of ordinary differential equations (ODE), together with the algebraic constraints imposed by the transmission network, form the dynamics of the administrative region in the form of differential-algebraic equations (DAE).

It is well known that DAE problems are very difficult to handle in general. The approach proposed here is to convert the DAE problem to an ODE problem by differentiating the network constraints under an assumption that holds for a very wide range of system operation. A standard state space nonlinear dynamical model for the administrative region in the form of unconstrained ODE's is obtained by combining local dynamics for individual units with the differentiated network constraints. Note that the resulting dynamical model is in an extended state space, since the coupling variables become also the states.

The developed structural dynamical model offers an essential, yet simple, vehicle for rigorous analysis of the power system dynamics. The model is exceptionally powerful for controlling inter-area dynamics at all time horizons. It is proven, with the obtained structural model, that the real power/frequency dynamics of power systems possess an important structural property – the structural singularity, as will be defined in this chapter. It is also shown that the reactive power/voltage dynamics of power systems, on the other hand, do not have this structural singularity, although numerical singularity can occur under particular operating conditions. It is further shown that the structural singularity has a systemwide impact on the dynamical behavior of the system. In this case, there exist some combinations of the states in the extended state space, defined as the *interaction variables*, that stay constant with time for any local controls, and can

be varied only by the tie-line flows with neighboring regions. In control terminology, this represents the case of an uncontrollable system under the given localized control structure presently used, and calls for new control designs to overcome this problem.

The developed structural dynamical model also provides a theoretically solid basis for hierarchical control design of power systems to reject load disturbances over the wide-spread frequency spectrum. Much simpler models than the detailed dynamics specifically for control design at different hierarchical levels are obtained by applying time scale separation techniques to the new structurally-based models proposed here. These simple models, or the *aggregate models*, represent the net effect of interactions among interconnected regions on specific hierarchical levels. They are exact, since no assumptions on weak interconnections among the subsystems are made. Details are given in the next chapter.

2.2 Modeling Issues

In this section, general modeling issues related to power system analysis and basic modeling assumptions made in the thesis are discussed. This section serves as the background material for the structural modeling and hierarchical control approach proposed in this thesis. It includes topics such as time scales, network and load modeling, control hierarchy, and the frequency/voltage decoupling assumption.

2.2.1 Time Scales

Modeling and control of large scale systems usually exploits significant time scale separation among a variety of processes. Due to these different time scales, dynamics and

responses of the system exhibit different characteristics. Much of the analysis work is presently available for studying shortest response of the system to fast disturbances. Very little systematic analysis is available for system responses over the mid- and long-term time horizons. In order to partly eliminate this gap, it is adopted in this thesis that for short-term stable operations steady state outputs of fast dynamics can be viewed as the moving equilibria under slower disturbances, forming a discrete event process (DEP) over longer time scale. A fundamental difference between this class of processes and the continuous dynamics is that a DEP under certain conditions on the continuous dynamics is driven solely by control actions and disturbances.

Electric power systems, generally large in size and complex in operation, typically display this special class of processes. The local (primary) controllers stabilize system dynamics to within a threshold of their steady state reference values with a very fast time constant. The steady state outputs of these primary controllers are regulated at a regional (secondary) level with a significantly longer time constant than the primary controllers, forming what can be viewed a DEP process. To fully optimize the operation of a system consisting of several electrically interconnected regions under varying loading conditions, the reference values of the output variables are adjusted at an even higher (tertiary) level with a still longer time constant than the secondary.

Most important sources of different time scales include different electrical distances within a large-scale interconnected network and loads which vary over different time scales. Power systems involve huge number of devices interconnected over far geographical and electrical distances. The connections among these devices within an administrative region (electric power utility) are relatively meshed and strong, compared to

very sparse, and normally weak tie-line interconnections among different administrative regions. The meshed or strong intra-area connections represent shorter electrical distances and the sparse or weak inter-area connections imply longer electrical distances. Loads typically have wide spread frequency spectrum. They are modeled in this thesis as containing dynamics at three qualitatively different time scales, fast fluctuations, mid-term and long-term variations. The controls responding at these three distinct time scales are the basis for a hierarchical control scheme to stabilize the frequency and voltage throughout the system.

As a convention throughout the thesis, we refer to the fast transient dynamics of the system as the *primary* process, with typical time constant T_p, the DEP on the mid-range time scale as the *secondary* process, with typical time constant T_s, and the slowest process a the *tertiary* process with time scale T_t. The primary process is simply the continuous dynamics of the system, the secondary process is the set value adjustment by the regional controls over mid-time horizon, and the tertiary process is associated with the slowest adjustment of system settings relevant for the entire interconnected system.

Since the secondary and tertiary processes are activated only at discrete times, any variable v of interest can be decomposed into

$$v = v(t) + v[k] + v[K], \quad k, K = 0, 1, 2, \cdots \tag{2.1}$$

where $v(t)$ is the continuous component associated with the primary dynamics with time scale T_p, the discrete secondary process is defined as $v[k] = v(kT_s)$, and $v[K] \triangleq v(KT_t)$ is the slowest component associated with the tertiary process. A schematic presentation of relevant time horizons is illustrated in Fig. 2.2.

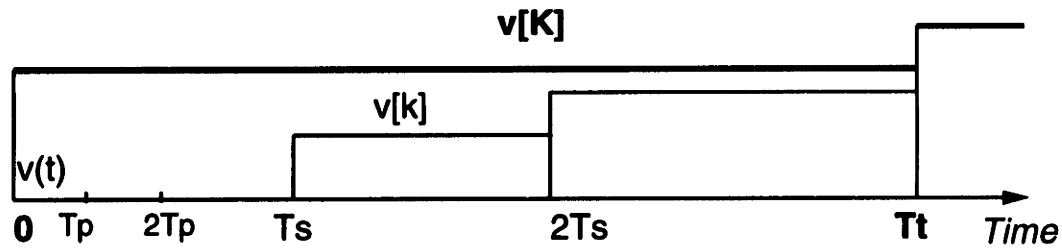

Figure 2.2: Multiple Time Scales

2.2.2 Network and Load Modeling

In large-scale power system studies, the transmission network is modeled as a linear circuit, normally with inductances, resistances and shunt capacitances. For the frequency range of interest in this thesis, dynamics of the transmission network are neglected. Under this modeling assumption, the transmission network effectively imposes algebraic constraints to the dynamics of the local generating units and their local controls. The constraints are simply the real and reactive power balances. Generator local dynamics in the form of ODE's, together with the algebraic network constraints lead to a constrained dynamical problem of a DAE (page 15) form.

Loads are modeled as sinks or sources of real power P_L and reactive power Q_L. The deviations from constant power sinks/sources are further modeled as external disturbances to the system. Although more realistic models include dependence on their voltage and frequency, these models are not presently actively used for on-line control of the interconnected system. Using the notation introduced in (2.1), loads in this thesis are represented by

$$P_L = P_L(t) + P_L[k] + P_L[K] \quad k, K = 0, 1, \cdots \tag{2.2}$$

$$Q_L = Q_L(t) + Q_L[k] + Q_L[K] \quad k, K = 0, 1, \cdots \tag{2.3}$$

for real power P_L and reactive power Q_L. In this equation, $P_L(t)$ and $Q_L(t)$ are the fast continuous fluctuations, $P_L[k]$ and $P_L[K]$ represent variations over the mid-term horizon, $Q_L[k]$ and $Q_L[K]$ correspond to variations of the load on the long-term horizon.

2.2.3 Control Hierarchy

Corresponding to the three different time scales, monitoring and control of large-scale power systems typically employs a hierarchical structure:

- *Primary control*: This level is most often entirely localized in the sense that controllers respond to the local output variable changes only. The main function of primary control is to correct for small, fast output deviations caused by fast load disturbances. Excitation and governor systems are the main primary controllers responsible for voltage and frequency controls, respectively.

- *Secondary control*: This level is concerned with changes at the regional level, considering interactions with the neighboring regions to be small. Its main function is to eliminate frequency and voltage deviations at certain critical locations over the mid-term time horizon. These deviations are caused by slow load deviations and the structural singularity associated with the frequency dynamics under the present localized primary control structure. Adjusting speed-changers of the governors and terminal voltages of the generators are the main control means at this level of hierarchy.

- *Tertiary control*: This level is concerned with the coordination of secondary controllers by incorporating effects of interactions on the quasi-static changes of the

interconnected system over the long-term time horizon. The ultimate goal of this coordination is to achieve a systemwide optimal performance over the long-term time horizon.

In terms of the load decomposition discussed in the previous section, the main purpose of the primary frequency and voltage controllers is to cancel the effects of the fast load fluctuations $P_L(t)$ and $Q_L(t)$. The regional secondary controllers are designed to control frequency and voltage under the slower load changes $P_L[k]$ and $Q_L[k]$. The systemwide tertiary controller is intended to update settings at secondary controllers in response to slow nominal load changes $P_L[K]$ and $Q_L[K]$ over the time horizon T_t.

2.2.4 Decoupling Assumption

It is well understood that in a static operation real power injections to a power system closely affect voltage angle differences across the transmission lines, and that reactive power injections closely affect the voltage magnitudes, under normal operating conditions. In other words, sensitivities of real powers to phase angle differences, and sensitivities of reactive powers to voltage magnitudes are relatively larger than the cross sensitivities of real powers to voltage magnitudes and reactive powers to phase angle differences. This property is referred to in the power systems literature as the real power/voltage decoupling assumption.

Under normal conditions, power systems operate in a quasi-steady state on slow time scales, i.e., the system reaches its steady state within the fast time scale T_p. Therefore, it is generally a valid assumption that real power/angle dynamics and reactive power/voltage dynamics are decoupled in normal operating conditions. In order

to exploit the most fundamental characteristics of power system dynamics, and not to confuse with complex mathematical expressions associated with the coupled dynamics, the decoupling assumption of real power/frequency and reactive power/voltage dynamics will be made throughout this thesis. This, however, does not imply that the decoupling assumption holds in general.

2.3 Structural Modeling

Let us first discuss the decomposition of power systems into various devices. A power system typically consists of the following three major components: 1) loads, 2) the transmission network, and 3) generator units. Loads are simply modeled as power sinks/sources. In this thesis, load deviations from their nominal constant power values are modeled as external disturbances to the system, and therefore are not measured. It is fully recognized in this thesis that more detailed knowledge of load dynamics could provide for better design of the system. However, since load models are quite uncertain, the approach proposed here is to view loads as uncertainties at different time scales for which controls are designed. This single fact makes a strong case for the need for on-line controls, instead of static off-line optimization scheme, such as OPF, assuming loads to be known. Dynamics of the transmission network are neglected for the time scale of interest to this thesis. As a result, the transmission network only imposes power balance constraints between generation and load. These two components are simply static and do not have any dynamical feature. Dynamics of power systems occur only at generator units, each of which has its own individual controls. These control units together with generators form the local dynamics of the system, which are

coupled together by the algebraic relationship imposed by the transmission network. A complete dynamical model of any power system is the combination of the local dynamics and the network coupling. This structural decomposition is schematically illustrated in Fig. 2.1.

2.3.1 Local Dynamics

Let us first discuss local dynamics of generator units. Define x^i_{LC} as the local states of generator i. One can express local dynamics of this generator in a general form as

$$\dot{x}^i_{LC} = f^i_{OP}(x^i_{LC}, u^i_{LC}, x^i_{CP}) \tag{2.4}$$

where u^i is the control input to the generator, and x^i_{CP} represents the coupling variables which relate local dynamics of different generator sets together. For example, in the case of real power/frequency dynamics, the coupling variable is simply the real power generation of the generator. Real power generations of different generators are coupled together by the transmission network that connect different generators. The primary task of the local controller is to stabilize the local output variables of the specific generator to their desired settings, which can be calculated locally or more often given by higher level controls. Assume that

$$y^i = C^i x^i_{LC} \tag{2.5}$$

is the vector of output variables of interest for generator i. Let y^i_{ref} represent the desired settings for output variables. The local control u^i_{LC} is typically a feedback control designed using the error signal

$$e^i = y^i - y^i_{ref} \tag{2.6}$$

After appropriate design of the local controller, the closed-loop dynamics of the generator set can be written as

$$\dot{x}^i_{LC} = f^i_{LC}(x^i_{LC}, y^i_{ref}, x^i_{CP}) \tag{2.7}$$

We now derive local dynamical models for all generator units in the network. As discussed in the previous section, we choose any administratively divided region as the base system for our study. Consider here such a region consisting of m generator units. Define the local states, output variable settings, and coupling variables for the region as

$$x_{LC} \triangleq \begin{bmatrix} x^1_{LC} \\ \vdots \\ x^m_{LC} \end{bmatrix}, \quad y_{ref} \triangleq \begin{bmatrix} y^1_{ref} \\ \vdots \\ y^m_{ref} \end{bmatrix}, \quad x_{CP} \triangleq \begin{bmatrix} x^1_{CP} \\ \vdots \\ x^m_{CP} \end{bmatrix} \tag{2.8}$$

Since Eq. (2.7) is true for any generator control set, one can simply obtain the local dynamical model for the entire region as

$$\dot{x}_{LC} = f_{LC}(x_{LC}, y_{ref}, x_{CP}) \tag{2.9}$$

where the nonlinear function is defined as

$$f_{LC}(x_{LC}, y_{ref}, x_{CP}) \triangleq \begin{bmatrix} f^1_{LC}(x^1_{LC}, y^1_{ref}, x^1_{CP}) \\ \vdots \\ f^m_{LC}(x^m_{LC}, y^m_{ref}, x^m_{CP}) \end{bmatrix} \tag{2.10}$$

2.3.2 Network Constraints

The transmission network imposes algebraic constraints on the coupling variables x_{CP} and a small subset of local state variables x_{LC}. With definition (2.8), it will be demonstrated in this thesis that the constraints are always given in the following structural form

$$g(x_{CP}, x_{LC}, F) = 0 \tag{2.11}$$

where the nonlinear function $g(\bullet,\bullet,\bullet)$ has the same dimension as that of the coupling variables. The term F represents tie-line flows into the region from its neighboring regions. This formulation assumes constant power loads. Any variations in the loads are viewed as disturbances to the system. The primary goal of power system control design is to reject the load disturbances. Details will be presented in the next chapter. The differential equation of local dynamics given in (2.9), together with this algebraic relationship, forms the dynamics of the system in the form of differential-algebraic equations (DAE).

It is well known that DAE problems are very difficult to handle in general. It is proposed here that the DAE problem is converted to ordinary differential equations (ODE), by differentiating the algebraic constraint equation (2.11) with respect to time. It follows that

$$J_{CP}\dot{x}_{CP} + J_{LC}\dot{x}_{LC} + J_F\dot{F} = 0 \tag{2.12}$$

where

$$J_{CP} \triangleq \frac{\partial g}{\partial x_{CP}}, \quad J_{LC} \triangleq \frac{\partial g}{\partial x_{LC}}, \quad \text{and} \quad J_F \triangleq \frac{\partial g}{\partial F} \tag{2.13}$$

are defined as the Jacobian matrices of the network constraints. Note that these Jacobian matrices are evaluated at the actual value of the state and flow variables (x_{CP}, x_{LC}, F), and therefore no approximations are introduced.

To derive a standard state space ODE model for the dynamics of the region, let us assume that the square matrix J_{CP} is nonsingular. If this is not the case, complicated phenomenon such as impasse points [17] will occur. This case is out of the scope of the thesis and will not be further discussed. Under this condition, Eq. (2.12) can be

equivalently written as

$$\dot{x}_{CP} = S_{LC}(x_{CP}, x_{LC}, F)\dot{x}_{LC} + S_F(x_{CP}, x_{LC}, F)\dot{F} \tag{2.14}$$

where

$$S_{LC}(x_{CP}, x_{LC}, F) \triangleq -J_{CP}^{-1}J_{LC} \quad \text{and} \quad S_F(x_{CP}, x_{LC}, F) \triangleq -J_{CP}^{-1}J_F \tag{2.15}$$

are defined as the sensitivity matrices of coupling variables to local states and flows, respectively. Again, these sensitivity matrices are functions of the state and flow variables, as explicitly indicated above. Eq. (2.14) represents an equivalent nonlinear ODE set for the network algebraic constraints.

2.3.3 Structural Dynamical Model

The local dynamical model (2.9), combined with the coupling dynamics given in (2.14), forms a complete set of ODE's for dynamics of the specific region under consideration,

$$\begin{bmatrix} \dot{x}_{LC} \\ \dot{x}_{CP} \end{bmatrix} = \begin{bmatrix} f_{LC}(x_{LC}, y_{ref}, x_{CP}) \\ S_{LC}(x_{CP}, x_{LC}, F)\dot{x}_{LC} + S_F(x_{CP}, x_{LC}, F)\dot{F} \end{bmatrix} \tag{2.16}$$

Or,

$$\begin{bmatrix} \dot{x}_{LC} \\ \dot{x}_{CP} \end{bmatrix} = \begin{bmatrix} f_{LC}(x_{LC}, y_{ref}, x_{CP}) \\ S_{LC}(x_{CP}, x_{LC}, F)f_{LC}(x_{LC}, y_{ref}, x_{CP}) + S_F(x_{CP}, x_{LC}, F)\dot{F} \end{bmatrix} \tag{2.17}$$

Define the state variables in the extended state space for the region under study as

$$x \triangleq \begin{bmatrix} x_{LC} \\ x_{CP} \end{bmatrix} \tag{2.18}$$

and the nonlinear function on the right hand side of (2.17) as

$$f(x, y_{ref}, F, \dot{F}) \triangleq \begin{bmatrix} f_{LC} \\ S_{LC}f_{LC} + S_F\dot{F} \end{bmatrix} \tag{2.19}$$

We obtain the nonlinear standard state space dynamical model for any administratively divided region as

$$\dot{x} = f(x, y_{ref}, F, \dot{F}) \tag{2.20}$$

Notice that the reference values for output variables, y_{ref} are updated more slowly than the transient dynamics by a higher level control center. The purpose of updating the reference y_{ref} is to render an optimal performance of the system accommodating the slowly varying component of the load fluctuations (fast component of the load variations is stabilized by the appropriate design of local controllers). This typical implementation of the control, referred to in this thesis as the hierarchical control structure, gives rise naturally to different time scales for the closed-loop dynamics. The following section will discuss the time scale separation associated with this particular structure.

Note also that this dynamical model is written explicitly in terms of tie-line flows into the region from neighboring systems. In Eq. (2.20), the tie-line flows act as an external input to the dynamics of the region under study. These flows play important roles in the inter-area behaviors of different regions within the interconnected system, as it will be studied in detail later. It will be shown that the decoupled real power/frequency dynamics are not completely controllable under the present control structure; the local control u_{LC} cannot regulate inter-area behaviors of the inter-connected system. The popular, but not well understood phenomenon of inter-area oscillations cannot be effectively suppressed with local governor controls, without significantly changing voltages throughout the network. In this case, additional control actions are needed to guarantee a desired performance of the system. This leads to the idea of direct flow control, as will be studied later in this chapter.

2.4 Structural Singularity

Detailed analysis of the structural dynamical model (2.20) of any region are given in this section. We define an important property of power system dynamics – the structural singularity, associated with the real power/frequency dynamics which will be studied in detail in Part II of the thesis. It is shown that for structural singular dynamics, there exists a combination of states that stays as constant independent of operating conditions unless the local reference values y_{ref} and/or tie-line flows vary. This combination of states is defined as the *interaction variable.* For an isolated system (no tie-line flows), the interaction variable will be constant if the reference values are not changed. This structural property is the fundamental concept behind the inter-area dynamics in electric power systems.

2.4.1 Definition of Structural Singularity

The state space dynamical model of any administrative region was derived in (2.20). From this general nonlinear model, we define the matrix

$$A(x, y_{ref}, F, \dot{F}) \triangleq \frac{\partial f}{\partial x}(x, y_{ref}, F, \dot{F}) \tag{2.21}$$

as the *system matrix* associated with each administrative region. Note that the system matrix is a function of variables $(x, y_{ref}, F, \dot{F})$. With the system matrix, we define the structural singularity as follows:

Definition 2.1 (Structural Singularity) *Any administrative region is defined as structurally singular if its system matrix $A(x, y_{ref}, F, \dot{F})$ defined in (2.21) is singular for any $(x, y_{ref}, F, \dot{F})$.*

2.4.2 Interaction Variables

It can be shown that the structural singularity has a profound systemwide impact on the dynamical behavior of the system. To better understand the fundamentals, and not to be confused with complicated mathematical expressions, we illustrate the analysis on structural singularity using a linearized model, noting that the principle carries over to the nonlinear model under the assumption of nonsingular J_{CP} in (2.12). Assume that for a given set of output variable references y_{ref}^{ss}, the steady state of Eq. (2.20) given by (x^{ss}, F^{ss}). The linearized model takes the form

$$\delta\dot{x} = A^{ss}\delta x + B^{ss}\delta y_{ref} + U^{ss}\delta F + V^{ss}\delta\dot{F} \tag{2.22}$$

where the prefix δ denotes deviation of the corresponding variable from its steady state value, e.g., $\delta x \triangleq x - x^{ss}$. Matrices A^{ss} and B^{ss} are given by

$$A^{ss} = A(x^{ss}, y_{ref}^{ss}, F^{ss}, 0) \tag{2.23}$$

$$B^{ss} = \frac{\partial f}{\partial y_{ref}}(x^{ss}, y_{ref}^{ss}, F^{ss}, 0) \tag{2.24}$$

In this model, the tie-line flows are viewed as external inputs to each region.

To simplify the notation, let us drop the prefix δ and the superscript ^{ss} on all variables, with the understanding that the model under study represents the linearized dynamics around the given steady state. Now one can rewrite (2.22) as

$$\dot{x} = Ax + By_{ref} + UF + V\dot{F} \tag{2.25}$$

For this model, we define the interaction variables as follows:

Definition 2.2 (Interaction Variable) *Any linear combination of the states, $z = Tx$, $T \neq 0$, that satisfies*

$$\dot{z}(t) \equiv 0 \tag{2.26}$$

in the absence of the reference value changes and the interactions among different regions, i.e. when $y_{ref} = 0$ and $F = 0$, is defined as the interaction variable of the administrative region under study.

This definition clearly indicates that any variations in time of the interaction variable are caused only by the interaction among different regions, and the active controls – the updating of the reference values, because they remain constant if the interactions and active controls are not present. As a result, the interaction variable captures properties of the interactions among interconnected regions.

Note from this definition that interaction variables are local variables associated with each region. There is no coupling among different regions, since the interaction variables are defined in terms of the disconnected regions. In other words, the interaction variables for region i are function of the state variables of region i only. As a result, the calculation of the interaction variables can be performed in a decentralized manner by each region separately.

Let us find the matrix T in the definition. Eq. (2.25), together with $z = Tx$, simply gives

$$\dot{z} = TAx + TBy_{ref} + TUF + TV\dot{F} \tag{2.27}$$

Under the condition stated in Definition 2.2, $y_{ref} = 0$ and $F = 0$, the above leads to

$$\dot{z} = TAx \tag{2.28}$$

Thus, we obtain the condition for calculating matrix T

$$TA = 0 \tag{2.29}$$

From this simple condition, it is obvious that no interaction variables exist for non-singular systems characterized by the existence of A^{-1}. For a singular system, assume that each row of the matrix L represents a left eigenvector of A corresponding to its zero eigenvalue, i.e.,

$$LA = 0 \tag{2.30}$$

It trivially follows that:

Proposition 2.1 (Existence of Interaction Variables) *Interaction variables exist only for singular systems, and are given by*

$$z = Lx \tag{2.31}$$

where matrix L contains all left eigenvectors of A corresponding to its zero eigenvalues.

2.4.3 Interaction Dynamics

Assume that the region under consideration is a singular system, i.e. A is singular. After calculating the interaction variables from (2.31) for a singular system, one can derive from (2.27) an aggregate model in terms of the reference and tie-line flow changes as

$$\dot{z} = TBy_{ref} + TUF + TV\dot{F} \tag{2.32}$$

This model defines changes in the interaction variables explicitly in response to the inter-regional flows and the output reference values. It is referred to as the *inter-area*

dynamics. Note from (2.32) that the inter-area dynamics correspond to the singular mode of the system, since any change in z is driven only by external inputs – the flow and reference value changes. This singular mode causes steady state errors in output variables. Appropriate designs must be done to eliminate this mode. This will be addressed in the next chapter.

Note that this model does not require weak interconnections, since it is based on the structural properties of the system. When interconnections are indeed weak, changes in the interaction variables will be slow, allowing for a singular perturbation-based formulation [18], [19]. When interconnections are strong, singular perturbation does not apply, while the model (2.32) still holds. It can be shown that for the case of weakly connected power systems the interaction variables as defined here are related to the slow variables of the aggregate model in [18].

It follows from Proposition 2.1 that interaction variables as defined in Definition 2.2 are not present for nonsingular systems. However, it is important at this point to observe that there exist variables which have the similar property as in Definition 2.2 on slower time scales than the time constant of transient dynamics. These variables, to be defined in the next chapter as the *interaction variables on secondary level*, are caused structurally by insufficient number of controls at the secondary level of power system control design, as discussed in Section 2.2.3. This will be fully introduced in the next chapter.

2.5 Summary

A new structurally-based modeling approach to large-scale electric power systems is proposed in this chapter. The approach is general enough so that the decomposition of the interconnected system into areas or regions (interchangeable throughout this thesis) can be arbitrary. For practical purposes, an area or region is chosen as an independent administrative region in this thesis.

Each region consists of generators typically at different locations. Dynamics of each generator i are represented by the local states x_{LC}^i and the coupling states x_{CP}^i. The local states and coupling states for the entire region, denoted by x_{LC} and x_{CP}, are the collection of the local states and coupling states, respectively, of all generators in the region, as defined in Eq. (2.8). The extended state variables x for the entire region are the combination of local states and coupling states of the region, as indicated by (2.18). The full dynamics of the region are then linearized. From the linearized dynamics, interaction variables, $z = Tx$, are defined in Definition 2.2. Conditions for calculating the interaction variables are given, and the interaction dynamics are derived.

Chapter 3

Hierarchical Control

3.1 Introduction

In this chapter we present a new hierarchical control design concept based on the structural models developed in the previous chapter. The need for control design is mostly promoted by the inevitable load variations, which consist of components of different time scales as introduced in Section 2.2.1. The main goal of local control design is to reject the fast component of load variations so that local output variables are stabilized to their reference values. This can be achieved if the resulting system under the given local control is a nonsingular and stable system. Load fluctuations can be successfully suppressed by an appropriate design as long as the the slowest eigenvalue of the system is faster than the fast component of load variations. It is shown in this thesis for the first time that suppression of fast load variations can only be fully achieved for nonsingular systems via local, decentralized control structure presently practiced.

Disturbance rejection cannot be achieved for a structurally singular system under

the given local control design, because the structural zero eigenvalues cannot be removed. As a consequence, steady state offsets in the output variables to their given reference values are necessarily present. The remedy for this structural singularity is to employ more centralized control structure than the simple localized control. In this thesis, a new approach to directly control inter-regional tie-line flows using FACTS (page 17) devices is proposed. The goal of the additional control is to remove the singular modes, which corresponds to the interaction dynamics in Eq. (2.32), so as the resulting system is nonsingular and stable. Theoretical background on the direct tie-line power flow control will be presented in this chapter, and its applications to the real power/frequency control of power systems will be given in Part II of the thesis.

Further higher level control actions are needed for both singular and nonsingular systems, due to the presence of slower components in load variations. Steady state values of output variables cannot be maintained at their given reference values on a slower time scale, because they are affected by the slow component in the load variations. This is true even for nonsingular systems, including those which are originally singular, but become nonsingular with appropriately designed FACTS controls discussed in this chapter. The reason is that steady state errors of the output variables, although zero on the short time scale, will be driven to nonzero values by the slow load variations.

This chapter introduces a hierarchical control design concept for nonsingular systems by slowly updating the reference values of output variables to suppress the slow drifting of output variables and to achieve a global optimality on the slow time scale. It is shown that control designs can be done at different hierarchical levels using much

simpler aggregate models than presently known in the literature directly relevant for the specific levels. This is fully illustrated later in context of reactive power/voltage control.

For singular systems, such as the real power/frequency dynamics, similar control designs are more complicated due to the more complicated relationship between controls and states on the slow time scale. This topic is still an open question, and is currently under active research sponsored by the Pennsylvania-New Jersey-Maryland (PJM) power pool, which is one of the largest electric pools in the United States.

3.2 Direct Tie-line Control for Singular Systems

As discussed above, steady state errors in the regulated output variables always exist for singular systems, due to the structural singularity. In this case, additional controls are needed to remove the structural singularity associated with the original control structure. In this section, an entirely novel approach to regulating the inter-area dynamics using the FACTS technology is proposed. It is possible with FACTS devices to directly vary the voltage phasor angle difference, or equivalently the power flow, across a transmission line. In other words, the tie-line flows can be viewed as additional controls to the system dynamics. With appropriate design of the new controls, the original singularity of the system can be removed and eigenvalues of the system can be placed in desired locations.

To include this control option into formulation in this thesis, let us use the standard control terminology by defining

$$u_F = F \tag{3.1}$$

as the supplementary control variables with the FACTS devices. The dynamics of the administrative region with this additional control can be derived from (2.25) as

$$\dot{x} = Ax + By_{ref} + Uu_F + V\dot{u}_F \tag{3.2}$$

Let us consider suitable feedback designs to remove the system singularity. Since the singular mode corresponds to the inter-area dynamics derived in (2.32), let us study further the inter-area dynamics under the new control u_F. With definition (3.1), the inter-area dynamics given in (2.32) can be written as

$$\dot{z} = TBy_{ref} + TUu_F + TV\dot{u}_F \tag{3.3}$$

It is clear from this equation that the singularity, when tie-line flows are not directly controlled, can be removed easily with a simple feedback of the interaction variables z, noting that the dimension of interaction variables is very low. It should be pointed out that implementation of the tie-line control is not restricted to either the fast transient time scale of system dynamics or the slow time scale of updating the reference values. Details of the control design to meet desired specifications are given in Part II.

3.3 Time Scale Separation

Because the updating of reference values of output variables is done typically more slowly than the time constant of the system transient dynamics, different time scales exist in the system dynamics over long time horizon. Time scale separation techniques can be used to simplify higher level control designs.

The linearized dynamical model for any administrative region was derived in Chap-

ter 2 as

$$\dot{x} = Ax + By_{ref} + UF + V\dot{F} \tag{3.4}$$

In this equation, vector F represents the tie-line flows into this region from its neighboring regions. The reference value y_{ref} is updated, by either the local level or higher level controls, at discrete instances to regulate the profiles of output variables of direct interest so that some predefined optimality is achieved. Due to physical limitations and practical considerations, the updating is typically done more slowly than the transient dynamics. This process of updating the reference values of individual controllers is often called the *secondary control.* Let us denote the time interval of the secondary control as T_s, i.e., the reference value is updated at instances kT_s, $k = 0, 1, \cdots$. Thus the reference value y_{ref} is constant in the interval $kT_s < t < (k+1)T_s$. Let us further denote $v_s[k] = y_{ref}(kT_s)$ as a discrete time sequence of the reference value. With this notation, Eq. (3.4) can now be written as

$$\dot{x} = Ax + Bv_s[k] + UF + V\dot{F} \tag{3.5}$$

The secondary control is to design an appropriate discrete time sequence $v_s[k]$ to achieve some prespecified optimality, as will be further discussed. Because the discrete sequence $v_s[k]$ varies more slowly than the transient dynamics, much simpler models can be derived to assist the secondary control design. Let us now carry out the detailed derivations. Because the time constant of the transient dynamics is much shorter than the secondary control time interval T_s, one can assume that all transient dynamics settle to a steady state before each time instance kT_s, i.e., $\dot{x} = 0$ at kT_s. Eq. (3.5) then reduces to

$$Ax + Bv_s[k] + UF = 0, \quad \text{at } t = kT_s \tag{3.6}$$

or

$$Ax[k] + Bv_s[k] + UF[k] = 0 \tag{3.7}$$

using the convention of (2.1). Eq. (3.7) determines a static relationship between the steady state equilibria of the system and the reference values to be adjusted by the secondary control.

The secondary level controls are designed to eliminate the slower steady state offset of some critical variables in the region under the slow drifting of disturbances. Let us express these critical variables for the secondary level as

$$x_s = Dx \tag{3.8}$$

The dimension of x_s is in general much lower than the dimension of x. The reference value $v_s[k]$ is updated on the time scale T_s so that slower steady state offset in x_s on the time scale T_s is eliminated. To derive the relationship between $x_s[k]$ and $v_s[k]$, we distinguish two important cases, the singular system and nonsingular system. Singular system corresponds to the real power/frequency dynamics without direct flow control, and the nonsingular system corresponds to the reactive power/voltage dynamics. For a singular system, i.e., matrix A in (3.7) is singular, the relationship between $x_s[k]$ and $v_s[k]$ derived from (3.7) is quite complicated. Details will be given in Part II. In the case of a nonsingular system, either the voltage dynamics or the frequency dynamics with direct flow control, the desired relationship between $x_s[k]$ and $v_s[k]$ can be easily determined from (3.7) as

$$x[k] = -A^{-1}Bv_s[k] - A^{-1}UF[k] \tag{3.9}$$

and therefore

$$x_s[k] = B_s v_s[k] + M_s F[k] \tag{3.10}$$

with $B_s \triangleq -DA^{-1}B$ and $M_s \triangleq -DA^{-1}U$.

Eq. (3.10) determines a quasi-static relationship between $x_s[k]$ and $v_s[k]$. This quasi-static relationship is best utilized for the secondary control design when transformed into a dynamical model. To introduce the secondary discrete time dynamical model, let us subtract (3.10) at two consecutive time instances kT_s and $(k+1)T_s$:

$$x_s[k+1] - x_s[k] = B_s(v_s[k+1] - v_s[k]) + M_s(F[k+1] - F[k]) \tag{3.11}$$

Define the update of the reference value, or the corrective control for the secondary level as

$$u_s[k] = v_s[k+1] - v_s[k] \tag{3.12}$$

and the change of tie-line flows as

$$F_s[k] = F[k+1] - F[k] \tag{3.13}$$

One obtains the secondary level discrete time dynamical model as

$$x_s[k+1] - x_s[k] = B_s u_s[k] + M_s F_s[k] \tag{3.14}$$

Model (3.14) is introduced as the simplest model for designing output feedback-based secondary level controllers at the regional level. This model can also be interpreted as representing a discrete event process of a moving equilibrium $x_s[k]$ driven by the discrete control actions $u_s[k]$ and the tie-line flows [8]. Variables $x_s[k]$ will be referred to as the *secondary level states.*

It should be pointed out that the corrective control signal $u_s[k]$ defined in (3.12) represents an implicit integral control, because, from (3.12),

$$v_s[l] = \sum_{k=0}^{l-1} u_s[k] + v_s[0] \tag{3.15}$$

for any integer l. It is this implicit integral control that rejects the steady state error in the output variables on the secondary level time scale.

3.4 Hierarchical Control Design

In this section we present the hierarchical control design methodology based on the time scale separation method discussed above. It is shown that the effect of neighboring regions can be easily accounted for in the regional control design, using the derived simple model at the secondary level.

3.4.1 Controllability

Let us first show a structural property associated with a control-driven system – the controllability of the system is determined by the relative dimensions of the states and controls. Assume that the dimension of the secondary level states $x_s[k]$ is n, and the dimension of the secondary level controls $u_s[k]$ is m. Recall that the controllability matrix of (3.14), with $F_s[k]$ treated as an external input, can be written as

$$\left[B_s \;\; 0 \;\; \cdots \;\; 0 \right] \tag{3.16}$$

This matrix has maximum rows of m and therefore maximum rank of m. If the number of controls m is less than the number of states n, as is typically always the case, this controllability matrix is always singular, and the system is not fully controllable. This property is a structural one since it is independent of the numerical values of the system.

As a result of this structural uncontrollability, only at most m states can be con-

trolled independently. Let us choose m critical states as the output variables to be regulated by the secondary control, expressed as

$$y_s[k] = C_s x_s[k] \tag{3.17}$$

with matrix C_s having dimension $m \times n$. Variations in the output variables $y_s[k]$ can be easily obtained from (3.14) as

$$y_s[k+1] - y_s[k] = C_s B_s u_s[k] + C_s M_s F_s[k] \tag{3.18}$$

Define the $m \times m$ square matrix $U_s = C_s B_s$. Then the above can be written as

$$y_s[k+1] - y_s[k] = U_s u_s[k] + C_s M_s F_s[k] \tag{3.19}$$

3.4.2 Conventional Secondary Control

The goal of the secondary level control is to stabilize the output variables $y_s[k]$ over the secondary time horizon to an optimal value determined by the tertiary control. The conventional secondary control takes the simple proportional form

$$u_s[k] = G(y_s[k] - y_s^{opt}[K]) \tag{3.20}$$

where $y_s^{opt}[K] \triangleq y_s^{opt}(KT_t)$ is the optimal value for the output variables on the even longer tertiary time scale T_t. This optimal value is calculated by the tertiary control, and is constant for secondary processes.

Under this conventional feedback control, secondary level closed-loop dynamical model for output variables is obtained as

$$y_s[k+1] - y_s[k] = U_s G(y_s[k] - y_s^{opt}[K]) + C_s M_s F_s[k] \tag{3.21}$$

The gain matrix G can be chosen to optimize a performance index at the regional level

$$J_s = \sum_{k=0}^{\infty} (y_s^T[k]\, Q\, y_s[k] + u_s^T[k]\, R\, u_s[k]) \tag{3.22}$$

for some matrices $Q = Q^T \geq 0$ and $R = R^T > 0$ specified by each region. The superscript ^{T} denotes the transpose of a matrix. The optimization is with respect to $u_s[k]$, and the result is the optimal gain matrix G. In this process, tie-line flows with neighboring regions are neglected, due to the large scale of the system and the desire to maintain decentralized nature of the regional control.

3.4.3 Improved Secondary Level Control

It is clear from (3.21) that tie-line flows viewed as an independent external input to the system affect the dynamics of the output variables. The conventional "optimal" control designed with interconnections neglected will no longer be optimal when implemented to the actual system where interconnections are indeed present. To fully compensate the effect of interconnections, we propose a modified feedback control law in the form

$$u_s[k] = G(y_s[k] - y_s^{opt}[K]) + HF_s[k] \tag{3.23}$$

where the term $HF_s[k]$ is to cancel the effect of $F_s[k]$ on output variables. Substituting (3.23) into (3.21) yields

$$y_s[k+1] - y_s[k] = U_s G(y_s[k] - y_s^{opt}[K]) + (U_s H + C_s M_s) F_s[k] \tag{3.24}$$

It is clear that if U_s is invertible, then the effects of the tie-line flows can be fully eliminated by simply choosing

$$H = -U_s^{-1} C_s M_s \tag{3.25}$$

With this choice of H, (3.24) reads

$$y_s[k+1] - y_s[k] = U_s K_s (y_s[k] - y_s^{opt}[K]) \tag{3.26}$$

with no flows entering into the equation. In other words, the region under study looks as if it were fully isolated from the rest of the system, as far as the output variables are concerned.

Note that the condition that U_s is invertible should not be viewed as restrictive; instead, it ought to be taken as one of the requirements for the choice of output variables. This is due to the fact that the matrix $(I + U_s K_s)$ is the system matrix for the output variables $y_s[k]$ seen from (3.21) or (3.26); therefore, if the matrix U_s were singular, the closed-loop system matrix $(I + U_s K_s)$ would always have an eigenvalue of 1. The consequence of this is that steady state errors are inevitable for the chosen output variables. To fully control all output variables, it is required that they are selected such that U_s is of full rank.

Note also that the control scheme presented here is totally decentralized, assuming that tie-line flows are locally measurable at each region level. No detailed information about neighboring regions is needed; only tie line flows are required, since they aggregate the net effect of detailed dynamics of neighboring regions. It is not an unrealistic assumption that tie-line flows are locally measurable.

3.4.4 Tertiary Level Control Design

As mentioned earlier, the tertiary level control is mainly concerned with regional coordination over the long time scale T_t. The ultimate goal of this level is to ensure that the interconnected system as a whole operates in an optimal fashion. It is implemented by

adjusting the optimal values y_s^{opt} of the secondary output variables over the time horizon T_t. Since inter-regional effects take place through tie-line flows, scheduling these flows is of direct concern for the tertiary control. In fact, the goal of tertiary level design, as proposed here, is to reschedule the tie-line flows according to a systemwide performance criterion.

There exists a trade-off between the settings of flows and the secondary level output variables. An ideal optimal operation at the tertiary level may require unrealistic setting at the secondary level, due to physical limitations and constraints. Thus, a typical performance criterion at the tertiary level should involve the trade-off between the scheduled flow and the optimal settings for the secondary level outputs. To solve this problem, one must have the relationship between the optimal setting $y_s^{set}[K]$ and the tie-line flows. This relationship, which reveals the effect of tie-line flows on the output variables of each region, is the aggregate model on the tertiary level to be derived in Part III.

3.5 Summary

A new hierarchical control design concept based on the structural models developed in Chapter 2 is presented. The main goal of the hierarchical control is to eliminate the structural singularities associated with singular systems and reject load variations of different time scales. The new concept is based on the use of FACTS devices to directly vary the power flows across a transmission line. This chapter also discusses higher level control designs for both singular and nonsingular systems to stabilize the system in the presence of slower components in load variations. Quasi-static discrete-time dynamical

models are derived on slower time scales, with $x_s[k]$ representing the state variables of interest at the discrete-time instance kT_s. The corresponding output variables are represented by $y_s[k]$.

Part II

Real Power/Frequency Control

Chapter 4

Modeling and Singularity

In Part I the structurally-based modeling and hierarchical control approach was presented conceptually. Here these theoretical concepts are applied specifically to real power/frequency dynamics of power systems. It is shown that real power/frequency dynamics under the present localized control constitute a structurally singular system as defined in Definition 2.1. Detailed discussions on the direct tie-line flow control to remove the structural singularity is presented. Quasi-static models for frequency on mid-term time scales will be derived under the assumption that the fast dynamics of the system are stabilized. Conceptual use of these new structural models for systemwide frequency regulation is proposed.

4.1 Modeling

In this section, the general structurally-based modeling approach proposed in Part I is used for modeling the real power/frequency dynamics. Load disturbances are explicitly modeled.

4.1.1 Local Dynamics

The typical structure for real power/frequency control can be represented by Fig. 4.1.

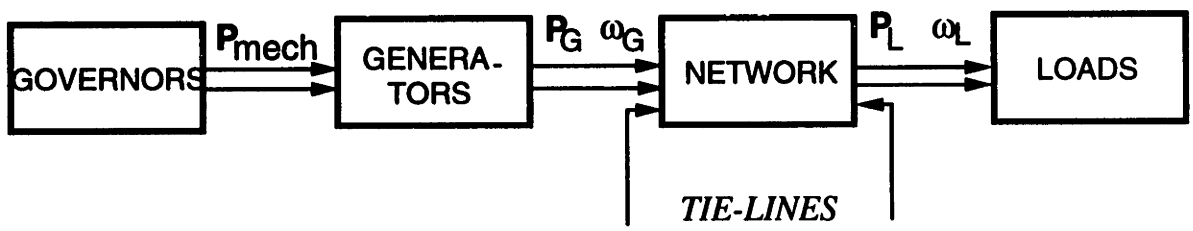

Figure 4.1: Typical Structure of Real Power/Frequency Control

The governor control regulates the mechanical power applied to the generator shaft to stabilize the frequency. Presently, the control structure is entirely localized in the sense that each governor control uses only the frequency error signal, defined as the difference of the measured frequency and the given reference value, of the particular generator to which it is connected. There does not exist a direct coupling among the controls of different generator units.

Let us first study the local dynamics of each generator unit. Consider any generator unit i. Since the generator is simply a rotating shaft, the dynamical model is simply the mechanical rotation equation

$$J^i\dot{\omega}^i = \tau_m^i - \tau_e^i - \tau_d^i \tag{4.1}$$

where ω^i is the rotating speed, or frequency of the generator, J^i is the inertia of the rotating shaft. The terms τ_m^i, τ_e^i, and τ_d^i represent the input mechanical torque, output electro-magnetic torque, and mechanical damping torque, respectively. To simplify notation, the subscript ^{i} will be dropped throughout the subsection. Eq. (4.1) then

becomes

$$J\dot{\omega} = \tau_m - \tau_e - \tau_d \tag{4.2}$$

This equation is typically converted into a more convenient form using power instead of the torque. Multiply (4.2) by ω. That leads to, by recognizing that multiplication of torque with frequency is power,

$$M\dot{\omega} = P_m - P_e - P_d \tag{4.3}$$

where $M = \omega J$, and P_m, P_e, and P_d are the input mechanical power, output electrical power, and mechanical damping power. Since the generator is operating very close to the nominal frequency ω_0 (60 Hz in US), one typically takes $M = \omega_0 J$ as a constant. The damping power P_d is usually small, and is assumed to be a linear function of the frequency, $P_d = D\omega$, where D is the damping coefficient. For the linear damping, Eq. (4.3) becomes

$$M\dot{\omega} + D\omega = P_m - P_e \tag{4.4}$$

The mechanical power P_m is regulated by the governor control. Consider a simple governor-turbine-generator (G-T-G) set shown in Fig. 4.2.

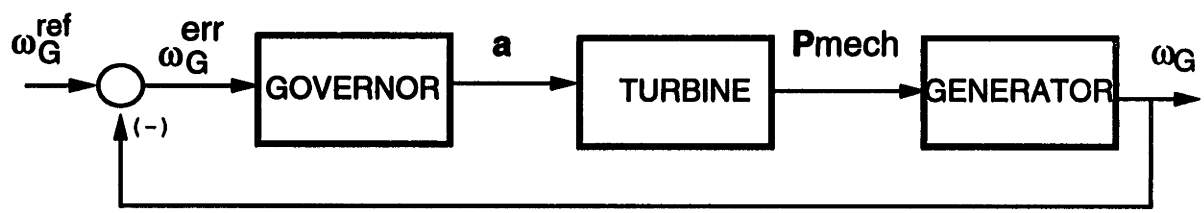

Figure 4.2: Primary Control Loop of a G-T-G Set

The governor regulates the valve opening a of the turbine, which in turn controls the mechanical power applied to the generator shaft P_m. We adopt the same notation

as in [20]. Turbine and governor are in general modeled as a first order system, given by

$$T_u \dot{P}_m = n(P_m, a) \tag{4.5}$$

$$T_g \dot{a} = m(a, \omega^{err}) \tag{4.6}$$

where T_u and T_g are the turbine and governor time constants. Frequency error signal is defined as $\omega^{err} = \omega - \omega^{ref}$, with ω_G^{ref} being the reference value for the governor.

The local state variables of the G-T-G set are defined as the frequency, mechanical power and valve position, given by

$$x_{LC} \triangleq \begin{bmatrix} \omega \\ P_m \\ a \end{bmatrix} \tag{4.7}$$

The local dynamical model of the G-T-G set is described in a nonlinear state-space form:

$$\dot{x}_{LC} = f_{LC}(x_{LC}, \omega^{ref}) - cP_e \tag{4.8}$$

where f_{LC} is the combination of (4.4)-(4.6), and the vector c is given by

$$c = \frac{1}{M} \begin{bmatrix} 1 \\ 0 \\ 0 \end{bmatrix} \tag{4.9}$$

Assume that there exists a nominal operating point given by $x_{LC}^0 = (\omega^0,\ P_m^0,\ a^0)$, and $P_e = P_e^0$. Define deviations of the local state variables from the nominal operating point as

$$\begin{aligned} \delta\omega &\triangleq \omega - \omega^0 \\ \delta P_m &\triangleq P_m - P_m^0 \\ \delta a &\triangleq a - a^0 \end{aligned} \tag{4.10}$$

or $\delta x_{LC} \triangleq x_{LC} - x_{LC}^0$. The linearized local dynamics can be derived as

$$\delta \dot{x}_{LC} = A_{LC}\delta x_{LC} + b\delta\omega_G^{ref} - c\,\delta P_e \tag{4.11}$$

where A_{LC} is the system matrix of local dynamics of each generator, and given by

$$A_{LC} = \begin{bmatrix} -D/M & 1/M & e_T/M \\ 0 & -1/T_u & K_t/T_u \\ -1/T_g & 0 & -r/T_g \end{bmatrix} \tag{4.12}$$

$$b = \frac{1}{T_g}\begin{bmatrix} 0 \\ 0 \\ 1 \end{bmatrix} \tag{4.13}$$

Quantities T_u, K_t, T_g, and r are constant parameters. See [20] for more details. To simplify notation, the prefix δ will be omitted throughout the thesis. With this convention Eq. (4.11) becomes

$$\dot{x}_{LC} = A_{LC}x_{LC} + b\omega_G^{ref} - cP_e \tag{4.14}$$

Now let us write the local dynamics for all generator units in the region. Eq. (4.14) is true for any generator, i.e.,

$$\dot{x}_{LC}^i = A_{LC}^i x_{LC}^i + b^i \omega_G^{i\,ref} - c^i P_e^i\ ,\ i = 1, \cdots, m \tag{4.15}$$

Define the local state, frequency reference, and the generator output for the region as

$$x_{LC} \triangleq \begin{bmatrix} x_{LC}^1 \\ \vdots \\ x_{LC}^m \end{bmatrix},\quad \omega_{ref} \triangleq \begin{bmatrix} \omega_{ref}^1 \\ \vdots \\ \omega_{ref}^m \end{bmatrix},\quad P_G \triangleq \begin{bmatrix} P_e^1 \\ \vdots \\ P_e^m \end{bmatrix} \tag{4.16}$$

and the regional local system matrix

$$A_{LC} = \begin{bmatrix} A_{LC}^1 & & \\ & \ddots & \\ & & A_{LC}^m \end{bmatrix} \tag{4.17}$$

and

$$b \triangleq \begin{bmatrix} b^1 & & \\ & \ddots & \\ & & b^m \end{bmatrix},\quad c \triangleq \begin{bmatrix} c^1 & & \\ & \ddots & \\ & & c^m \end{bmatrix} \tag{4.18}$$

One obtains the local dynamical model for the entire region as

$$\dot{x}_{LC} = A_{LC}x_{LC} + b\omega_G^{ref} - cP_G \tag{4.19}$$

The vector of generator power outputs P_G is the coupling variables x_{CP} introduced in Chapter 2, which serve as the link to local dynamics of other generators via the transmission network. This is discussed next.

4.1.2 Network Coupling

Consider any single region with m generators. Network constraints are typically expressed in terms of nodal type equations that require complex valued power into the network $\hat{S}^N$ to be equal to the complex valued power $\hat{S} = P + jQ$ injected into each node

$$\hat{S}^N = \hat{S} \tag{4.20}$$

where $\hat{S}^N = P^N + jQ^N$ is the vector of net complex power injections to all nodes, which can be written as

$$\hat{S}^N = \text{diag}(\hat{V})\hat{\mathbf{Y}}_{bus}^*\hat{V}^* \tag{4.21}$$

where $\hat{\mathbf{Y}}_{bus}$ is the admittance matrix of the network, $\hat{V} = Ve^{j\delta}$ is the vector of all nodal voltage phasors, with magnitude V and phase δ. The notation diag(•) stands as the diagonal matrix with each element of the vector as the diagonal element. Here we focus only on the real power constraints. The constraints for the reactive power will be discussed in detail in the next part of the thesis. The real part of this equation becomes

$$P^N = P^N(\delta, V) \tag{4.22}$$

Further, the real power injected into each generator terminal on the interconnected system, P, generally is the sum of the generator power output P_G and the real power flow from the neighboring areas. Let us define the vector of the real power flow from the neighboring areas into all generator nodes as

$$F_G \triangleq \begin{bmatrix} F_G^1 \\ \vdots \\ F_G^m \end{bmatrix} \tag{4.23}$$

Then it is obvious that $P_G^N = F_G + P_G$. The network constraints for the real power balance can be further written as

$$P_G^N(\delta, V) = F_G + P_G \tag{4.24}$$

Similarly, since the real power from the load into the network can be written as the difference of real power flow injected into the network at the load terminal F_L and the real power absorbed by the load P_L, i.e.

$$P_L^N = F_L - P_L \tag{4.25}$$

the network constraints (4.22) at the load nodes are expressed as

$$P_L^N(\delta, V) = F_L - P_L \tag{4.26}$$

assuming that the positive direction for tie-line flows is the injection into the network, and the positive direction for loads is leaving the the network. Note that F_G and F_L represent real power flows throughout Part II of the thesis. The separation of the power injection into the part of the injection from the actual device and the part from the interconnecting tie-lines with the neighboring subsystems is essential for establishing structural models of the interconnected systems introduced here.

Differentiating these equations under the decoupling assumption ($\partial P^N/\partial V = 0$) obtains

$$F_G + P_G = J_{GG}\delta_G + J_{GL}\delta_L \tag{4.27}$$

$$F_L - P_L = J_{LG}\delta_G + J_{LL}\delta_L \tag{4.28}$$

where

$$J_{ij} = \frac{\partial P_i^N}{\partial \delta_i}, \quad i,j = G,L \tag{4.29}$$

are the Jacobian matrices evaluated at the given equilibrium operating point. Assuming J_{LL} to be invertible under the normal operating conditions, we define one of the most important matrices associated with a transmission network, the sensitivity matrix,

$$C_\omega \triangleq -J_{LL}^{-1}J_{LG} \tag{4.30}$$

to express frequency deviations at loads ω_L in terms of frequency deviations at generators ω_G and fluctuations in load power. It follows from (4.28) that

$$\delta_L = C_\omega\delta_G + J_{LL}^{-1}(F_L - P_L) \tag{4.31}$$

or by differentiating it with respect to time

$$\omega_L = C_\omega\omega_G + J_{LL}^{-1}(\dot{F}_L - \dot{P}_L) \tag{4.32}$$

where

$$\omega_G = \dot{\delta}_G \triangleq \begin{bmatrix} \omega^1 \\ \vdots \\ \omega^m \end{bmatrix} \tag{4.33}$$

Relationship (4.32) defines the explicit dependence of load frequencies on generator frequencies determined by the network constraints. Combining (4.31) and (4.27), and defining the other two most important matrices associated with a transmission network

$$K_P \triangleq J_{GG} + J_{GL}C_\omega \tag{4.34}$$

and

$$D_P \triangleq -J_{GL}J_{LL}^{-1} \tag{4.35}$$

results in

$$P_G = K_P\delta_G + D_P P_L - F_e \tag{4.36}$$

Here F_e represents effective tie-line flow as seen by each generator and is given as

$$F_e \triangleq F_G + D_P F_L \tag{4.37}$$

It follows after taking derivative with respect to time on both sides of (4.36) that

$$\dot{P}_G = K_P\omega_G - \dot{F}_e + D_P\dot{P}_L \tag{4.38}$$

This equation defines the relationship among all the generator real power outputs P_G, the tie-line flows into the subsystem, and the loads variations, through the network characteristics specified by the two important matrices K_P and D_P.

It should be noted that any (portion of) network is fully characterized by the three matrices (K_P, C_ω, D_P), with K_P reflecting the effect of the generator frequencies on the generator real power outputs, C_ω relating the generator frequencies to the load frequencies, and D_P representing different electrical distances of loads at different locations seen by the generators. The structural properties of these three matrices determine the fundamental features of the power system primary real power/frequency dynamics. They have a direct impact on important issues such as the inter-area oscillations. These properties also have a systemwide effect on the higher level dynamics. Detailed studies on these matrices will be presented in the next section.

4.1.3 Regional Dynamics

The state space formulation of the linearized local dynamics of all the governor control sets on the system (4.19), together with the network constraint equation (4.38), forms the closed-loop dynamic model of the interconnected system. To derive this, let us first repeat Eq. (4.38) here

$$\dot{P}_G = K_P \omega_G - \dot{F}_e + D_P \dot{P}_L \tag{4.39}$$

Generator frequencies are part of the local generator states, given by

$$\omega_G = E x_{LC} \tag{4.40}$$

with the matrix

$$E = \text{BlockDiag}(e^1, \cdots, e^m) = \begin{bmatrix} e^1 & & \\ & \ddots & \\ & & e^m \end{bmatrix} \tag{4.41}$$

and $e^i = \begin{bmatrix} 1 & 0 & \cdots & 0 \end{bmatrix}^i$, with the dimension matching the dimension of the local states x^i_{LC}, $i = 1, \cdots, m$. Local dynamics are derived in (4.19). Combining these two equations together, the standard state space linearized model of the single region within the interconnected system in terms of the tie-line flows explicitly takes the form

$$\begin{bmatrix} \dot{x}_{LC} \\ \dot{P}_G \end{bmatrix} = \begin{bmatrix} A_{LC} & -c \\ K_P E & 0 \end{bmatrix} \begin{bmatrix} x_{LC} \\ P_G \end{bmatrix} - \begin{bmatrix} 0 \\ \dot{F}_e \end{bmatrix} + \begin{bmatrix} 0 \\ D_P \end{bmatrix} \dot{P}_L \tag{4.42}$$

The system matrix for the region is given by

$$A = \begin{bmatrix} A_{LC} & -c \\ K_P E & 0 \end{bmatrix} \tag{4.43}$$

The augmented state variables within each area to be used throughout this thesis are defined as

$$x \triangleq \begin{bmatrix} x_{LC} \\ P_G \end{bmatrix} \tag{4.44}$$

instead of traditionally used

$$x_{old} = \begin{bmatrix} x_{LC} \\ \delta_G \end{bmatrix} \tag{4.45}$$

The state coordinate transformation at each machine level is the mapping from the variables defined in (4.45) into (4.44). With these new state variables the general structure of an arbitrarily interconnected system is given in (4.42). At this point we could directly use the model formulation proposed here to re-visit the question regarding the information obtained from the static load flow equations in analyzing small-signal stability. This was recently studied in [21]. It follows in a very straightforward way that the small-signal stability properties of an isolated system ($F_e = 0$) are dependent only on the properties of the static network constraints, i.e. on the properties of the matrix $K_P E$, when the local system matrices A_{LC} of all components are stable. This observation shows that as long as the local dynamics at each component level are stable, the small-signal stability information obtainable from matrix A is equivalent to the information obtainable from the static load flow equations. This claim is independent from the complexity of particular components.

From a structural view the choice of electric real power outputs of the generators P_G as the state variables is a natural choice for the state variable since it can be directly interpreted in terms of generators' interactions with the transmission system. Notice that this model is not a simple generalization of the swing equations often used for transient stability analysis. The state variable used here is P_G instead of the state δ_G commonly employed in the swing equations. The significance of the new choice for the state variables and the relationship with the traditional ones will be studied next.

4.2 Analysis

In this section a detailed analysis of the real power/frequency dynamics is given, much in the same spirit as in Chapter 2. Let us first exploit the structural singularity of the real power/frequency dynamics.

4.2.1 Network Properties

The transmission network has distinct properties that directly contribute to the inter-area oscillations and other important dynamical features. The decoupled Jacobian matrix J is defined as

$$J \triangleq \frac{\partial P^N}{\partial \delta} = \begin{bmatrix} J_{GG} & J_{GL} \\ J_{LG} & J_{LL} \end{bmatrix} \tag{4.46}$$

with submatrices $J_{ij},\ i,j = G,L$ shown in (4.27)-(4.28). Define further

$$K_P^b \triangleq K_P|_{\text{No electrical losses}} \tag{4.47}$$

when the network is (real power) lossless. With these definition, some important network properties are listed as the following Proposition.

Proposition 4.1 (Network Properties) *For any (portion of) network, the following is true:*

1. $J\mathbf{1} = 0$
2. $K_P\mathbf{1} = 0$
3. $C_\omega\mathbf{1} = \mathbf{1}$
4. $\mathbf{1}^T K_P^b = 0$

where $\mathbf{1}$ *is the column vector with all 1's such that all operations are meaningful.*

All of the above propositions are direct consequence of the fact that the row sum of the incidence matrix is zero [22]. Note that $K_P\mathbf{1} = 0$ simply implies that, for any network, K_P is singular with $\mathbf{1}$ as the right eigenvector corresponding to its zero eigenvalue. The last conclusion in the proposition states further that, for a lossless network, matrix K_P^b has $\mathbf{1}^T$ also as its left eigenvector corresponding to the zero eigenvalue.

4.2.2 Structural Singularity

Singularity of matrix K_P for any network leads to a fundamental characterization of the regional system dynamics. For this, we have

Proposition 4.2 (Structural Singularity) *For any (portion of) network, lossy or lossless, any generator type, the system matrix A defined in (4.43) is always singular.*

This is a direct result of the singularity of K_P. Let the left eigenvector of K_P corresponding to its zero eigenvalue be l^T, i.e.,

$$l^T K_P = 0 \tag{4.48}$$

Consider the row vector

$$L \triangleq \begin{bmatrix} 0 & l^T \end{bmatrix} \tag{4.49}$$

with the same number of 0's as the dimension of x_{LC}. It is easy to check that

$$LA = \begin{bmatrix} 0 & l^T \end{bmatrix} \begin{bmatrix} A_{LC} & -c \\ K_P E & 0 \end{bmatrix} = \begin{bmatrix} l^T K_P E & 0 \end{bmatrix} = 0 \tag{4.50}$$

i.e. matrix A is also singular with the vector L given in (4.49) as its left eigenvector corresponding to the zero eigenvalue. Details on the systemwide effect of this structural singularity will be discussed next.

4.2.3 Inter-Area Dynamics

Inter-area variables were defined in Definition 2.2. It is emphasized that with the structurally-based modeling approach no weak interconnection assumption is required. To derive the inter-area dynamical model, let us recall that the state space model of a single region is given by

$$\begin{bmatrix} \dot{x}_{LC} \\ \dot{P}_G \end{bmatrix} = \begin{bmatrix} A_{LC} & -c \\ K_P E & 0 \end{bmatrix} \begin{bmatrix} x_{LC} \\ P_G \end{bmatrix} - \begin{bmatrix} 0 \\ \dot{F}_e \end{bmatrix} + \begin{bmatrix} 0 \\ D_P \end{bmatrix} \dot{P}_L \tag{4.51}$$

with the system matrix

$$A = \begin{bmatrix} A_{LC} & -c \\ K_P E & 0 \end{bmatrix} \tag{4.52}$$

Let the inter-area variables defined in Definition 2.2 be $z = Tx$. It has been shown that

$$T = L = \begin{bmatrix} 0 & l^T \end{bmatrix} \tag{4.53}$$

where $l^T K_P = 0$. The inter-area variable becomes

$$z = Tx = l^T P_G \tag{4.54}$$

This inter-area variable has a clear physical meaning that it is the combination of the real power outputs of all generators in the region according to the left eigenvector of K_P matrix. This particular combination remains constant if interactions are removed and there is no load variation. As tie-line flows or loads vary, the inter-area variable will vary with time.

The dynamical model for the inter-area variable is of the form

$$\dot{z} = -T \begin{bmatrix} 0 \\ \dot{F}_e \end{bmatrix} + T \begin{bmatrix} 0 \\ D_P \end{bmatrix} \dot{P}_L \tag{4.55}$$

or simply

$$\dot{z} = -l^T(\dot{F}_e - D_P \dot{P}_L) \tag{4.56}$$

Clearly it is seen that the inter-area variable z varies due to the tie-line flows, for a constant power load. Eq. (4.56) defines exactly the relationship between these two. It is also seen that the fundamentally the inter-area dynamics represent the regional net real power exchanges. This kind of interactions among subsystems are referred to as *inter-area power interactions.*

4.2.4 Computation of Inter-Area Variables

Since the inter-area variables are defined for individual separate region, the computation of inter-area variables can be done by each region separately. For each region, the computation involves only the calculation of the left eigenvector L of matrix A corresponding to its zero eigenvalues, as specified by

$$LA = 0 \tag{4.57}$$

In general, it is desired to have a stable local dynamics, i.e. the governor control design is such that each matrix A_{LC} is of full rank. This assumption is normally met since local controls are typically designed such that the local dynamics are stable. Under this condition, the singularity of matrix A is directly caused by the singularity of matrix K_P. In this case, we can take L as

$$L = \begin{bmatrix} 0 & l^T \end{bmatrix} \tag{4.58}$$

where l^T is the left eigenvector of matrix K_P corresponding to its zero eigenvalue, i.e.

$$l^T K_P = 0 \tag{4.59}$$

Let us discuss the calculation of l^T. It is emphasized that (4.59) can be easily solved by simple Gauss elimination-like method. But a structural approach for the solution seem more physically meaningful. It has been shown in Proposition 4.1 that, for a lossless network, we have a surprisingly simple, but meaningful solution $l^T = \mathbf{1}^T$. This particular structure is by no means coincident, it represents a fundamental requirement for the network – the power balance.

For a (real power) lossy network, since the losses are in general very small, we can use a perturbation method to obtain an approximate solution based on the lossless solution $l^T = \mathbf{1}^T$. The approximate solution is expected to be quite accurate if the losses are not unreasonably high. Numerical example will show later that the approximation gives a simple but quite satisfactory answer. Again, this approach is an alternative to the numerical Gauss method, but more physically meaningful. Let us write l as

$$l = l^b - l^g = \mathbf{1} - l^g \tag{4.60}$$

where $l^b = \mathbf{1}$ corresponds to the eigenvector of the lossless K_P matrix, and l^g is added to account for losses. When the losses are small, the term l^g is expected to be also small. Condition (4.59) becomes

$$l^T K_P = (l^b - l^g)^T (K_P^b + K_P^g) = 0 \tag{4.61}$$

Recognizing from Proposition 4.1 that $l^b K_P^b = 0$, and neglecting higher order term $l^{gT} K_P^g$ due to small losses, one obtains

$$l^{gT} K_P^b = l^{bT} K_P^g \tag{4.62}$$

Furthermore, without loss of generality, one could assume the form for l^g to be

$$l^{gT} = \begin{bmatrix} 0 & l_2^g & \cdots & l_m^g \end{bmatrix} \tag{4.63}$$

since the transformation l^T is unique only up to a constant scalar, and one can always choose the first element of l^T to be the first element of l^{bT}, and therefore first element of l^{gT} is always 0.

Let us denote

$$l_-^{gT} \triangleq \begin{bmatrix} l_2^g & \cdots & l_m^g \end{bmatrix} \tag{4.64}$$

Then Eq. (4.62) can be written as

$$\begin{bmatrix} 0 & l_-^{gT} \end{bmatrix} K_P^b = l^{bT} K_P^g \tag{4.65}$$

Since the first row of K_P^b is multiplied by zero, it can be eliminated. Define matrix

$$E_1 \triangleq I \Big|_{\text{Without 1st Column}} \tag{4.66}$$

Then it is easy to see that for any matrix M,

$$ME_1 = M \Big|_{\text{Without 1st Column}} \tag{4.67}$$

$$E_1^T M = M \Big|_{\text{Without 1st Row}} \tag{4.68}$$

With this notation, Eq. (4.65) now becomes

$$l_-^{gT} E_1^T K_P^b = l^{bT} K_P^g \tag{4.69}$$

Further, let us split K_P^b and K_P^g as follows:

$$K_P^b = \begin{bmatrix} K_{P1}^b & \vdots & K_{P-}^b \end{bmatrix} = \begin{bmatrix} K_{P1}^b & \vdots & K_P^b E_1 \end{bmatrix} \tag{4.70}$$

$$K_P^g = \begin{bmatrix} K_{P1}^g & \vdots & K_{P-}^g \end{bmatrix} = \begin{bmatrix} K_{P1}^g & \vdots & K_P^g E_1 \end{bmatrix} \tag{4.71}$$

where K_{P1}^b and K_{P1}^g represent the first column of K_P^b and K_P^g. Since both K_P^b and K_P^g satisfy

$$K_P^b \mathbf{1} = 0 \quad \text{and} \quad K_P^g \mathbf{1} = 0 \tag{4.72}$$

from Proposition 4.1, we have

$$K_{P1}^b = -K_P^b E_1 \mathbf{1} \quad \text{and} \quad K_{P1}^g = -K_P^g E_1 \mathbf{1} \tag{4.73}$$

Thus,

$$K_P^b = \left[\begin{array}{c:c} -K_P^b E_1 \mathbf{1} & K_P^b E_1 \end{array} \right] \tag{4.74}$$

$$K_P^g = \left[\begin{array}{c:c} -K_P^g E_1 \mathbf{1} & K_P^g E_1 \end{array} \right] \tag{4.75}$$

Eq. (4.69) becomes

$$l_-^{gT} E_1^T \left[\begin{array}{c:c} -K_P^b E_1 \mathbf{1} & K_P^b E_1 \end{array} \right] = l^{bT} \left[\begin{array}{c:c} -K_P^g E_1 \mathbf{1} & K_P^g E_1 \end{array} \right] \tag{4.76}$$

Or

$$l_-^{gT} E_1^T K_P^b E_1 \mathbf{1} = l^{bT} K_P^g E_1 \mathbf{1} \tag{4.77}$$

$$l_-^{gT} E_1^T K_P^b E_1 = l^{bT} K_P^g E_1 \tag{4.78}$$

Eq. (4.77) will be automatically satisfied if Eq. (4.78) is satisfied. This redundancy is always the case due to the singularity of K_P.

Let us now consider Eq. (4.78) only. Under normal operating conditions, matrix K_P^b is rank deficient only by 1. In this case, matrix $E_1^T K_P^b E_1$, which is the matrix K_P^b with first row and first column eliminated, has full rank. Therefore, one can solve for l_-^{gT} from Eq. (4.78) as

$$l_-^{gT} = l^{bT} K_P^g E_1 (E_1^T K_P^b E_1)^{-1} \tag{4.79}$$

Using the fact that $l^b = \mathbf{1}$, one derives

$$l^{gT} = \left[\begin{array}{c|c} 0 & \mathbf{1}^T K_P^g E_1 (E_1^T K_P^b E_1)^{-1} \end{array} \right] \tag{4.80}$$

This is the desired expression for the perturbation to the left eigenvector of K_P corresponding to its zero eigenvalue. It is valid for small real power losses.

It is interesting to recognize that when matrix K_P has rank lower than $(m-1)$, there exists a possibility of having more than one interaction variable per area. These additional interaction variables are simply caused by the non-existence of any solution to the static network constraints (4.21), and are independent from the relative inertia and damping coefficient values of generators, as well as from the type of governor controls. Although an open question remains if such operating points would be feasible, a near loss of rank would be of definite practical interest. For example, one scenario of additional loss of rank in the matrix K_P would be when the system operates at unusually high real power transfers. The inter-area oscillations have been recognized in context of this operating mode [4].

4.2.5 Interpretation of Inter-Area Variables

Let us now discuss the physical meaning of the inter-area variables defined in 2.2. Since inter-area variables are defined when interconnections are removed, i.e. they are defined separately for each region, we focus on a single region for our study. First, for the (real power) lossless case, it has been shown that $l^T = \mathbf{1}^T$. The inter-area variable can, from (4.54), be further written as

$$z = l^T P_G = \mathbf{1}^T P_G = \sum_{j=1}^{m} P_e^j \tag{4.81}$$

i.e. the inter-area variable is the sum of the real power outputs of all the generators in this region, or the total generation of the region. Under the conditions specified in Definition 2.2, i.e. when there are no tie-line flow exchanges with the neighboring regions, and no load variations, the total generation of the region must be constant, equaling the constant load demand. It is clear that the definition of the inter-area variables in Definition 2.2 captures this fundamental property of the network.

For the case of a lossy network, part of the generation must be absorbed by the losses in the network, and the other part of the generation must be balanced with the loads. Therefore, the total generation of the region minus the power absorbed by the losses must be a constant under the conditions in Definition 2.2. This portion of the power absorbed by the losses is precisely described by the correction term $l^{gT}P_G$. In fact it can be shown that the term $l^{gT}P_G$ is exactly the total real power loss of the region. Thus we see here again the requirement of power balance for the network. This power balance requirement is the fundamental property of the network. It will have a systemwide effect on higher level dynamics also.

4.2.6 Comparisons with Conventional Models

The choice of electric real power outputs P_G of generators as state variables facilitates greatly the study of inter-area dynamics. For comparison, let us discuss conventional models, which employ generator phase angles as state variables. The local dynamical model, under the condition that updating the reference values is inactive, has been obtained as

$$\dot{x}_{LC} = A_{LC}x_{LC} - cP_G \tag{4.82}$$

where the generator power P_G is replaced by the network coupling relation in (4.36)

$$P_G = K_P\delta_G + D_P P_L - F_e \tag{4.83}$$

Together, the global linearized model of an area takes the form

$$\dot{x}_{LC} = A_{LC}x_{LC} - c(K_P\delta_G + D_P P_L - F_e) \tag{4.84}$$

and the trivial relation

$$\dot{\delta}_G = \omega_G = Ex_{LC} \tag{4.85}$$

is used. The most often used model in the conventional state variables is the so-called swing dynamical model, i.e. there is no governor control, and the mechanical power applied to the generator shaft is constant. The primary dynamics become

$$M\ddot{\delta}_G + D\dot{\delta}_G + K_P\delta_G + D_P P_L - F_e = 0 \tag{4.86}$$

with

$$M = \begin{bmatrix} M^1 & & \\ & \ddots & \\ & & M^m \end{bmatrix} \quad \text{and} \quad D = \begin{bmatrix} D^1 & & \\ & \ddots & \\ & & D^m \end{bmatrix} \tag{4.87}$$

being the inertia and damping matrices. This model loses the clear structural properties of the system matrix A as stated in Proposition 4.2. Also it is not easily generalized to more complicated cases.

The new state variables P_G can be viewed as a linear transformation from the conventional state variables δ_G as specified in (4.83)

$$P_G = K_P\delta_G + D_P P_L - F_e \tag{4.88}$$

or simply

$$P_G = K_P\delta_G \tag{4.89}$$

if one neglects the inputs to the system. This is not a conventional transformation in the sense that the transformation matrix K_P is always singular for any network, as stated in Proposition 4.1. This singular transformation proves to be very efficient for the basic understanding of inter-area oscillations in power systems.

Let us first briefly present the existing results in the literature. For the conventional model (4.86), storage variables have been proposed [19]. These storage variables are defined as

$$\xi = M\omega_G + D\delta_G \tag{4.90}$$

Note that the defined storage variables have the dimension of the number of generators, not just a single scalar for an area. The question is how the generalized definition of the interaction variables introduced in Definition (2.2) is related to this widely accepted approach to modeling inter-area variables. To answer this, we first interpret the previous work from the viewpoint of Definition (2.2).

If we perform the calculation of the inter-area variables for the model (4.86) in the old state variables, it can be easily shown that the resulting area variable is

$$z_{old} = l^T\xi = l^T(M\omega_G + D\delta_G) \tag{4.91}$$

where $l^T K_P = 0$, the same left eigenvector of P_G corresponding to the zero eigenvalue. In other words, the scalar inter-area variable defined here when applied to the conventional model is the same linear combination of the storage variables as the inter-area variable

$$z = l^T P_G \tag{4.92}$$

in the new state space proposed here, with the left eigenvector l^T of P_G. The relation between the two inter-area variables is derived from (4.86) (with $P_L = 0$ and $F_e = 0$)

as

$$z = -\dot{z}_{old} \tag{4.93}$$

since

$$P_G = K_P \delta_G = -(M\dot{\omega}_G + D\omega_G) = -\dot{\xi} \tag{4.94}$$

In the context of mechanical variables, inter-area variable z can be explained as the force, and the inter-area variable z_{old} can be viewed as the momentum modulo mechanical losses.

There are a few drawbacks with the conventional model. Conceptually, first of all, the inter-area variable $z_{old} = l^T(M\omega_G + D\delta_G)$ misleadingly indicates that generator local dynamics directly participate in the inter-area mode, since all quantities involved are mechanical ones constituting the generator local dynamics. Although these local dynamics quantities show up in the inter-area dynamical equation, the particular expression $(M\omega_G + D\delta_G)$ actually implies the electrical power balance, as we see next.

Second, structurally, the form $z_{old} = l^T(M\omega_G + D\delta_G)$ is valid only for the linear damping. When the damping takes a nonlinear form, the expression is completely not valid. But, the inter-area variable $z = l^T P_G$ still holds. This is because the inter-area variable reflects the fundamental requirement of the power (force) balance for an isolated system without any disturbances. The expression $(M\omega_G + D\delta_G)$ is useful just because it is another form of the power (force) balance, for

$$(M\omega_G + D\delta_G) = -\int P_G(\tau)d\tau \tag{4.95}$$

through the dynamical equation. For different forms of damping, expression $(M\omega_G + D\delta_G)$ becomes meaningless, while the basic power (force) balance will still hold. This

clearly reveals that the choice of the power outputs P_G as state variables captures the fundamental properties of the system.

Third, from the point of view of control design to suppress inter-area oscillations, the inter-area variable $z_{old} = l^T(M\omega_G + D\delta_G)$ involves the measurements of m angles δ_G and m frequencies ω_G, and the inertia matrix M and the damping matrix D. It is very hard to get accurate numerical values for these parameters. In the new state space, the inter-area variable $z = l^T P_G$ only involves the measurements of m generator power outputs, which are measured anyway. No parameters regarding the local dynamics are needed.

4.2.7 An Example

In this section, we study a small example power system to illustrate the theoretical concepts developed in this thesis. The example is the 5-bus power system given in [23], also shown in Fig. 4.3.

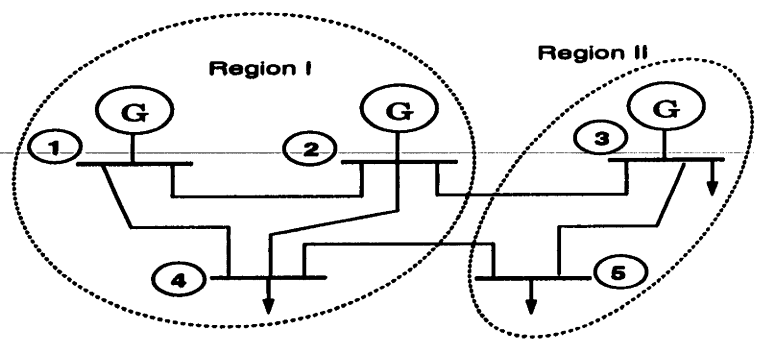

Figure 4.3: An Interconnected 5-bus Power System

This example will be used throughout this thesis consistently to show the structural decompositions and control designs. The system is composed of two regions. Region I includes generator buses #1, #2 and the load bus #4. Region II includes generator #3 and load #5. There are two tie-lines connecting generator #4 to #3, and load #4

G-T-G Set Parameters							
	M	D	e_T	T_u	K_t	r	T_g
#1	10	5	1696	.2	10744	19	.25
#2	5	4	1696	.2	10744	19	.25
#3	3	4	1696	.2	10744	19	.25
Line Parameters							
	#1 - #2	#1 - #4	#2 - #4	#3 - #5	#2 - #3	#4 - #5	
b	10	10	10	10	.5	.5	
g	1	1	1	1	.05	.05	
Load Flow Data							
	#1	#2	#3	#4	#5		
V	1	1	1	.9802	.9502		
δ	0	.0157	-.191	-.0575	-.3013		

Table 4.1: Per Unit Data of the 5-Bus Example

to #5. The data used in the simulation are listed in Table 4.1.

All simulations are done using the software MATLAB. The K_P matrix for each region are calculated as

$$K_P^I = \begin{bmatrix} 14.8977 & -14.8977 \\ -14.9446 & 14.9446 \end{bmatrix} \quad \text{and} \quad K_P^{II} = 0 \tag{4.96}$$

Clearly, each row in the K_P matrix sums up to zero, i.e.

$$K_P^I \begin{bmatrix} 1 \\ 1 \end{bmatrix} = 0 \quad \text{and} \quad K_P^{II}\ 1 = 0 \tag{4.97}$$

It is easy to check that the left eigenvector of K_P corresponding to the zero eigenvalue is given by

$$l^{I\,T} = \begin{bmatrix} 1 & 0.9969 \end{bmatrix} \quad \text{and} \quad l^{II\,T} = 1 \tag{4.98}$$

For the purpose of illustration, let us consider only the swing dynamics. In this case, the closed-loop eigenvalues for the disconnected and connected system are computed and shown in Table 4.2.

Disconnected System	Region I			Region II	
	$-0.3487 \pm 2.0825j$	-0.6025	0	-1.3333	0
Connected System	$-0.3509 \pm 2.100j$	$-0.4201 \pm 0.2503j$		-1.5523	0

Table 4.2: Closed-Loop Eigenvalues - Lower Damping

From Table 4.2, it is seen that each disconnected region has a zero eigenvalue. One zero eigenvalue remains at zero when the regions are connected, while two eigenvalues -0.6025 and 0 move together to the complex eigenvalues $-0.4201 \pm 0.2503j$. These two additional oscillatory eigenvalues correspond to the inter-area oscillations. The frequency of the inter-area oscillations $\omega = 0.2503$ is much smaller than the other frequency $\Omega = 2.100$ to yield the so-called slow intra-area oscillations.

Figure 4.4 shows the response of the system. Obviously, both fast intra- and slow inter-area oscillations are seen. As expected, the inter-area variable z^I captures the slow inter-area oscillations.

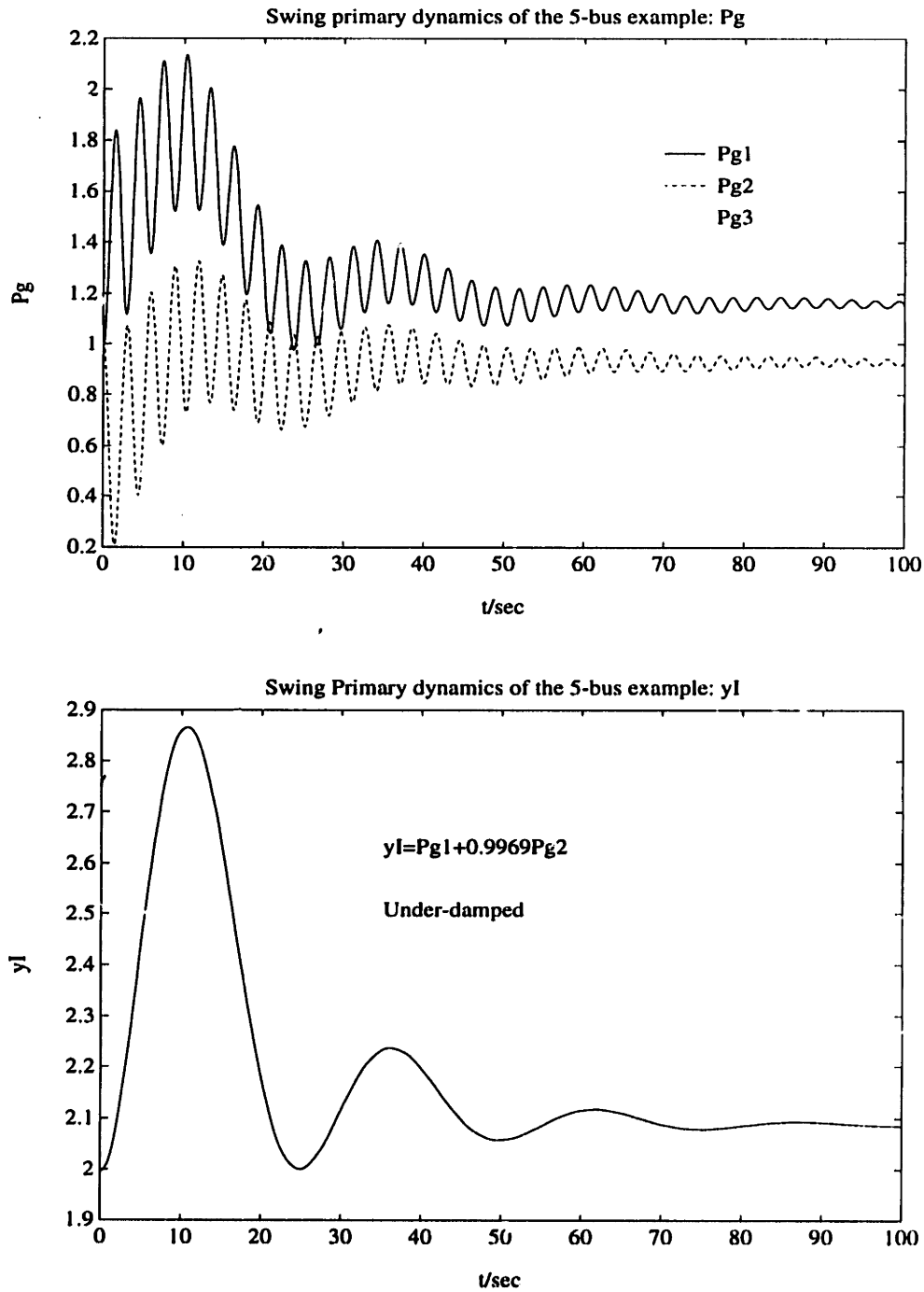

Figure 4.4: Inter-Area Oscillations

4.3 Quasi-Static Model

In this section, a simple discrete time dynamical model on the secondary time scale is derived. The purpose of the regional secondary control is to update the frequency reference value for each participating G-T-G set at discrete time instance kT_s so that steady state frequency errors are eliminated. The discrete-time actions of updating frequency reference values result in a DEP in frequencies on the secondary level.

Let us start with the closed-loop primary dynamical model (4.42),

$$\begin{bmatrix} \dot{x}_{LC} \\ \dot{P}_G \end{bmatrix} = \begin{bmatrix} A_{LC} & -c \\ K_P E & 0 \end{bmatrix} \begin{bmatrix} x_{LC} \\ P_G \end{bmatrix} + \begin{bmatrix} b \\ 0 \end{bmatrix} \omega_G^{ref}[k] - \begin{bmatrix} 0 \\ \dot{F}_e \end{bmatrix} + \begin{bmatrix} 0 \\ D_P \dot{P}_L \end{bmatrix} \tag{4.99}$$

Assume that the governor controls are designed such that the closed-loop transient dynamics are fast relative to the updating of reference values. Under this assumption one can write $\dot{x} = 0$, *at* kT_s, $k = 0, 1, \cdots$, i.e., the system settles to steady state at these discrete time instances kT_s. Let us first consider the local dynamics of each G-T-G set, derived before in (4.19),

$$\dot{x}_{LC} = A_{LC} x_{LC} + b\omega_G^{ref}[k] - cP_G \tag{4.100}$$

The assumption of fast transient dynamics yields

$$A_{LC} x_{LC}[k] = -b\omega_G^{ref}[k] + cP_G[k] \tag{4.101}$$

or

$$x_{LC}[k] = -A_{LC}^{-1} b\omega^{ref}[k] + A_{LC}^{-1} cP_G[k] \tag{4.102}$$

since A_{LC}, given in (4.12), is invertible. One can further calculate

$$A_{LC}^{-1} = \frac{1}{\Delta} \begin{bmatrix} -rM & -rT_u & -(e_T + K_t)T_g \\ K_t M & -(rD + e_T)T_u & -DK_t T_g \\ M & T_u & -DT_g \end{bmatrix} \tag{4.103}$$

with $\eta = rD + e_T + K_t$. Substituting this back into (4.102) simply gives

$$\begin{bmatrix} \omega[k] \\ P^m[k] \\ a[k] \end{bmatrix} = \frac{1}{\eta} \begin{bmatrix} e_T + K_t \\ DK_t \\ D \end{bmatrix} \omega^{ref}[k] + \frac{1}{\eta} \begin{bmatrix} -r \\ K_t \\ 1 \end{bmatrix} P_G[k] \tag{4.104}$$

Since we are interested in the frequency variations only on the secondary level, let us consider only the first row,

$$\omega[k] = \frac{e_T + K_t}{\eta} \omega^{ref}[k] - \frac{r}{\eta} P_G[k] \tag{4.105}$$

or

$$\omega[k] = (1 - \frac{r}{\eta} D)\omega^{ref}[k] - \frac{r}{\eta} P_G[k] \tag{4.106}$$

Define the *droop constant* of any G-T-G set as

$$\sigma \triangleq - \frac{\partial \omega[k]}{\partial P_G[k]} \Big|_{\omega^{ref}[k]=0} \tag{4.107}$$

The physical meaning of the droop constant is that it represents the sensitivity of the steady state frequency deviation to the deviation of steady state real power output of the G-T-G set, when the frequency setting is kept at a constant, or the secondary level control is inactive. A small droop constant indicates that real power output variations have a small effect on the steady state frequency variations. A flat droop characteristic, i.e., $\sigma = 0$, implies that the steady state frequency always reaches the reference value, no matter how the real power output varies. Clearly, an integral control must be involved in the primary controller in this case, so that the steady state error of the primary local control vanishes.

With this general definition, one simply obtains the droop constant for the G-T-G set discussed here as

$$\sigma = \frac{r}{\eta} = \frac{r}{rD + e_T + K_t} \tag{4.108}$$

It then follows from (4.11) that the steady-state transfer function of the G-T-G set for specified $P_G[k]$ is

$$\omega[k] = (1 - \sigma D)\omega^{ref}[k] - \sigma P_G[k] \tag{4.109}$$

where D is the generator damping constant.

This is the quasi-static relationship among the frequency deviation, reference value, and real power output variation of each G-T-G set. This relationship is completely decentralized, in the sense that no coupling between different G-T-G sets occur except through the local output variables P_G. *This complete decentralization is possible only if the real power output of each G-T-G set is chosen as a state variable as done in this thesis.* Real power output variations of all G-T-G sets in the network will be coupled, and the coupling is exactly the network relationships discussed before.

Let us derive the secondary level relationship for a region consisting of m such G-T-G sets. Since relationship (4.109) is completely decentralized and true for each G-T-G set, the secondary level relationship for the entire region is simply obtained by putting relationship (4.109) for each G-T-G set together. To do this, we define the generator frequency vector and power output vectors as

$$\omega_G \triangleq \begin{bmatrix} \omega_G^1 \\ \vdots \\ \omega_G^m \end{bmatrix} \tag{4.110}$$

and the diagonal droop matrix and damping matrix as

$$\sigma \triangleq \begin{bmatrix} \sigma_1 & & \\ & \ddots & \\ & & \sigma_m \end{bmatrix} \quad \text{and} \quad D \triangleq \begin{bmatrix} D_1 & & \\ & \ddots & \\ & & D_m \end{bmatrix} \tag{4.111}$$

Then the decentralized quasi-static model for all m G-T-G sets can be obtained as

$$\omega_G[k] = (I - \sigma D)\omega_G^{ref}[k] - \sigma P_G[k] \tag{4.112}$$

where I is the $m \times m$ identity matrix.

Vector $P_G[k]$ is coupled to all generator angles by the following equation derived in (4.83),

$$P_G[k] = K_P\delta_G[k] - F_e[k] + D_P P_L[k] \tag{4.113}$$

Eq. (4.112) is combined with (4.113) to yield

$$\omega_G[k] = (I - \sigma D)\omega_G^{ref}[k] - \sigma(K_P\delta_G[k] - F_e[k] + D_P P_L[k]) \tag{4.114}$$

Writing (4.114) at two successive LFC sampling instances kT_s and $(k+1)T_s$, one obtains

$$\omega_G[k+1] - \omega_G[k] = (I - \sigma D)(\omega_G^{ref}[k+1] - \omega_G^{ref}[k]) - \sigma K_P(\delta_G[k+1] - \delta_G[k])$$

$$+ \sigma(F_e[k+1] - F_e[k]) - \sigma D_P(P_L[k+1] - P_L[k]) \tag{4.115}$$

Since

$$\delta_G[k+1] - \delta_G[k] \approx T_s\omega_G[k] \tag{4.116}$$

model (4.115) expressed in terms of $\omega_G[k]$ only takes the form

$$\omega_G[k+1] = (I - \sigma K_P T_s)\omega_G[k] + (I - \sigma D)(\omega_G^{ref}[k+1] - \omega_G^{ref}[k])$$

$$+ \sigma(F_e[k+1] - F_e[k]) - \sigma D_P(P[k+1] - P[k]) \tag{4.117}$$

Model (4.117) is defined in terms of system variables at discrete times kT_s, $k = 0, 1, \cdots$ only. General theory of control design for such systems introduced in Chapter 3 is applicable to this model.

The discrete-time corrective signal $(\omega_G^{ref}[k+1] - \omega_G^{ref}[k])$ is the control action for the secondary level. To allow for generating units not participating in the secondary level control, let us separate the participating and nonparticipating generators as

$$\omega_G = \begin{bmatrix} \omega_s \\ \omega_n \end{bmatrix} \tag{4.118}$$

where ω_s and ω_n represent the participating and nonparticipating generators, respectively. The term $(\omega_G^{ref}[k+1] - \omega_G^{ref}[k])$ can now be written as

$$\omega_G^{ref}[k+1] - \omega_G^{ref}[k] = \begin{bmatrix} \omega_s^{ref}[k+1] - \omega_s^{ref}[k] \\ \omega_n^{ref}[k+1] - \omega_n^{ref}[k] \end{bmatrix} \tag{4.119}$$

It is obvious that for the nonparticipating generators

$$\omega_n^{ref}[k+1] - \omega_n^{ref}[k] \equiv 0, \quad \forall\, k \tag{4.120}$$

Let us define the actual secondary LFC control signal as

$$u_s[k] \triangleq \omega_s^{ref}[k+1] - \omega_s^{ref}[k] \tag{4.121}$$

From these definitions, we can rewrite the control term as

$$\omega_G^{ref}[k+1] - \omega_G^{ref}[k] = \begin{bmatrix} u_s[k] \\ 0 \end{bmatrix} = \begin{bmatrix} I \\ 0 \end{bmatrix} u_s[k] \triangleq B_s u_s[k] \tag{4.122}$$

where I is the $p \times p$ identity matrix with p being the number of participating generators.

Let us further define the net tie-line flow effect as

$$F_s[k] = F_e[k+1] - F_e[k] \tag{4.123}$$

and also define the disturbance at the secondary level as

$$d_s[k] = P_L[k+1] - P_L[k] \tag{4.124}$$

With these definitions, we derive the discrete-time dynamics of the generator frequencies at the secondary level as

$$\omega_G[k+1] = (I - \sigma K_P T_s)\omega_G[k] + (I - \sigma D)B_s u_s[k] + \sigma F_s[k] - \sigma D_P d_s[k] \tag{4.125}$$

This is the secondary level dynamical model for all generator frequencies in terms of the frequency setting changes and tie-line flow changes.

Load frequencies ω_L are expressed in terms of the generator frequencies ω_G by Eq. (4.32):

$$\omega_L = C_\omega \omega_G + J_{LL}^{-1}(\dot{F}_L - \dot{P}_L) \tag{4.126}$$

which leads to, with all time derivatives vanishing at discrete times kT_s,

$$\omega_L[k] = C_\omega \omega_G[k] \tag{4.127}$$

This relationship determines changes in load frequencies in terms of changes in generator frequencies.

The output variables for the secondary control include part or all of the generators and possibly some loads. Inclusion of load frequencies allows for demand side management of the secondary frequency regulations. Let us define the output variables as

$$\omega_o[k] = C_1 \omega_G[k] + C_2 \omega_L[k] \tag{4.128}$$

where C_1 and C_2 are matrices with 0's and 1's to pick up the desired output variables. Using (4.127) to express $\omega_L[k]$ in terms of the state variables $\omega_G[k]$, we obtain the output equation of the secondary level frequency control as

$$\omega_o[k] = C_s \omega_G[k] \tag{4.129}$$

where the output matrix is simply $C_s = C_1 + C_2 C_\omega$.

Eqs. (4.125) and (4.129) constitute the simple discrete-time dynamical model for variables of interest on the secondary level. This simple model forms a basis for the secondary level frequency control.

Here a numerical example is used to confirm that the derived simple quasi-static models agree with the detailed transient models evaluated on the secondary level time

scale T_s. In the simulation, secondary level control is not activated, i.e., $u_s[k] = 0$, $\forall k$. The entire system is considered as a single area. Because this region is isolated, there is no tie-line flow. We compare the time domain responses of the system under a given load variation, obtained using the full complicated primary models and the much simpler secondary level models. All initial conditions are set to zero. Figure 4.5 shows the linearly varying load at bus #4 and the responses of three generator frequencies to this load variation, with the primary and secondary models. The following is observed from the numerical simulations:

- Frequencies of generators #1 and #2 are almost equal. This is because the two lines connecting bus #4 to generators #1 and #2 are the same. Generator #3 is nearly unperturbed by the load disturbance occurring at bus #4, because the two tie-lines are weak;

- Time responses of generator frequencies roughly follow inversely load fluctuations, i.e., load increases result in frequency decreases, and vice versa;

- Time domain responses of the system obtained using complete model (4.42) is indistinguishably identical to the responses obtained using much simpler models (4.125) and (4.129). However, calculations involved with the quasi-static models are significantly simpler and easier, compared to the calculations with the original detailed models.

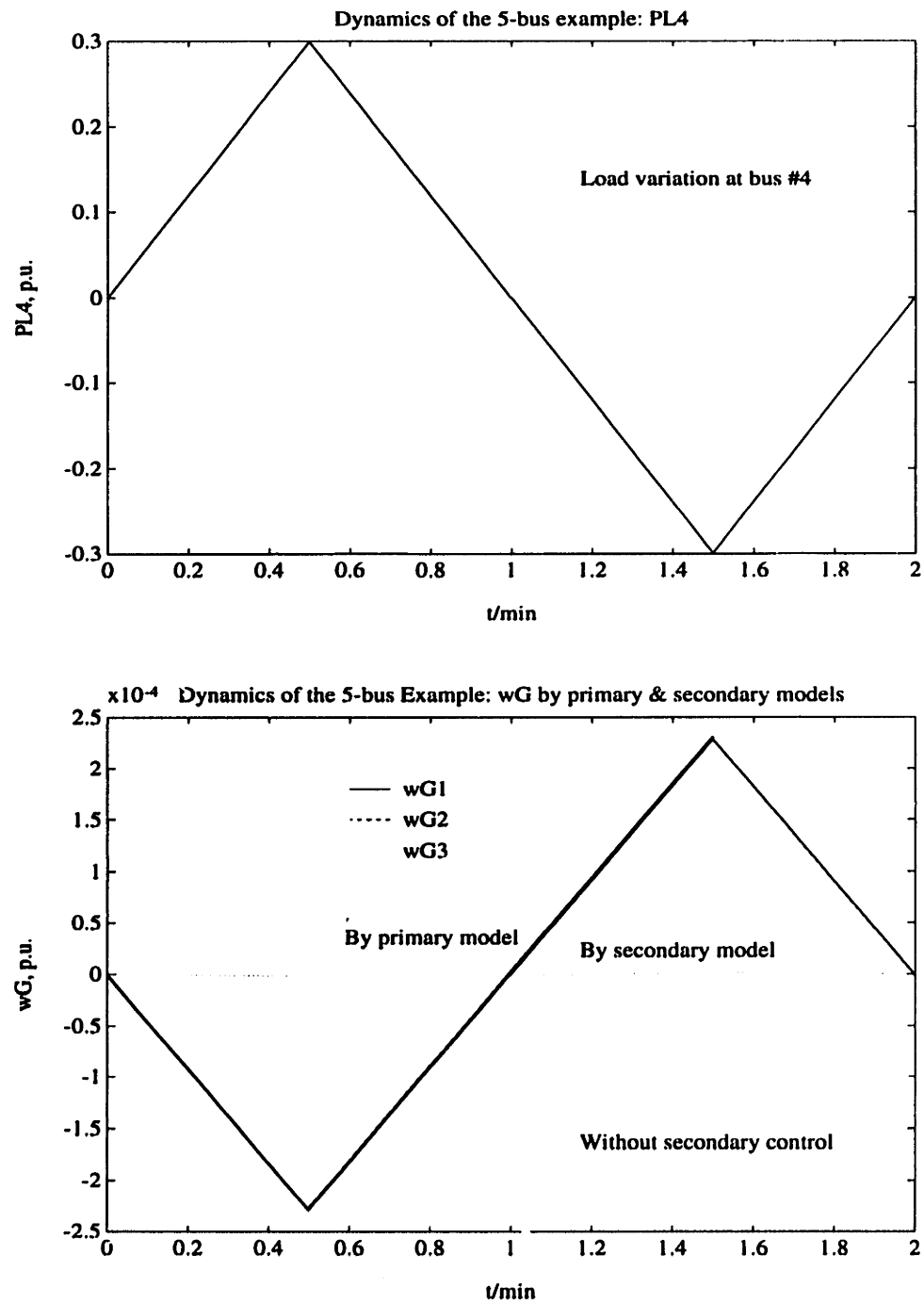

Figure 4.5: Load Variation and Frequency Response

4.4 Summary

In this chapter, a structurally-based modeling approach for real power/frequency dynamics of an interconnected power system is presented. Dynamics of the system are formulated by combining the local dynamics of individual generators and the network couplings. The concept of structural singularity for large-scale power systems is defined. It is shown that the decoupled real power/frequency dynamics of power systems are structurally singular. Discrete-time dynamical models on slower time scales are derived. The modeling approach provides a solid basis for systematic control designs to be discussed in the next chapter.

Chapter 5

Control Designs

5.1 Direct Flow Control

As discussed in Chapter 4, inter-area dynamics represent singular modes of the system under the present local control structure. Due to small dampings these singular modes often occur as oscillatory. Under weak interconnections, the oscillations become slow and persistent [24] [4]. As shown before, the structural singularities cannot be removed by any design under the present local control structure. In this thesis, we propose a new control scheme to remove the structural singularities by directly regulating tie-line flows using the fast power-electronic switched controllers presently being developed and tested. These controllers are often referred to as the FACTS devices [25], [26]. The idea of the proposed new control scheme is to change the dynamical characteristics of the inter-area modes by a feedback control so that the oscillatory behavior of the inter-area modes becomes exponential and settles in a desired time constant. First the case when all tie-lines are equipped with the FACTS control devices is studied. Detailed control design procedures are given. Next, the case where only a limited number of tie-lines are equipped with the controllers is briefly discussed.

5.1.1 All Tie-Lines Directly Controlled

As proposed in the general theoretical setting in Chapter 3, tie-line flows act as direct control inputs to the regional dynamics using FACTS devices. The additional control inputs are used to remove the structural singularity under the present local controls. Consider any administratively divided region within an interconnected system. If all components of the equivalent tie-line flows F_e are assumed to be the direct control variables with FACTS devices, model (4.56) can be viewed from a control design point as being of the form

$$\dot{z} = -l^T u + d \tag{5.1}$$

where $u = \dot{F}_e$ is the additional control variables for the administrative region, l^T is the participation factor vector, and $d = l^T D_P \dot{P}_L$ is the disturbance caused by the typically not measurable load variations $\dot{P}_L$. The equivalent tie-line flows F_e defined in (4.37) as a combination of flows into area generator nodes F_G and into the load nodes F_L are the new control variables to be designed according to specifications of the inter-area dynamics. If the inter-area dynamics are to meet particular response characteristics, including elimination of slow, persistent oscillations, specific flows F_G and/or F_L will need to be controlled. Notice that model (5.1) of inter-area dynamics can be seen as entirely control/disturbance driven. In the ideal case when all tie-lines are equipped with the additional control hardware capable of directly regulating real power flows, each area could directly regulate its inter-area variable z responsible for interactions with the neighboring systems by simply regulating it to the scheduled value z^{ref}, according to the general form

$$u = G_p e + G_i \int e dt + G_d \dot{e} \tag{5.2}$$

where $e = z - z^{ref}$ is the error of the inter-area variables, G_p, G_i and G_d are the gains corresponding to the proportional, integral and differential controls. It can be seen from (4.37) that the equivalent tie-line flows F_e corresponding to each specific area can be achieved by a variety of combinations of individual tie-line flows into the boundary generators, F_G, and into the boundary loads F_L. Eq. (4.37) can be used to decide on most effective locations of individual controllers which could achieve F_e needed to stabilize the inter-area variables to its scheduled value z^{ref}. Fig. 5.1 shows schematics of such controls on the 5-bus example.

For the purpose of illustration, let us take the simple form of the control with only a proportional control, i.e.

$$u = G_p(z - z^{ref}) \tag{5.3}$$

Under this control, the inter-area dynamical model in (4.56) becomes

$$\dot{z} = A_z(z - z^{ref}) + d \tag{5.4}$$

where $A_z = -l^T G_p$. Note that there is in general only one singular mode corresponding to each region. Therefore, the inter-area dynamics are in general a scalar system. The control gain vector G_p is chosen such that the scalar A_z is a negative number with sufficiently large magnitude to ensure the settling time. This is done easily because the left eigenvector l^T is roughly the vector with all 1's. The constant number z^{ref} determines the steady state value of the inter-area variable. Since the inter-area variable is basically the total area generation, modulo losses, the number z^{ref} will have a decisive effect on the steady state total area generation, and the steady state tie-line flows. It can be determined in a way such that the scheduled tie-line flows are achieved in steady state.

Let us use the same 5-bus example introduced in Fig. 4.3. Schematics of the direct tie-line controls on the 5-bus example are illustrated in Fig. 5.1.

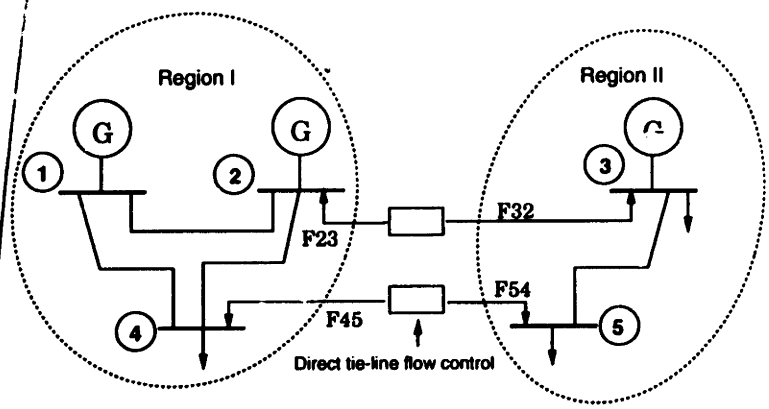

Figure 5.1: Direct Tie-Line Control

In this example, $F_G^I = [0 \;\; F_{23}]^T$; $F_G^{II} = F_{32}$; $F_L^I = F_{45}$; $F_L^{II} = F_{54}$. It follows that the inter-area variables are measurable directly through measurements of real power generations of the region. In this example, inter-area variables are given in the form

$$z^I = {l^I}^T P_G^I = P_{G1} + .9969 P_{G2} \tag{5.5}$$

$$z^{II} = {l^{II}}^T P_G^{II} = P_{G3} \tag{5.6}$$

The equivalent flows are calculated from Eq. (4.37) as

$$F_e^I = \begin{bmatrix} \frac{\partial P_{G1}}{\partial \delta_4} \\ \\ \frac{\partial P_{G2}}{\partial \delta_4} \end{bmatrix} [\frac{\partial P_{L4}}{\partial \delta_4}]^{-1} F_{45} - \begin{bmatrix} 0 \\ \\ F_{23} \end{bmatrix} \tag{5.7}$$

$$F_e^{II} = [\frac{\partial P_{G3}}{\partial \delta_5}][\frac{\partial P_{L5}}{\partial \delta_5}]^{-1} F_{54} - F_{32} \tag{5.8}$$

The inter-area dynamics of the system explicitly in terms of load disturbances are expressed from (4.56) as

$$\dot{z}^I = {l^I}^T (\dot{F}_e^I - \begin{bmatrix} \frac{\partial P_{G1}}{\partial \delta_4} \\ \\ \frac{\partial P_{G2}}{\partial \delta_4} \end{bmatrix} [\frac{\partial P_{L4}}{\partial \delta_4}]^{-1} \dot{P}_{L4}) \tag{5.9}$$

and

$$\dot{z}^{II} = l^{II\,T}(\dot{F}_e^{II} - [\frac{\partial P_{G3}}{\partial \delta_5}][\frac{\partial P_{L5}}{\partial \delta_5}]^{-1}\dot{P}_{L5}) \tag{5.10}$$

To illustrate by simulation the effects of direct tie-line flow control on the inter-area dynamics, let us first re-write the system model (4.42) in terms of voltage phase angle differences. For the same 5-bus example, one has

$$\dot{x} = Ax + N\dot{\Delta} + \dot{d} \tag{5.11}$$

where $\Delta = [\Delta_1 \quad \Delta_2]^T$, and Δ_1 is the phase angle difference across the line connecting nodes #2 and #3, Δ_2 the phase angle difference across the line connecting nodes #4 and #5. Matrix N is related to the tie-line impedances. $\dot{d} = [0 \; -D_P]^T\dot{P}_L$ is the system disturbance due to load variations. It can be shown that only the total (net) power generation of each region is important for inter-area dynamics regulation. Thus, one can assume $\Delta_2 = 0$ for simplicity. Assume further a lossless system, and define $u = -Z_1\dot{\Delta}_1$ as the control signal, where Z_1 is the impedance of the first tie-line. Using these notations, the open-loop dynamical model of the region (4.42) becomes

$$\dot{x} = Ax + bu + \dot{d} \tag{5.12}$$

where $b = [0 \;\; 0 \;\; 0 \;\; 1 \;\; 0 \;\; -1]^T$. The open loop inter-area dynamics take the form

$$\dot{z}^I = u + \dot{P}_4 \tag{5.13}$$

$$\dot{z}^{II} = -u + \dot{P}_5 \tag{5.14}$$

For this small power system the order of the full model (5.12) is three times the order of the local state space x_{LC} augmented by one, and the dimension of the model representing inter-area dynamics (5.13)-(5.14) is only two. In general, for realistic size

power systems the orders of the two models differ drastically. The proposed tie-line control design uses only the low-order model (5.13) or (5.14).

It is clear that once oscillations in either of z^I or z^{II} are suppressed, there will be no inter-area oscillations. This is obvious for the 2-area system, since inter-area oscillations are consequences of the power exchange between the two areas. As a result, control design can be done from either side. In this case, since $z^{II} = P_{G3}$, controlling y^{II} needs only one measurement (compared to two for z^I). To illustrate this, assume

$$u = G_p(z^{II} - z^{II\ ref}) \tag{5.15}$$

where $z^{II\ ref}$ is a constant target to be appropriately chosen. The closed-loop dynamics (5.13)-(5.14) for the inter-area dynamics have the form

$$\dot{z}^I = G_p(z^{II} - z^{II\ ref}) + \dot{P}_4 \tag{5.16}$$

$$\dot{z}^{II} = -G_p(z^{II} - y^{II\ ref}) + \dot{P}_5 \tag{5.17}$$

Clearly the stability requirement for z^{II} dictates $G_p > 0$.

Shown in Fig. 5.2 is the case for $z^{II\ ref} = .929$ and $G_p = .1$, and $z^{II\ ref}$ is chosen to be the steady-state value of net tie-line flow out of area II prior to adding the new controller. G_p is chosen such that the settling time for the inter-area dynamics is roughly 46 seconds. Initial conditions for all states are unity.

As a comparison, Fig. 5.3 shows responses of the system when there is no direct tie-line flow control. Clearly the slow mode corresponding to the inter-area oscillations is eliminated by the proposed control method.

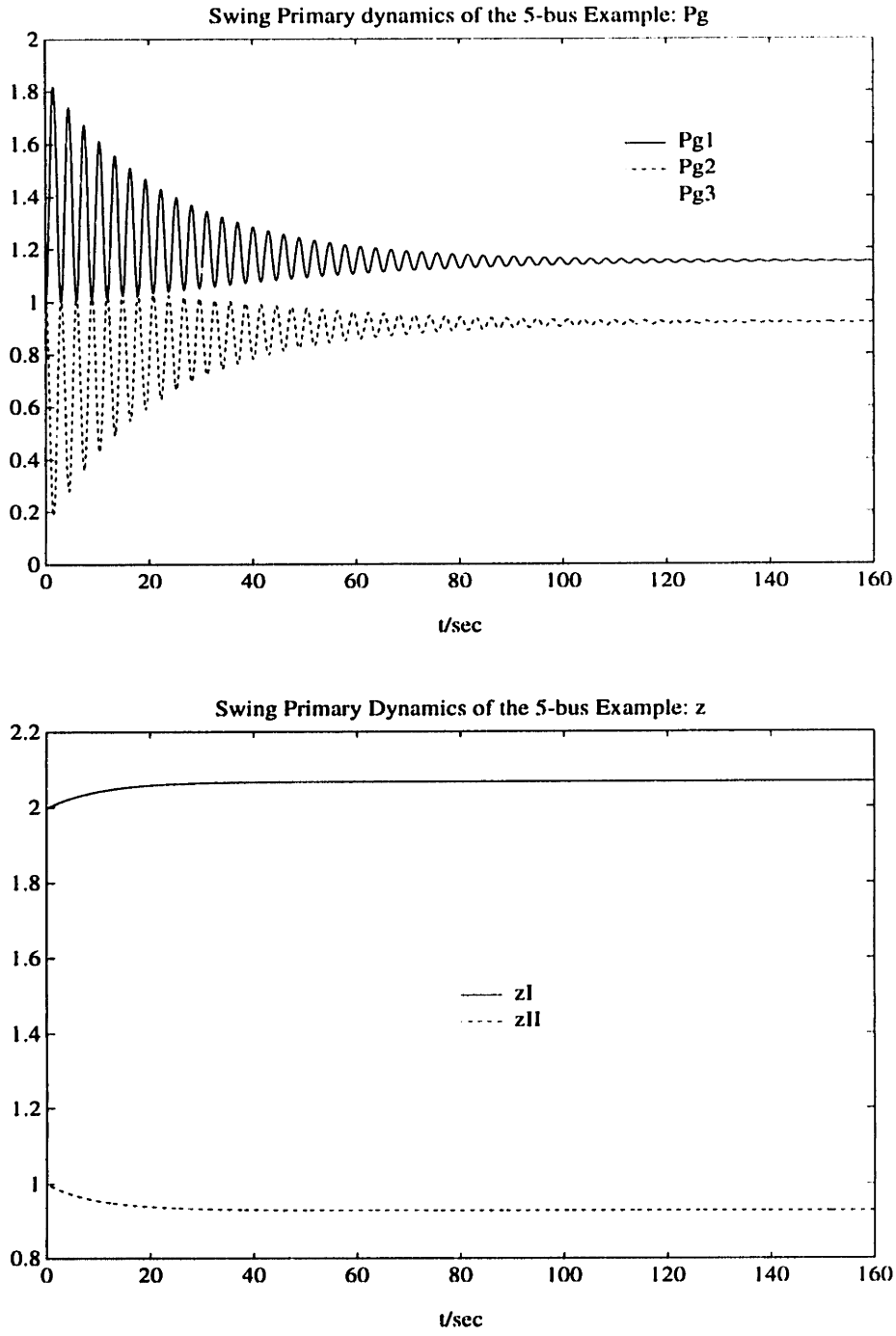

Figure 5.2: System Responses After Control

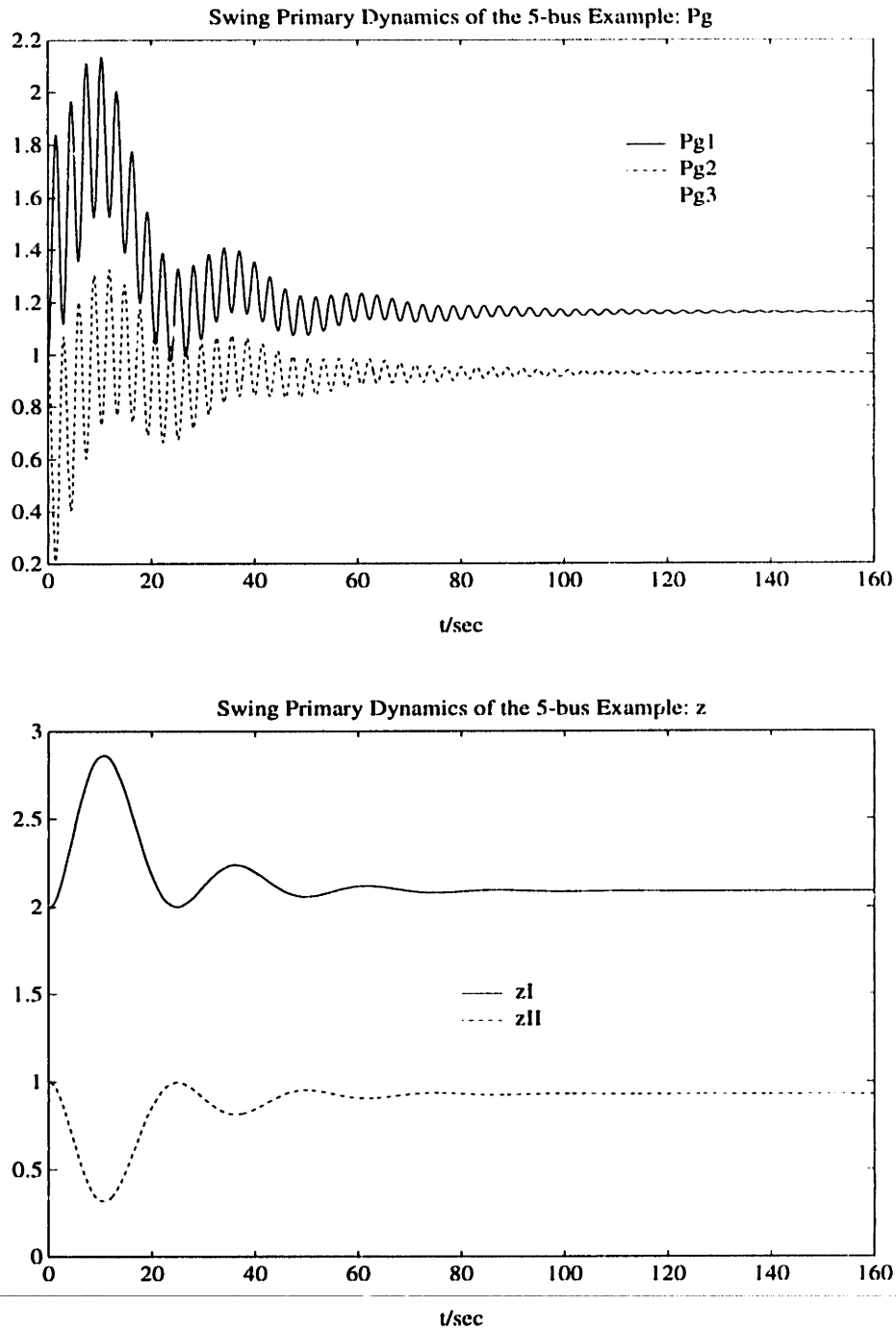

Figure 5.3: System Responses Before Control

5.1.2 Only A Subset of Tie-Lines Directly Controlled

The fact that the inter-area behavior is contained in the inter-area variable z provides some interesting opportunities for the application of the $\mathcal{H}_\infty$ design methodology to the use of FACTS devices for improved transmission grid response. In order to formulate the problem, we make the following assignments, to follow the notation of [27]. First, we separate the tie-line flows into a controlled group and an uncontrolled one, F_c and F_u, respectively, via a signed permutation matrix U:

$$\begin{bmatrix} F_G \\ F_L \end{bmatrix} = U \begin{bmatrix} F_u \\ F_c \end{bmatrix} \tag{5.18}$$

so that

$$F_e = F_G - D_P F_L = B_c F_c + B_u F_u \tag{5.19}$$

In addition, for the moment it will be assumed that $\dot{P}_L = 0$. We can then write the system model (4.42)as:

$$\dot{x} = Ax + B_c F_c + B_u F_u \tag{5.20}$$

$$z = Lx \tag{5.21}$$

or

$$\dot{x} = Ax + B_c u + B_u w \tag{5.22}$$

in the same notation of [27]. At this point the controlled output, the disturbance and the input have been defined adequately for the purposes of the $\mathcal{H}_\infty$ minimization. Appropriate weighting functions $W(j\omega)$ could be defined at the output and input, to tailor the behavior of the resulting controller. Emphasis could be placed on damping a particular inter-area mode, for example, by placing higher weighting at that frequency. Further research is needed to establish accurate solutions to this problem.

In summary, a new approach to regulating the inter-area dynamics via direct tie-line flow control using a reduced-order model relevant for the inter-area dynamics is proposed for the first time. The approach allows for a systematic control design regarding both best placement of the controllers and their control logic. It is shown that the inter-area dynamics can be regulated using standard designs for low-order linear dynamical systems. An underlying assumption that the new control does not destabilize the intra-area dynamics regulated by generator controls needs to be verified as part of the proposed design. The design is based on reduced decentralized measurement structure at each regional level. The physical devices for controlling the inter-area oscillations are assumed to be capable of directly controlling flows of transmission lines on which they are located. These FACTS devices are typically controlled by fast power electronic switchings.

5.2 Frequency Regulation

In this section, the simple discrete-time dynamical model for an administrative region within an interconnected power system derived in Chapter 4 is used for control designs at higher levels to offset the effects of neighboring regions and load disturbances. Control designs at the secondary level and tertiary level are studied separately.

5.2.1 Secondary Control

It is shown here that the fairly simple quasi-static dynamical model of the frequency is basic to developing decentralized secondary level controllers. The proposed secondary level control schemes provide a system-theoretic support for the ingenious concept of

AGC, and help to answer many open questions stated, for example, in [1], [28] and [29].

The main task of the secondary level control is to eliminate steady state deviations of frequencies at critical locations from their scheduled values. The secondary level control, often referred to as also the Load Frequency Control (LFC), is implemented by updating the reference values of governor speed-changers of the G-T-G sets participating at this control level at discrete time instance kT_s, $k = 0, 1, \cdots$. In practice LFC is often combined with generation scheduling needed to optimize total fuel cost for meeting a given load at each regional level. The simplest static optimization method for distributing total P_G among all generators according to their production costs needed to maintain the average frequency at each subsystem level is the Economic Dispatch method. This optimization task is generally not coordinated with LFC and this is known as one of the open issues in the LFC area [30]. The mathematical formulation of optimal LFC proposed in this thesis naturally overcomes this issue since the contribution of each generator to the average frequency is defined as dependent on the electric properties of the transmission network.

It is important to recognize that the secondary level control should keep operations at each regional level as autonomous as possible. In other words, the secondary level control should be designed so that deviations in mechanical outputs of the G-T-G sets are introduced to respond to the load deviations within the same region, while suppressing unintentional changes in real power tie-line flows. This requirement is based on the widely accepted Area Control Principle [7].

Control Design

The secondary level quasi-static discrete-time model for an administrative region within an interconnected system was derived in Eq. (4.125), and is repeated here as

$$\omega_G[k+1] = (I - \sigma K_P T_s)\omega_G[k] + (I - \sigma D)B_s u_s[k] + \sigma F_s[k] - \sigma D_P d_s[k] \qquad (5.23)$$

The secondary level control signal $u_s[k]$ is to cancel the effect of the load and tie-line flow variations to eliminate the steady state frequency deviations. Since the number of tie-lines is small, and tie-line flows are in general being monitored in practice, a new control logic on the secondary level to stabilize frequencies is proposed as follows:

$$u_s[k] = G_s(\omega_o[k] - \omega_o^{set}[K]) + H_s F_s[k] \qquad (5.24)$$

where $\omega_o^{set}[K]$ is the set value for the output frequencies defined in Eq. (4.129). The settings are changed on a longer time scale T_t by the tertiary level control to achieve best performance over the time horizon T_t. The gain matrices G_s and H_s are to be determined.

Under this control law, the closed-loop dynamics on the secondary level become

$$\omega_G[k+1] = (I - \sigma K_P T_s)\omega_G[k] + (I - \sigma D)B_s G_s(\omega_o[k] - \omega_o^{set}[K])$$
$$+ [(I - \sigma D)B_s H_s + \sigma]F_s[k] - \sigma D_P d_s[k] \qquad (5.25)$$

Using the output equation $\omega_o[k] = C_s\omega_G[k]$, one obtains

$$\omega_G[k+1] = A_s\omega_G[k] - (I-\sigma D)B_s G_s\omega_o^{set}[K] + [(I-\sigma D)B_s H_s + \sigma]F_s[k] - \sigma D_P d_s[k] \qquad (5.26)$$

where

$$A_s \triangleq (I - \sigma K_P T_s) + (I - \sigma D)B_s G_s C_s \qquad (5.27)$$

is the closed-loop system matrix of the secondary level dynamics.

The purpose of the additional term $H_s F_s[k]$ in the control law is to cancel the effect of tie-line flows from the neighboring regions, so that each region has effectively decoupled dynamics. The decoupling can be achieved if

$$(I - \sigma D)B_s H_s + \sigma = 0 \tag{5.28}$$

In general, both generator damping and the droop constants are very small, so that matrix $(I - \sigma D)$ is invertible. In this case to derive a unique solution for H_s from (5.28), one must require that B_s be nonsingular. From the structure of B_s defined in Eq. (4.122), it is clear that nonsingularity of B_s is equivalent to all generators participating in the secondary frequency control. In this case, $B_s = I$, and we can simply choose

$$H_s = -(I - \sigma D)^{-1}\sigma \tag{5.29}$$

to cancel the effect of neighboring regions. With this choice of H_s, the region under study looks as if it were disconnected from the rest of the system. The closed-loop dynamics of the region take on the form

$$\omega_G[k+1] = A_s\omega_G[k] - (I - \sigma D)B_s G_s \omega_o^{set}[K] - \sigma D_P d_s[k] \tag{5.30}$$

with no coupling among different regions occurring in this equation. Unless all generators participate in the secondary control, complete cancellation of tie-line flows in all generator frequencies is not possible. In this case, only partial cancellation for some state variables can be achieved.

The gain matrix G_s can be determined by specifying the desired closed-loop dynamics, as will be seen from the numerical example in the next section, or by formulating

an optimal control problem. A linear quadratic performance criterion for the region can be written as

$$J_s = \sum_{k=0}^{\infty} (\omega_o^T[k] Q \omega_o[k] + u_s^T[k] R u_s[k]) \tag{5.31}$$

for $Q = Q^T \geq 0$ and $R = R^T > 0$. Depending on the relative importance of quality of frequency regulation and fuel cost associated with specific G-T-G sets, the weighting matrices Q and R in the performance criterion will vary. The optimization, with respect to the secondary controls $u_s[k]$, determines the optimal gain G_s. The generalized formulation here allows for including frequencies of all generators and loads participating in LFC, instead of conventionally used criterion in terms of average frequency only [8], [18].

The performance criterion reflects specifications of the output variables at the regional level. It is sufficiently general to allow for specifying different frequency quality requirements at different individual generators and/or loads throughout the area. In light of the new regulatory constraints on operating power systems in this country, this feature is taking on a new importance. The jointly owned units, non-utility owned units and the large loads participating in the Demand-Side Management are potentially the points in the system whose requirements need such monitoring and would belong to the set $\omega_o[k]$. Note that it is possible to relate generator frequency variations ω_G as the output variable to which both primary and secondary controllers respond to the load frequency variations ω_L as the relevant operating specifications. Their relationship is the simple one derived in Eq. (4.127). This is not presently being done, but with the formulation proposed here it is fairly straightforward to do.

Note that formulations here clearly separate the governor controllers at the primary

level and the secondary level, while more conventional formulation combines the two levels into one PI controller which responds to the average frequency changes ω; the proportional part comes from the primary level, and the integral part form the secondary. Physically these are two different control loops, and the formulation in this thesis for the first time provides two separate mathematical models (4.42) and (4.125)-(4.129). A further comparison of the proposed formulation for the secondary frequency control with the ACE-based AGC implementation shows that the two formulations are actually consistent in terms of the measurement structure employed at this level. Notice, however, that the need for defining the frequency bias for the ACE signal is entirely eliminated with the proposed control scheme. The gain G_s is designed according to the desired frequency quality at different locations in the area ω_o. The gain H_s is a function of the transmission network parameters, and is computed according to (5.29).

A Numerical Example

The same 5-bus example given in Fig. 4.3 is used here to illustrate the proposed control scheme. To simplify the computation, we choose all three generators to participate in the secondary LFC control. In this case, $B_s = I$. The output variables are simply the three generator frequencies, so that $C_s = I$. The gain H_s is chosen according to (5.29). In this case, Eq. (5.30) are simplified to

$$\omega_G[k+1] = A_s\omega_G[k] - (I - \sigma D)G_s\omega_o^{set}[K] - \sigma D_P d_s[k] \tag{5.32}$$

with $A_s = (I - \sigma K_P T_s) + (I - \sigma D)G_s$. To further simplify calculations, the gain G_s is chosen such that the three generator frequencies have a decoupled identical dynamics.

i.e. $A_s = \lambda I$ for some scalar constant λ. With this choice of A_s, one simply obtains

$$G_s = (I - \sigma D)^{-1}[(\lambda - 1)I + \sigma K_P T_s)] \tag{5.33}$$

Fig. 5.4 shows the same linearly varying load at bus #4 as in Fig. 4.5, and the generator frequency responses to this load change with and without the secondary LFC. The scalar constant λ is chosen to be $\lambda = -1$. The figure clearly indicates that the proposed secondary control scheme eliminates the situation of frequencies inversely following the load variations, as shown in Fig. 4.5. It also significantly reduces the steady state frequency errors.

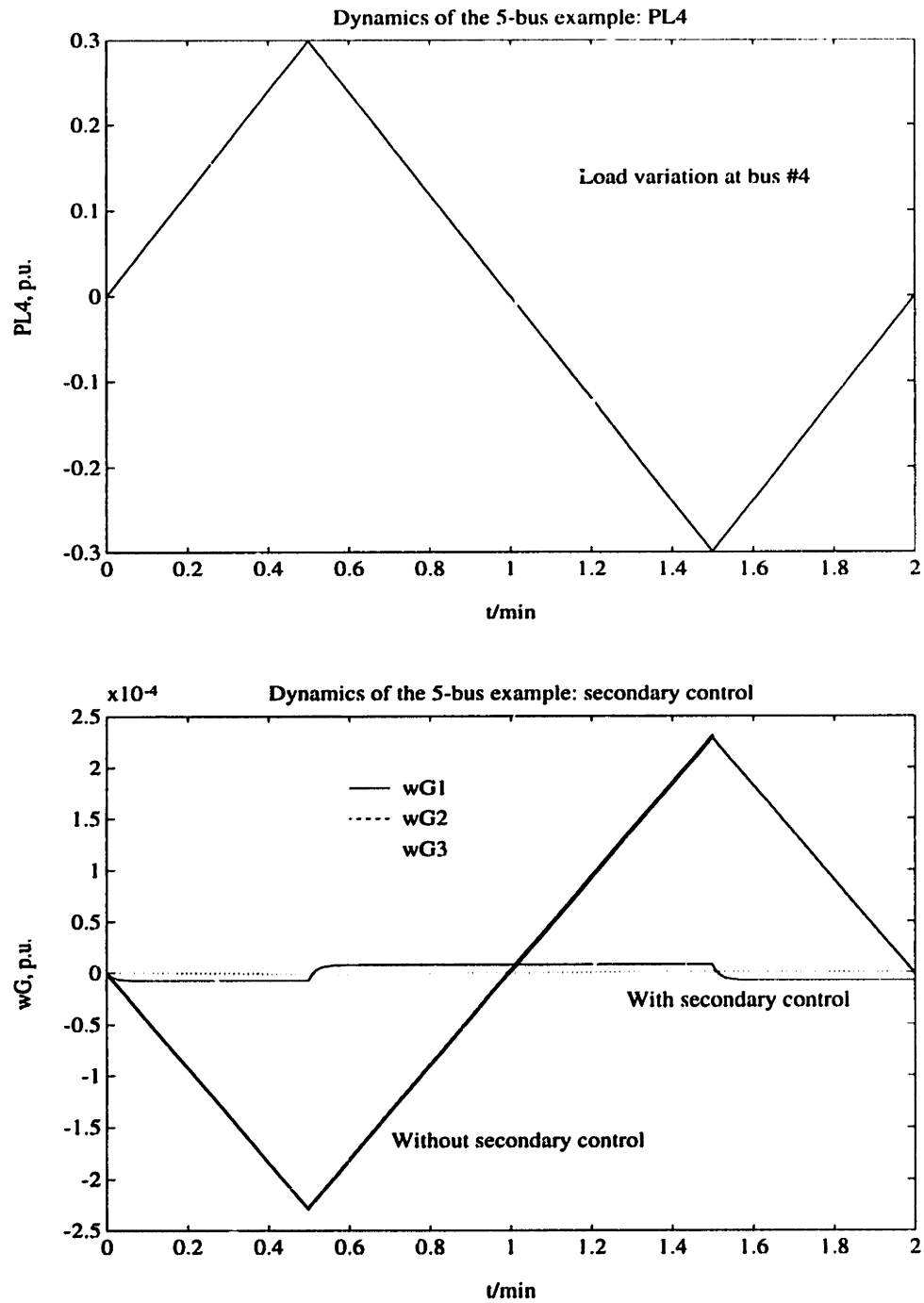

Figure 5.4: Load Variation and Frequency Response

5.2.2 Tertiary Control

As introduced in Chapter 3, the main goal of the tertiary real power/frequency control is to coordinate the regional secondary controllers in such a way that the global interconnected system operates in an optimal fashion. To be more specific, the goal of the tertiary level real power/frequency control is to optimally reschedule the tie-line flows in response to the load variations $P_L[K]$, while maintaining the system frequency. At present this task is carried out by agreement between several areas at a time when needed. The concept is referred to in [1] for example, as the "central AGC". The tertiary level is envisaged as particularly effective when the load-generation mismatch in a specific subsystem exceeds the capacity of the secondary level controls, which only stabilizes flows to their scheduled values. When certain control and/or output limits are reached in the stressed area the scheduled exchange should be changed to facilitate help from the neighboring areas. At present this is done in an asynchronous, ad-hoc manner. If this process were to become automated, it could be implemented much in the same way as the digital AGC, only at a much slower sampling rate T_t. We observe here that the presence of slow deviations in the average frequency documented in [28] can be explained by the inadequate tie-line flow schedules.

The relevant output variables at the tertiary level are the generator frequencies and the tie-line flows. There exists a potential conflict between the setting of tie-line flows and the system frequency, because the tie-line flows and frequency are dependent on each other. An arbitrary setting for the tie-line flows could cause the system frequency to be offset from the desired value (60 Hz in US, for example). This explains why in practice the regional control is proportional to the time integral of a combination of the

frequency deviation and the tie-line flow deviation, simply because when the tie-line flow setting is not properly chosen, neither of the deviations can be driven to zero. As a compromise, their combination is targeted to be vanished.

Conceptually, three types of implementation at this level can be envisioned: fully centralized, fully decentralized, and combination of the two. The fully centralized approach entitles the tertiary level decision maker to assign all set values of $y[K]$ for the feedback controllers so that a system-wide performance criterion is optimized. When the performance criterion is chosen as the total fuel cost needed to produce generation for meeting the anticipated load, the tie-line scheduling leads to what is known as a security constrained economic dispatch. The real advantage of the formulation proposed here is that it does not require full information structure, but only monitoring of critical load frequencies and tie-line flows, and is therefore amenable to full automation.

The fully decentralized approach preserves the right of subsystems to schedule generations at their level in order to meet its own performance criterion, and allows for the individual regions within the interconnected system to compete and make their own decisions. The dynamical properties of the rest of the system are not assumed to be known for the individual regions. In this case, each region measures the tie-line flows into it from the neighboring regions, and, based on the measurements, determines the control strategies to optimize its own performance criterion. In this case, each region is completely independent and assumes no dynamical properties of the other regions.

The combined centralized/decentralized approach to the tertiary level scheduling preserves the decentralized structure of the control implementation, but assumes structural properties of the other regions on the interconnected system. In other words,

each region has the knowledge of dynamical structures of the other regions. Based on the shared knowledge of the dynamical structures of other regions and on-line measurements of the tie-line flows, each individual regions make their decisions to optimize their own performance criteria. Intuitively, this approach would result in a system-wide performance in between the fully centralized and fully decentralized implementations. This approach can be formulated into the framework of theoretical games.

In the tertiary control automation, one of the most important relationships is the one which relates the frequency schedules to the tie-line flow schedules. The relationship between the system frequency and tie-line flows helps the proper setting of tie-line flows such that the system frequency is kept at the desired value and the global system as a whole is operating in an optimal fashion. It presents an essential tool for consistent optimal scheduling of the tie-line flows.

However, this important relationship is still an open research question. It is not easily derived because the secondary level dynamical model (4.125) is not a control-driven model due to the droop characteristics of the generator primary control. As a result, state variables can still evolve with time even when the system is subject to no tie-line flows and disturbances, as a consequence of the generator dynamics. We believe that the structurally-based aggregation method proposed here can be used and extended to solve this problem. Research effort should be directed to developing meaningful tertiary level control schemes and comparing the new control schemes to the already existing AGC. More involved problems such as point-to-point real power wheeling need further extensive research. However, the new structural modeling and aggregation approach proposed in this thesis provides a basis for most sophisticated

frequency regulation schemes of present and future power systems under the truly dynamical operating mode.

5.3 Summary

This chapter presents a new hierarchical control design concept for the real power/frequency dynamics of power systems, based on the structural models developed in Chapter 4. The main goal of the direct tie-line control based on FACTS devices is to eliminate the structural singularity associated with the real power/frequency dynamics. Systemwide frequency regulation on longer time scales is also discussed. Simulations show that the new control scheme significantly reduces frequency fluctuations in the presence of load variations.

Part III

Reactive Power/Voltage Control

Chapter 6

Voltage Dynamics Modeling

6.1 Introduction

The work on reactive power/voltage dynamics presented in this thesis is motivated by the practical need to regulate load voltages over mid-term and long-term time horizons according to a specified performance by changing generator voltage settings. While the voltage control of an interconnected large-scale power system is widely recognized as a very important problem, its basic formulation and solutions are often utility specific. Most often the voltage control is viewed as an entirely static problem, whose solution is identical to a centralized open-loop optimization-based reactive power/voltage management. The most common tool for solving this optimization problem is the OPF based algorithm. This approach computes changes in generator voltages needed to regulate load voltages on the entire interconnected system. It assumes availability of the full information of the system and requires a large amount of data which is typically not available when the system is experiencing unusual operating conditions. Moreover, this approach does not provide an easy balance between coordination and competition, which is of practical interest in coordination of regions.

A second approach to voltage control coordination relies on decomposition of a large system into regions and an on-line decentralized closed-loop reduced information structure for controlling regions. For instance, the French power system has been committed to a full automation of system-wide voltage regulation while employing an intuitive reduced information structure at the regional level. The dynamical model of voltage on mid-term and long-term time horizons, as is shown in this chapter, is a load variation and control-driven model, in the sense that any variations in voltages with time are caused only by the control signal or the disturbances. It will be shown in Chapter 7 of this thesis that for this kind of control-driven models, only certain number of states can be fully controlled. The maximum number of states that can be fully controlled is equal to the number of controls. Therefore only at most the same number of load voltages as the generators can be independently controlled. These states chosen to be independently controlled are referred to as the *pilot load voltages*. The pilot load voltages are controlled within each region by regional controllers, assuming that neighboring regions have negligible effects. In this case the responsibility for coordinated voltage regulation is shared among regional closed-loop controllers or the secondary voltage controllers, and the operators at the national control center or the tertiary level.

This work in the thesis was largely sponsored by the Electricité De France (EDF). As the French power network has become increasingly meshed during the past decade and is operated closer to the prespecified voltage limits, a tertiary level coordination of the regional secondary voltage controllers has become critical to improve the security and economics of the entire system. Under mild system changes, it is often sufficient to rely on the operator's expertise to provide coordinating signals from the national level.

If time permits and if the results of the state estimation are available, the operator could employ computer tools such as OPF to assist him in the decision making. However, when the interconnected network experiences unusual reactive power deficiency, typically in one region at a time, it is important to provide the dispatchers quickly with adequate coordination strategies.

The main goal of this part of the thesis is to develop new concepts for coordination of secondary voltage controllers at the national level which preserves a reduced, pilot point-based information structure. As in the frequency dynamics case, a structurally-based decomposition approach is taken to derive the regional voltage dynamical model consisting of local dynamics of individual devices and the network coupling. A remarkable feature is that although the reactive power/voltage control has a parallel structure to the real power/frequency control, these two models represent fundamentally different systems. As shown in Part II, the real power/frequency dynamics are structurally singular. It is, however, not the case for reactive power/voltage dynamics, unless a specific numerical singularity occurs. The structurally singularity of real power/frequency dynamics is due to the fact that the real power across a transmission line depend on the phase angle difference across the line only. A constant offset on both angles makes no difference for real power transfer. However, the reactive power across a transmission line is not a function of the voltage difference only, so that a constant offset on both voltages does change the reactive power flow. Due to the nonexistence of singular modes in voltage dynamics, there is no need for a direct flow control, as proposed in the frequency case, except for unusual operating conditions in which voltage dynamics become numerically singular.

On the other hand, a different type of structural singularity occurs at the secondary level quasi-static control-driven voltage models due to insufficient number of controls. Interaction variables associated with this type of structural singularities are defined as the *quasi-static interaction variables.* Both the continuous interaction variables in the frequency dynamics and the quasi-static interaction variables of voltage dynamics represent singular modes of the system evolving at different time scales. The most important property of these two kinds of singularities is that they are structurally inherent rather than numerically coincident, as already shown for the case of frequency dynamics. These structural singularities on different time scales reveal most fundamental dynamical properties of power systems. An important breakthrough as a result of the structural decomposition is that the interaction variables defined here represent physically measurable variables, such as reactive tie-line flows. This provides a basis for automated feedback control designs because interaction variables are physically measurable.

It should be emphasized that, in contrast to many standard techniques on system decomposition which assume weak or sparse coupling among the regions, the structural approach developed in this thesis does not depend on this assumption, as already seen in the case of real power/frequency dynamics. The decomposition is entirely based on the structural properties of the system. In the particular case of weak interconnections, the structural interaction variables defined here can be shown to represent the slow dynamics obtained using the singular perturbation method.

6.2 Modeling

Having introduced structurally based models for real power/frequency control at different levels of hierarchy in the previous chapters, we revisit the present state-of-the-art in voltage control via generators. There are many reactive devices present in modern electric power systems. To avoid confusion, we consider only reactive power scheduling of generators. It is shown here that an effective formulation of voltage control at all levels lends itself naturally to exploiting the same structural properties as in designs of real power/frequency controls of large-scale electric power systems. This fact appears not to have been recognized in the literature, mainly because of the somewhat inaccurate notion that a single average frequency can be associated with each subsystem, while voltages could be quite non-uniform throughout a voltage control area. The need for more refined frequency measurements and specifications throughout each subsystem is described in the previous chapters, and a model formulation which "unbundles" frequencies at the locations of interest is proposed as more realistic, particularly when considering regulatory changes imposed on operating power systems in the future. Depending on electric characteristics of each subsystem non-uniformity in frequency deviations could be significant. Formula (4.32) explicitly defines how frequencies vary at specific locations in the system as a function of real power generation and demands.

The second fundamental issue in comparing the concepts for frequency and voltage control automation is the issue of reactive losses which are much larger than the real power losses. A closer look into the systems oriented literature in the area of real power/frequency dynamics quickly reveals that the most elegant derivations are proposed under the assumption of no real power losses. It is expected that attempts to

extend such existing formulations for real power dynamics to reactive power will not succeed. It is with this issue in mind that we emphasize that the formulation proposed here does not make any assumptions regarding losses, i.e., the linearized real and reactive power flows are not assumed to be lossless. Since the entire concept proposed in this thesis is not dependent on the above two "facts", which create potential qualitative differences in control concepts for real and reactive power, we suggest a structurally based concept for voltage control automation which is parallel to the real power/frequency control introduced in Part III of this thesis. Prior to describing technical details, it is important to observe that in Part II of the thesis we have established a structural approach to support an automated control scheme of LFC already operating. On the other hand, while primary level voltage controllers are fully automated, the secondary level voltage automation based on a parallel principle to LFC is being implemented in France and Italy only. Moreover, a tertiary level voltage automation has not yet been implemented anywhere in the world. We propose, first, that the secondary level voltage control automation can be improved relative to the existing implementations in France and Italy [16], by taking into account the effects of neighboring areas at each subsystem level. Second, the tertiary level voltage coordination can be fully developed following general parallelism with the AGC.

To establish a background for the automatic voltage control, let us recognize that the structural settings for deriving models of voltage dynamics are identical to the ones exploited in real power dynamics illustrated in Figure 4.1. Primary voltage dynamics defined by the electromagnetic changes at each generator and the excitation system controls can be expressed in the same structural form as the frequency dynamics in (4.42) by introducing local state variables. These local state variables define the local

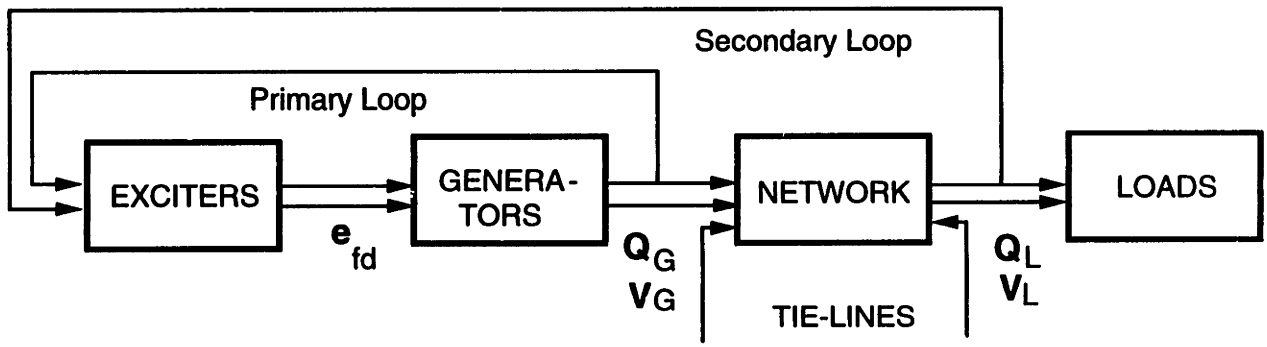

Figure 6.1: Typical Structure of Reactive Power/Voltage Control

primary voltage dynamics of each generator-excitation system in response to terminal voltage deviations from its reference value.

6.2.1 Local Dynamics

The general structure of reactive power/voltage control of power systems can be represented by Fig. 6.1.

The excitation system controls the field voltage input to the generator using the error signal between the measured generator terminal voltage and a given reference value. The goal is to maintain the generator terminal voltage at the prespecified setting.

As in the real power/frequency control case, the dynamics of all the generators are coupled together through the transmission network via the reactive power outputs of all generators. The transmission network imposes an algebraic constraint on the total reactive power injections into the network, and couples all the generator power outputs together. It also couples generators to the loads.

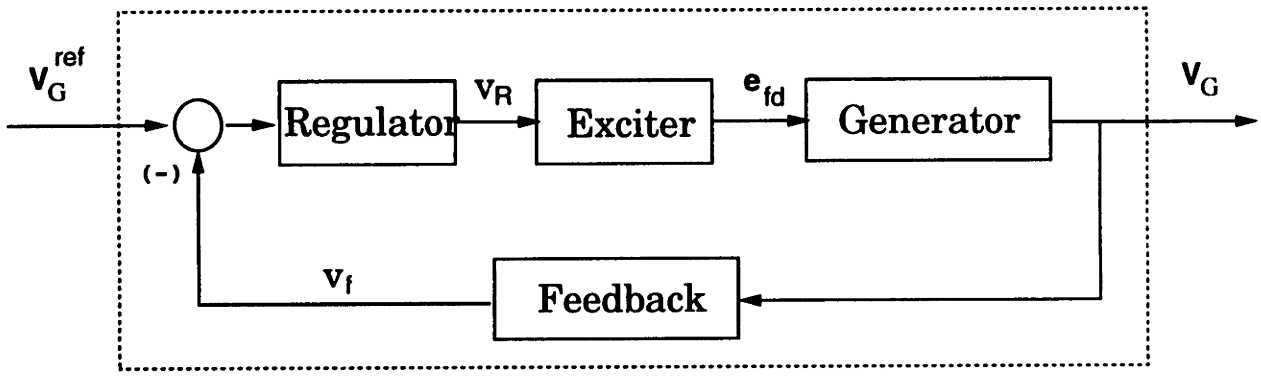

Figure 6.2: A Typical Excitation System

Let us first consider the local dynamics of individual excitation system and generator set. A schematic block diagram for the excitation control system is shown in Fig. 6.2.

A typical excitation system consists of the regulator, exciter and the excitation feedback compensator. Detailed modeling of dynamics of each component and notations can be found in [31] [13]. The regulator is described by

$$T_a \dot{v}_R = K_a v_f - \frac{K_a K_f}{T_f} e_{fd} - v_R - K_a (V_G - V_G^{ref}) \tag{6.1}$$

where e_{fd} is the field voltage of the exciter, V_G the generator terminal voltage, and V_G^{ref} the reference value for the generator terminal voltage.

The exciter dynamics can be modeled in the following form

$$T_e \dot{e}_{fd} = -(K_e + S_e) e_{fd} + v_R \tag{6.2}$$

Generator dynamics are typically given by

$$T'_{d0} \dot{e}'_q = -e'_q - (x_d - x'_d) i_d + e_{fd} \tag{6.3}$$

neglecting the effects of damper winding, i.e., $e'_d = 0$. where i_d is the reactive current

out of a generator. Current component i_d is also a function of the states, known as the network constraint. Under the assumption $e'_d = 0$, it is obtained

$$i_d = \frac{Q_G}{e'_q} \tag{6.4}$$

since $Q_G = e'_q i_d - e'_d i_q$.

Finally the compensator is of the form

$$T_f \dot{v}_f = -v_f + \frac{K_f}{T_f} e_{fd} \tag{6.5}$$

Define the local states of each generator as

$$x_{LC} = [v_R \;\; e_{fd} \;\; e'_q \;\; v_f]^T \tag{6.6}$$

One can write Eqs. (6.1)-(6.5) together in a nonlinear state space form as

$$\dot{x}_{LC} = f_{LC}(x_{LC}, Q_G, V_G^{ref}) \tag{6.7}$$

recognizing that $V_G = e'_q$ since $V_G = \sqrt{e'^2_q + e'^2_d}$ and $e'_d = 0$. This model of local dynamics is of the general form (2.9). In this model, the generator reactive power output Q_G is the coupling variable x_{CP} in the general local dynamics model (2.9). This variable couples dynamics of all generators connected through the network. This coupling, known as the network constraints, are discussed next.

6.2.2 Network Constraints

As in the real power/frequency case, generator reactive power outputs Q_G are determined by the interactions with other generators and loads via the transmission network. Derivations here are very similar to those for the real power/frequency dynamics. Consider any administrative region with m generators and n loads within an interconnected

system. The complex power constraint for the transmission network is stated in (4.21). The real part of the equation, i.e. the real power/frequency constraint, has been discussed in Part II. The imaginary part is the reactive power/voltage constraint. Similar to (4.22), let us write the imaginary part of (4.21) as

$$Q^N = Q^N(\delta, V) \tag{6.8}$$

where

$$\delta \triangleq \begin{bmatrix} \delta_G \\ \delta_L \end{bmatrix} \quad \text{and} \quad V \triangleq \begin{bmatrix} V_G \\ V_L \end{bmatrix} \tag{6.9}$$

are the nodal voltage angles and magnitudes. Define the reactive power tie-line flows from the neighboring areas into all generator nodes, and all load nodes, as

$$F_G \triangleq \begin{bmatrix} F_G^1 \\ \vdots \\ F_G^m \end{bmatrix} \quad \text{and} \quad F_L \triangleq \begin{bmatrix} F_L^1 \\ \vdots \\ F_L^n \end{bmatrix} \tag{6.10}$$

Note that throughout Part III of the thesis, we use F_G and F_L to represent the reactive power tie-line flows. Then it is obvious that $Q_G^N = F_G + Q_G$. The network constraints for the real power balance can be further written as

$$Q_G^N(\delta, V) = F_G + Q_G \tag{6.11}$$

Same relationship is true for the load buses, i.e.

$$Q_L^N = F_L - Q_L \tag{6.12}$$

the network constraint (6.8) at the load nodes are expressed as

$$Q_L^N(\delta, V) = F_L - Q_L \tag{6.13}$$

assuming again that the positive direction for tie-line flows is the injection into the network, and the positive direction for loads is leaving the the network. Similar to the

real power/frequency case, we separate reactive power injections into the part of the injection from the generators or loads and the part from the interconnecting tie-lines with the neighboring regions.

These represent algebraic constraints to the network variables like bus voltage vector V. They add severe difficulties to the local dynamical models in differential equations. To eliminate the algebraic constraints, we take differentiation on the algebraic constraints. Here the real/reactive power decoupling assumption is made again. In terms of reactive power relations, the decoupling assumption is expressed as

$$\partial Q^N / \partial \delta = 0 \tag{6.14}$$

Under this assumption, differentiating the above constraints yields

$$\dot{F}_G + \dot{Q}_G = J_{GG}\dot{V}_G + J_{GL}\dot{V}_L \tag{6.15}$$

$$\dot{F}_L - \dot{Q}_L = J_{LG}\dot{V}_G + J_{LL}\dot{V}_L \tag{6.16}$$

where

$$J_{ij} = \frac{\partial Q_i^N}{\partial V_j}, \quad i,j = G,L \tag{6.17}$$

are the Jacobian matrices evaluated at the given equilibrium operating point. Assuming J_{LL} to be invertible under the normal operating conditions, we define one of the most important matrices associated with a transmission network

$$C_V = -J_{LL}^{-1} J_{LG} \tag{6.18}$$

to express voltage deviations at loads V_L in terms of voltage deviations at generators V_G and fluctuations in load power. It follows from (6.16) that

$$\dot{V}_L = C_V \dot{V}_G + J_{LL}^{-1}(\dot{F}_L - \dot{Q}_L) \tag{6.19}$$

where

$$V_G \triangleq \begin{bmatrix} V_G^1 \\ \vdots \\ V_G^m \end{bmatrix} \tag{6.20}$$

Relationship (6.19) defines the explicit dependence of load voltages on generator voltages determined by the network constraints. Combining (6.19) and (6.15), and defining the other two most important matrices associated with a transmission network

$$K_Q \triangleq J_{GG} + J_{GL}C_V \tag{6.21}$$

and

$$D_Q \triangleq -J_{GL}J_{LL}^{-1} \tag{6.22}$$

result in

$$\dot{Q}_G = K_Q\dot{V}_G - \dot{F}_e + D_Q\dot{Q}_L \tag{6.23}$$

Here F_e represents effective reactive tie-line flow as seen by each generator and is defined as

$$F_e \triangleq F_G + D_Q F_L \tag{6.24}$$

Eq. (6.23) defines the relationship among the generator reactive power outputs Q_G, generator voltages, the tie-line flows into the subsystem, and the reactive load variations, through the network characteristics specified by the two important matrices K_Q and D_Q.

It should be noted that any (portion of) network is fully characterized by the three matrices (K_Q, C_V, D_Q), with K_Q reflecting the effect of the generator frequencies on the generator real power outputs, C_V relating the generator frequencies to the load frequencies, and D_Q representing different electrical distances of loads at different locations seen by the generators. It is easily shown that matrix K_Q does not have the

structural singularity associated with matrix K_P for the real power/frequency dynamics, although under extreme operating conditions numerical singularities are possible.

6.2.3 Structural Dynamical Model

Local dynamical model (6.7) and the network relationship (6.23) combine to form the structural dynamical model for reactive power/voltage of the administrative region. Define the state variables of the region as in (2.18). Voltage dynamics of the region can be written in a standard nonlinear state space form as

$$\dot{x} = f(x, V_G^{ref}, \dot{F}_e) \tag{6.25}$$

where the nonlinear function f is the combination of (6.7) and (6.23). This model is of the general form (2.20).

In contrast to the real power/frequency dynamics, the network matrix K_Q is in general not singular. As a result, the voltage dynamics as described in (6.25) are not structurally singular. Because of this nonsingularity, inter-area voltage oscillations in general do not exist, except in the case of numerical singularities. Also there is in general no need for direct tie-line flow control, as in the frequency case to remove the structural singularity. Furthermore, there do not exist the interaction variables as defined in (2.2). However, as will be discussed next, there exists another type of quasi-static interaction variables on the secondary level, which reflect a different type of structural singularity – insufficient number of controls for the quasi-static voltage dynamical model.

6.3 Quasi-Static Voltage Model

Typical designs of the excitation system yield very fast transient dynamics, relative to the secondary time scale T_s. A quasi-static voltage dynamical model can be derived when the reference value V_G^{ref} is updated at discrete time instance kT_s. FIRST set all derivatives in (6.25) to zero. This leads to an algebraic equation

$$f(x, V_G^{ref}, 0) = 0 \text{ at } kT_s \tag{6.26}$$

The linearized equation for this is

$$A\delta x + B\delta V_G^{ref} = 0 \text{ at } kT_s \tag{6.27}$$

where A is nonsingular. This nonsingularity determines a unique relationship between the generator voltage V_G, which is part of the state variables, and the reference value V_G^{ref}. For simplicity, let us simply write

$$\delta V_G[k] = \alpha\, \delta V_G^{ref}[k] \tag{6.28}$$

In other words, generator terminal voltages are directly proportional to the reference values.

The secondary level control of the reactive power/voltage is to regulate load voltage profiles with generator terminal voltages. To derive the relationship between load voltages and generator terminal voltages, let us consider any administrative region within an interconnected system. From the network relationship (6.19) derived in the previous section one can obtain the following quasi-static discrete-time model, by integrating (6.19) from the secondary time instance kT_s to the next instance $(k+1)T_s$,

$$V_L[k+1] - V_L[k] = C_V(V_G[k+1] - V_G[k]) + J_{LL}^{-1}[(F_L[k+1] - F_L[k])$$

$$- (Q_L[k+1] - Q_L[k])] \tag{6.29}$$

As in the frequency control case, let us define the secondary corrective control signal

$$u_s[k] \triangleq V_G[k+1] - V_G[k] \tag{6.30}$$

the tie-line flow changes

$$F_s[k] \triangleq F_L[k+1] - F_L[k] \tag{6.31}$$

and the secondary level load disturbances

$$d_s[k] \triangleq Q_L[k+1] - Q_L[k] \tag{6.32}$$

Eq. (6.29) then becomes

$$V_L[k+1] - V_L[k] = C_V u_s[k] + D_s(F_s[k] - d_s[k]) \tag{6.33}$$

with $D_s \triangleq J_{LL}^{-1}$. This is the desired secondary level discrete-time dynamical model for a region within an interconnected system.

To write this in standard control notation, let us define the secondary level states as

$$x[k] \triangleq V_L[k] \tag{6.34}$$

Then equation (6.33) is rewritten as

$$x[k+1] - x[k] = C_V u_s[k] + D_s(F_s[k] - d_s[k]) \tag{6.35}$$

where $F_s[k]$ and $d_s[k]$ act as the disturbances to the system with control $u_s[k]$. The difference between $F_s[k]$ and $d_s[k]$ is that the flow can be measured, while the loading variations are rarely measured in practice. They are either estimated or simply treated as a real disturbance.

It is emphasized that the discrete-time dynamical model (6.35) is a control- or disturbance-driven model, in the sense that, if all disturbances (including tie-line flows) are not present, and the corrective control is inactive, then $x[k] = \text{constant}, \forall k$. Clearly control actions are needed to bring the system (6.35) back to the nominal operation, if the system is perturbed away from the nominal operation by disturbances.

It is also worth noting that the secondary level control is an implicit integral control. We see from (6.30) that the secondary level control $u[k]$ is a corrective signal, i.e. it updates the previous generator voltage $V_G[k]$ to get the next value. This corrective action is equivalent to an integral control. It is this implicit integral control that can eliminate steady state errors in the load voltages caused by system disturbances.

6.4 Quasi-Static Interaction Variables

The secondary quasi-static voltage dynamical model for any region explicitly in terms of the tie-line flows has been derived as

$$x[k+1] - x[k] = C_V u_s[k] + D_s(F_s[k] - d_s[k]) \tag{6.36}$$

where $x[k] = V_L[k]$ is the state vector consisting of all load voltages. The dimension of the sensitivity matrix C_V is $n \times m$, where n being the number of load buses, and m the number of generator buses that participate in the secondary level regulation. In general it is true that $n > m$, i.e. the number of load buses is larger than the number of generator buses participating in the secondary level control.

Under the condition of $n > m$, one can easily verify that the closed-loop system using any feedback control is singular, because matrix C_V has maximum rank of m.

This structural singularity due to the relative numbers of controls and states. This is a general property for any control-driven systems. In exploiting this structural singularity of the quasi-static voltage dynamics, we first give the following definition.

Definition 6.1 (Quasi-Static Interaction Variables) *Any linear combination of the states, $z[k] = Tx[k]$, $T \neq 0$, that satisfies*

$$z[k+1] - z[k] \equiv 0, \quad \forall k \tag{6.37}$$

for any secondary control actions, and in the absence of interactions among regions and the disturbance, i.e., $F_s = 0$ and $d_s = 0$, is defined as the quasi-static interaction variable of the administrative region under study.

The same notation as the continuous interaction variables is used here to indicate the same characteristics of the two. The meaning is clear from the context under study. Similar to the continuous interaction variables defined in Part II, the quasi-static interaction variables do not vary with time when interconnections are removed and load disturbances are not present. For the interconnected system, therefore, any variations of the interaction variables with time are entirely due to the interactions among regions or load disturbances. It should be noticed from the definition that the interaction variables are not unique. In fact, any combinations of the interaction variables are still interaction variables.

Let us derive the condition for the transformation matrix T. Combining (6.37) and (6.36) yields

$$z[k+1] - z[k] = T(V_L[k+1] - V_L[k]) = TC_V u_s[k] + TD_s(F_s[k] - d_s[k]) \tag{6.38}$$

Under the conditions in the definition, $F_s[k] \equiv 0$ and $d_s[k] \equiv 0$, we arrive at

$$z[k+1] - z[k] = TC_V u_s[k] \tag{6.39}$$

In order to have $z[k+1] - z[k] \equiv 0$ for any control $u_s[k]$, matrix T must satisfy

$$TC_V = 0 \tag{6.40}$$

This is the desired equation for calculating T. Note that matrix C_V has maximum rank $m < n$, and therefore, equation (6.40) has nonzero solutions for T. It is quite easy to solve T from (6.40), since it is a simple algebraic equation, and can be solved with Gauss Elimination method. The need for eigenstructure analysis is completely avoided.

Note that the definition for interaction variables is for any secondary control, meaning that the interaction variables are independent of the specific secondary control. Equivalently, the secondary control cannot affect the interaction variables. Any variations of the interaction variables are uniquely due to the interactions with other regions or the load variations. The matrix T, as a result, will not be dependent on the specific form of the secondary control.

An interesting difference between the continuous and quasi-static interaction variables can be noted. For any single region, the dimension of the continuous interaction variable is in general one, because the system is normally rank-deficient by one. For the quasi-static interaction variables, as shown above, the dimension is the difference between the number of states and that of controls. This difference indicates the fundamentally different causes for the two types of interaction variables.

Once the interaction variables are determined from (6.40), one can further derive

the dynamical model for these interaction variables. Eqs. (6.38) and (6.40) simply lead to

$$z[k+1] - z[k] = TD_s(F_s[k] - d_s[k]) \tag{6.41}$$

This is the desired dynamical model for the interaction variables. This simple model relates the interaction variables to the tie-line flows and load variations. It is of crucial importance for the secondary voltage control and tertiary level coordination, as is discussed in more detail in the next chapter.

Notice that the definition for interaction variables does not assume numerically weak interconnections. Rather, it reflects a structural property of the system, different numbers of the states and controls. It is interesting to relate the interaction variables defined above to the slow variables in singular perturbation analysis when the interconnections are indeed weak. It is easily seen from the interaction dynamical model (6.41) that, in the weak interconnection case, the interaction variables do vary more slowly than the rest of the states. One can rigorously prove that, in the weak interconnection case, the interaction dynamics derived here will be the slow subsystem in the singular perturbation analysis.

Let us now demonstrate the interaction variables and their properties by a small 9-bus example network given in Fig. 6.3.

Region I consists of buses #1 and #7, the rest is region II. The pilot points are buses #1, #2, and #3. The feedback gain G_s is designed such that the pilot voltages settle exponentially in 3 minutes. The load is assumed to have a step increase at bus #5 at $t = 0$; thus the effect of $d_s[k]$ is seen in changes of the initial conditions for all the load voltages. This small example will be used throughout to demonstrate the

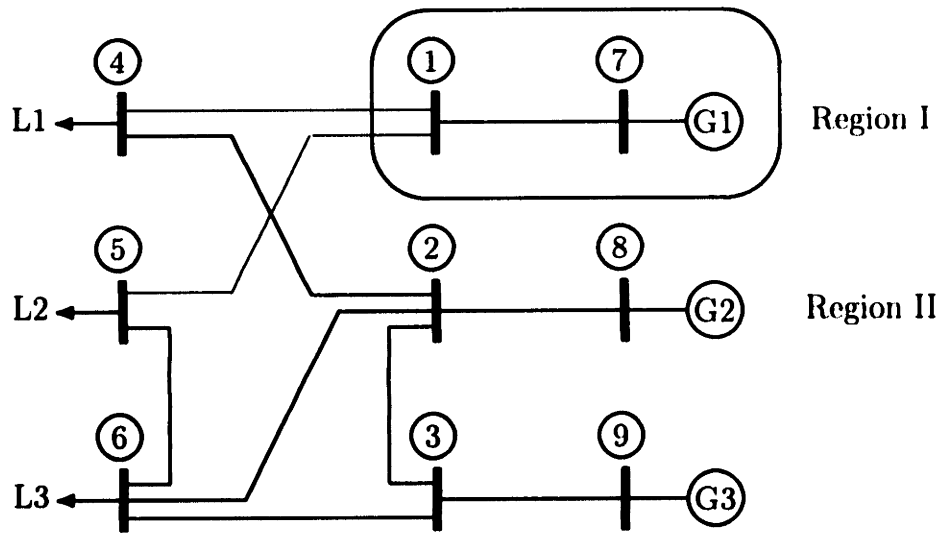

Figure 6.3: The 9-Bus Example

developed concepts. Simulations for the EDF network will also be given, but only for the purpose of illustrating the tertiary level control. The numerical data used in the simulations for the 9-bus system are given in Table 6.1.

Line Parameters										
	#1-4	#1-5	#1-7	#2-3	#2-4	#2-6	#2-8	#3-6	#3-9	#5-6
b	5	7	7.69	15.67	21.55	7.19	8.33	12.49	10	9.8
g	0	.15	0	0	1.02	.34	0	.31	0	0
Nominal Operating Point										
	#1	#2	#3	#4	#5	#6	#7	#8	#9	
V	1	1	1	1	1	1	1	1	1	
δ	0	0	0	0	0	0	0	0	0	

Table 6.1: Per Unit Data of the 9-Bus Example

The sensitivity matrix for region I, which has only one generator bus and one load bus, is simply

$$C_V^I = 1 \tag{6.42}$$

The sensitivity matrix for region II, which has two generator buses and five load buses,

is calculated as

$$C_V^{II} = \begin{bmatrix} .55 & .45 \\ .37 & .63 \\ .55 & .45 \\ .44 & .56 \\ .44 & .56 \end{bmatrix} \tag{6.43}$$

Let us use condition (6.40) to calculate the matrix T. For region I, condition $T^I C_V^I = 0$ simply gives $T^I = 0$. This means that region I does not have any interaction variables. For region II, condition $T^{II} C_V^{II} = 0$ leads to one independent solution

$$T^{II} = \begin{bmatrix} 21.55 & 0 & -21.55 & 0 & 0 \\ 0 & 0 & 0 & 9.8 & -9.8 \\ 7.19 & 12.49 & 0 & 9.8 & -29.48 \end{bmatrix} \tag{6.44}$$

There are three independent interaction variables given by

$$z^{II} = \begin{bmatrix} 21.55(x_2 - x_4) \\ 9.8(x_5 - x_6) \\ 7.19x_2 + 12.49x_3 + 9.8x_5 - 29.48x_6 \end{bmatrix} \tag{6.45}$$

To see the physical meaning of these interaction variables, let us rewrite the above equation as

$$z^{II} = \begin{bmatrix} 21.55(x_2 - x_4) \\ 9.8(x_5 - x_6) \\ 7.19(x_2 - x_6) + 12.49(x_3 - x_6) + 9.8(x_5 - x_6) \end{bmatrix} \tag{6.46}$$

Note that the interaction variables are given in the differences of bus voltages, with the coefficients being exactly the line inductances. Therefore, these interaction variables exact represent the power flows on the lines, since the power flow on each line is exactly the voltage difference across the line multiplied by the line inductance, for the nominal operating conditions given in Table 6.1. Preservation of physical meaning of the interaction variables is important for both regional control and tertiary coordination, as will be shown in the next chapter.

6.5 Summary

This chapter presents a structurally-based modeling approach for reactive power/voltage dynamics of an interconnected power system. Dynamics of the system are formulated by combining the local dynamics of individual generators and the network couplings. It is shown that the decoupled reactive power/voltage dynamics of power systems are not structurally singular. Quasi-static dynamical models on slower time scales are derived. The structural models developed here will be used for systemwide voltage control on slower time scales in the the next chapter.

Chapter 7

Voltage Regulation

As discussed in the previous chapter, voltage regulation of power system involves the excitation system to stabilize the generator terminal voltages to their given reference values. These reference values are adjusted at discrete time instances slowly by the higher level controls. Significant effort has been given to analysis, modeling and design of excitation systems. This thesis will not further discuss these issues concerning the designs of fast primary controls. Emphasis here is on higher level control designs – the slow updating of the reference values for excitation systems. The ultimate goal is to develop a reliable, automated regional and systemwide voltage control to enhance secure and economical operation of power systems.

7.1 Regional Voltage Control

The simple control-driven model (6.35) is basic to developing decentralized secondary level voltage controllers. This control level is referred to in France and Italy as the *Automatic Voltage Control* (AVC) [16]. Its main function is to respond to the reactive load disturbances $d_s[k] = Q_L[k+1]-Q_L[k]$. The AVC is implemented on generator units

whose voltage set points $V_G^{ref}[k]$ are automatically changed to respond to deviations in load voltages $V_L[k]$ at the chosen subset of loads, the critical "pilot point" loads, $V_c[k] = C_s V_L[k]$. Because the maximum number of states that can be fully controlled is equal to the number of active controls (the number of participating generators), the number of pilot point loads is always less or equal to the number of participating generators.

Similarly to the AGC concepts, the AVC at the secondary level should be designed in such a way to keep operation of subsystems as autonomous as possible given control constraints. Its main objectives are to:

- Reschedule $V_G^{ref}[k]$ at each subsystem level to meet reactive load deviations $Q_L[k]$, $k = 0, 1, \cdots$;
- Regulate voltages $V_c[k]$ to $V_c^{set}[K]$,
- Maintain $F[K] \approx 0$ as long as reserves within each area are available (area control principle),
- Optimize subsystem performance (total reactive reserve or total transmission losses).

The formulation offered in this thesis enables one to perform optimization of a chosen performance criterion in a coordinated manner with the voltage regulation at the pilot point loads. It follows that the secondary control law of general form (7.5) or (3.23) will achieve the above objectives. It is important to recognize that the "participation factors" of different units are directly determined by the optimal gain G_s for any

given power network, no additional economic dispatch type functions are required at a subsystem level.

Consider, within an interconnected system, an area with n load buses and m generators participating in the secondary control. The dynamical equation for all the load voltages is given by

$$x[k+1] - x[k] = C_V u_s[k] + D_s(F_s[k] - d_s[k]) \tag{7.1}$$

where the dimension of the sensitivity matrix C_V is $n \times m$. In general, $n > m$. Under this condition, one can easily prove the following:

Proposition 7.1 (Controllability) *The dynamical system given in (6.36) is not fully controllable.*

Proof Let us write the controllability matrix for (6.36) as

$$Q_c = \begin{bmatrix} B & AB & \cdots & A^{n-1}B \end{bmatrix} = \begin{bmatrix} C_V & 0 & \cdots & 0 \end{bmatrix} \tag{7.2}$$

since $A = 0$ for the control-driven system. Because the sensitivity matrix C_V has maximum rank m, the system is not fully controllable.

As a result, not all load voltages can be fully controlled. Only the same number of loads as the number of generators can be fully controlled. This leads to the idea of pilot load voltages, the number of which does not exceed the number of generators participating in the secondary level control.

Due to this controllability issue, the maximum number of loads that can be controlled is equal to the number of active controls. Let us choose m output variables or

the pilot loads as

$$y[k] = C_s x[k] \tag{7.3}$$

The control-driven dynamical model for these pilot loads can be simply obtained as

$$y[k+1] - y[k] = C_c u_s[k] + D_c(F_s[k] - d_s[k]) \tag{7.4}$$

where $C_c = C_s C_V$ is the sensitivity matrix of the critical pilot voltages relative to the control, and $D_c = C_s D_s$. This is the basic model for secondary control design. Note that C_c is a square matrix.

7.1.1 Conventional Secondary Level Control

The present state of secondary voltage regulators is based only on the regional measurements, i.e. regional pilot point voltages. The effect of interconnecting flow changes due to changes in the neighboring regions is not considered directly. One consequence of this is that under certain conditions the secondary controller may cause a significant overshoot or not reach the set value within the prespecified time intervals.

The goal of the secondary level regulation is to maintain the pilot voltages (output variables) at their prespecified set values when the system is under disturbances. A simple proportional feedback law takes the form

$$u_s[k] = G_s(y[k] - y^{set}[K]) \tag{7.5}$$

where $y^{set}[K] \equiv y^{set}(KT_t)$ is the set value for the pilot voltages on the tertiary level time scale. This set value is adjusted by the tertiary level control on the even longer time scale T_t, and is a constant for the secondary control process, see Figure 2.2 for reference.

Under this control law, the secondary level closed-loop dynamical model becomes

$$x[k+1] - x[k] = C_V G_s (C_s x[k] - y^{set}[K]) + D_s (F_s[k] - d_s[k]) \tag{7.6}$$

and the pilot voltage dynamics are simply

$$y[k+1] - y[k] = C_c G_s (y[k] - y^{set}[K]) + D_c (F_s[k] - d_s[k]) \tag{7.7}$$

Let $A_s = C_c G_s$. We then rewrite the above as

$$y[k+1] - y[k] = A_s (y[k] - y^{set}[K]) + D_c (F_s[k] - d_s[k]) \tag{7.8}$$

One requirement for the choice of pilot voltages is that the resulting matrix C_c must be nonsingular. If matrix C_c is singular, then A_s will be singular for any gain matrix G_s. The discrete-time closed-loop system matrix $I + A_s$ will always have an eigenvalue of 1. The consequence of this is that the system will have a linear combination of the pilot voltages that cannot be moved by any control actions, i.e. not all pilot voltages can be fully controlled. In other words, steady state errors are inevitable for the chosen pilot voltages. To fully control the pilot voltages, it is required that the pilot points are selected such that C_c is of full rank.

The secondary level control design is to choose the appropriate gain G_s. The conventional control design neglects the effect of neighboring regions, i.e. it assumes $F_s[k] = 0$. Under this simplification, the model for pilot voltage dynamics becomes

$$y[k+1] - y[k] = A_s (y[k] - y^{set}[K]) - D_c d_s[k] \tag{7.9}$$

where $d_s[k]$ is treated as disturbances to the system. The problem of determining the feedback main matrix G_s can be formulated as an optimal control problem with

some performance criterion. An alternative way is to specify the desired closed-loop dynamics for the pilot voltages. The choice commonly used in EDF is to specify the closed-loop dynamics so that all pilot load voltages are completely decoupled with each other and exponentially reaching their set values within a specified time constant. This can be easily done by choosing the closed-loop system matrix $(I + A_s)$ to be a fully decoupled diagonal matrix with desired time constant. An example for the choice of time constant typically used in France is three (3) minutes. Equivalently, this is achieved by choosing

$$A_s = \lambda I \tag{7.10}$$

where λ is a scalar such that the pilot voltages settle to their steady state in the given time. For the specified decoupled dynamics, the time domain response of all pilot voltages will be purely exponential and no overshoot or undershoot will occur. Using the given A_s, one can solve for the gain matrix as

$$G_s = C_c^{-1}\lambda \tag{7.11}$$

under the assumption that pilot voltages are well chosen such that matrix C_c is non-singular.

Under the conventional control, the actual dynamics of the pilot voltages become

$$y[k+1] - y[k] = \lambda(y[k] - y^{set}[K]) + D_c(F_s[k] - d_s[k]) \tag{7.12}$$

The flow $F_s[k]$ is a function of the state variables. Therefore the effective dynamics of the pilot voltages are not purely exponential. In fact, overshoot or undershoot have been observed in some cases. The numerical example to be given later will illustrate the phenomenon.

7.1.2 Improved Secondary Level Control

We propose in this section possible ways to improve the secondary level voltage control, by taking into consideration the effect of interconnections, while preserving its decentralized nature. The proposed control laws will be such that they cancel out the effect of interactions based on additional feedback signals which use the reactive power flow measurements.

It is clear from (7.6) or (7.8) that tie-line flows viewed as an independent external input to the system affect the voltage dynamics. The conventional design of the secondary control, i.e. the design of G_s is typically done neglecting the interconnections with the neighboring regions, due to the large scale of the system and the desire to maintain the decentralized nature of the secondary level control. The "optimal" control designed this way will in general not be optimal anymore when implemented to the actual system where interconnections are indeed present. To fully compensate the effect of interconnections, we propose a new control feedback law in the form

$$u_s[k] = G_s(y[k] - y^{set}[K]) + HF_s[k] \tag{7.13}$$

where the first term is the same as the conventional secondary control control. The additional term $HF_s[k]$ is to cancel the tie-line flows on the dynamics of the pilot voltages. It will be shown that complete cancellation of the tie-line flows for the dynamics of the pilot voltages is possible with an appropriate choice of the matrix H. Substituting this improved control law into (7.4) leads to

$$y[k+1] - y[k] = A_s(y[k] - y^{set}[K]) + (C_cH + D_c)F_s[k] - D_cd_s[k] \tag{7.14}$$

It is clear that, when C_c is invertible, the tie-line flows can be fully eliminated in the

pilot voltage dynamics by choosing

$$H = -C_c^{-1} D_c \tag{7.15}$$

With this choice of H, equation (7.14) reads

$$y[k+1] - y[k] = A_s(y[k] - y^{set}[K]) - D_c d_s[k] \tag{7.16}$$

with no flows entering into the equation. In other words, the region under study looks as if it were completely isolated with the rest of the system, as far as pilot voltage dynamics are concerned.

It is noted that, due to the controllability issue discussed in Proposition 7.1, tie-line flows can be fully canceled only for as many as m (the number of active controls) load voltages. Since we choose m pilot points, flows can be canceled for all pilot voltages.

It is also noted that the control scheme presented here is fully decentralized, assuming the tie-line flows are locally measurable from each region. No detailed information about neighboring regions is needed; only tie line flows, which aggregate the net effect of detailed dynamics of the neighboring regions, are required. It is not an unrealistic assumption that tie-line flows are locally measurable.

7.1.3 The 9-Bus Example

Let us now illustrate the results by the small 9-bus example network given in Figure 6.3. Figure 7.1-a) shows the pilot voltage responses using the conventional feedback law given in (7.5). It is seen that, due to tie-line interactions, overshoot occurs and settling time is longer than supposed. Figure 7.1-b) shows the pilot voltage responses with the improved feedback control given in (7.13).

It is clear that the additional term $HF_s[k]$ improves the responses in both eliminating the overshoot and ensuring the prompt settling. This improvement is expected to be significant when tie-lines are strong and meshed.

Figure 7.2 shows the comparison between the non-pilot voltage responses using the conventional and improved feedback control. Again improvement is appreciable.

These figures also show that no oscillatory modes exist in the time domain responses of the load voltages, for either conventional secondary control or improved secondary control.

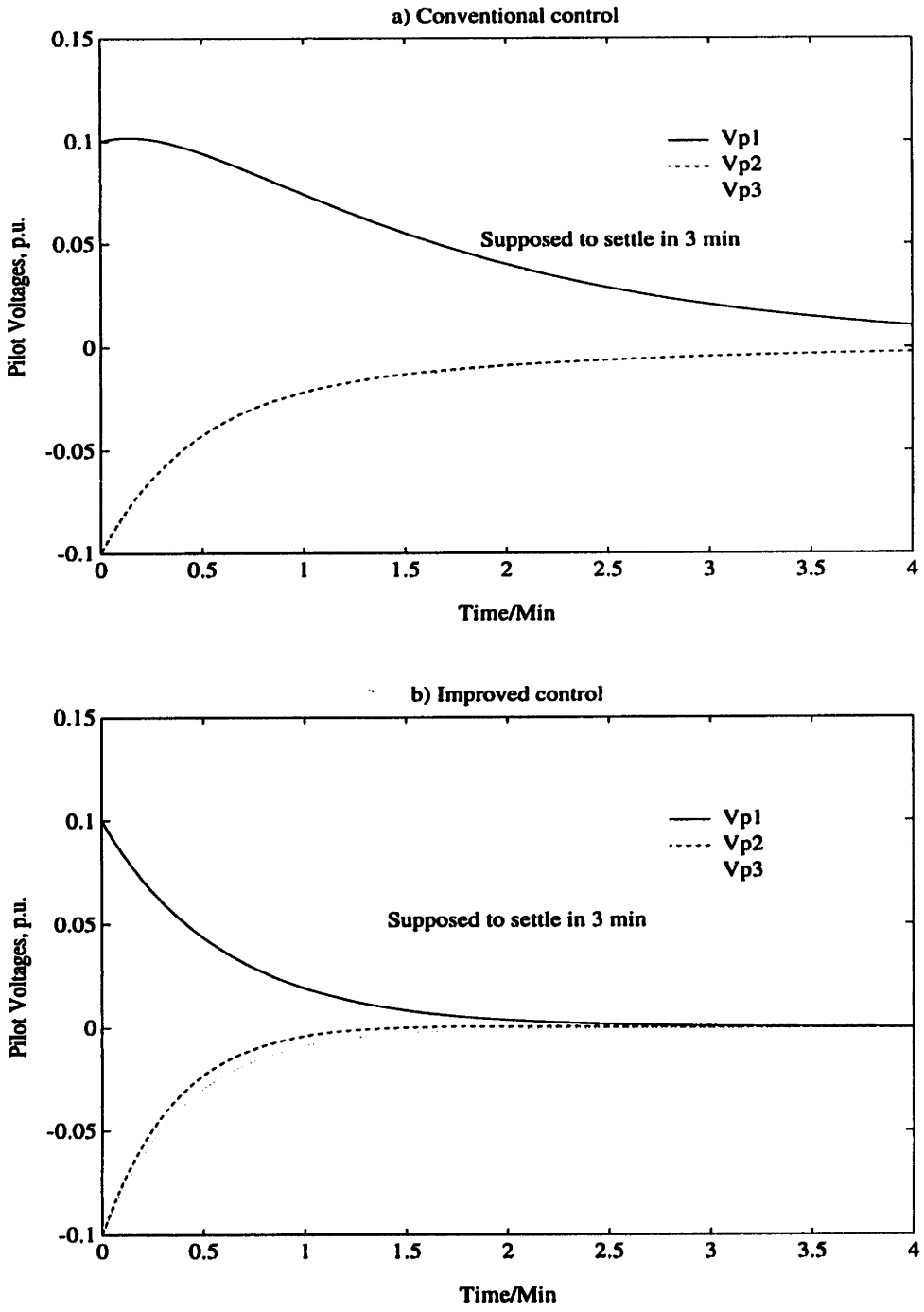

Figure 7.1: Pilot Voltages: a) Conventional, b) Improved

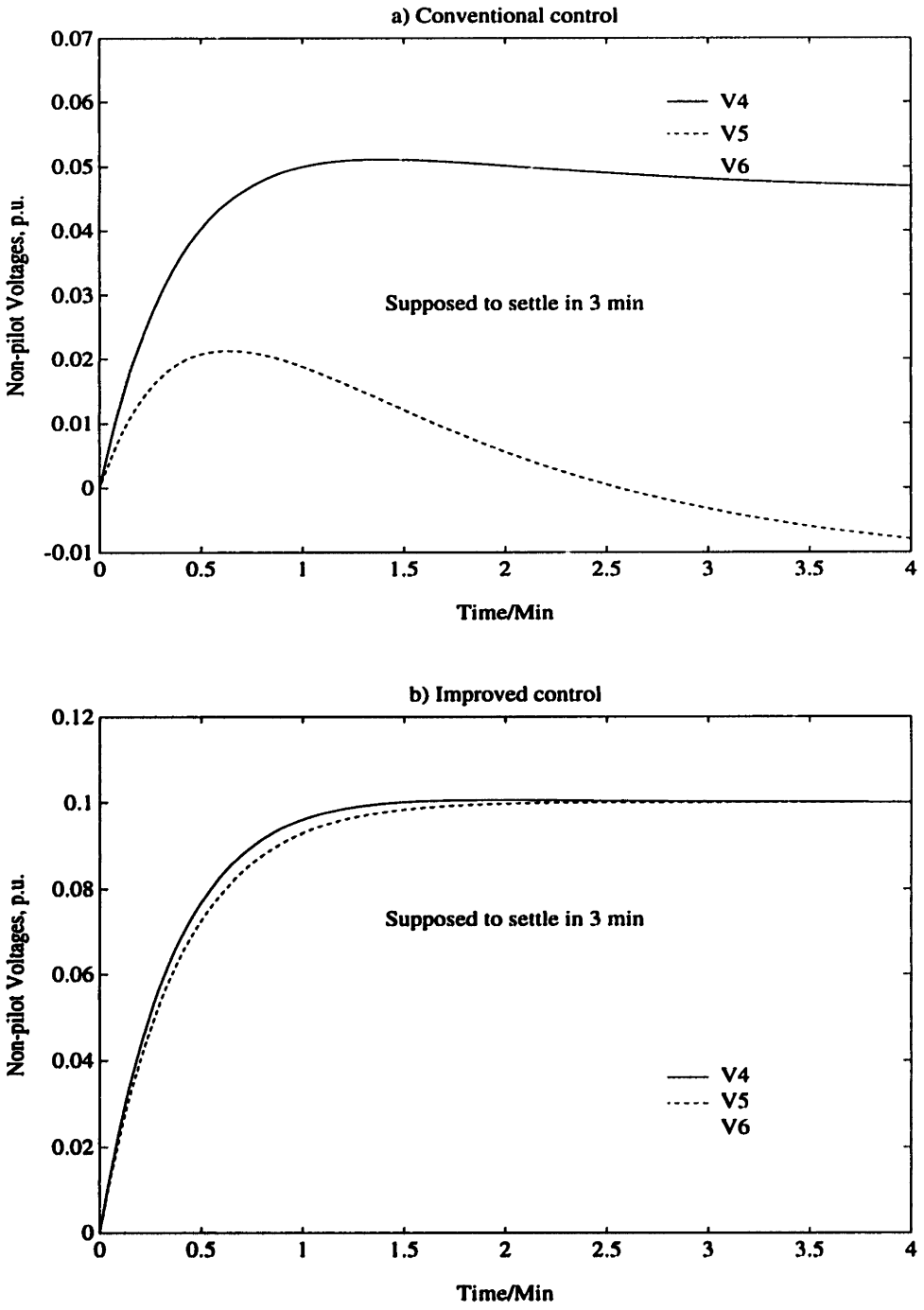

Figure 7.2: Nonpilot Voltages: a) Conventional, b) Improved

7.2 Tertiary Coordination

7.2.1 Introduction

With an increased tendency towards large energy transfer over long distances, the problem of maintaining voltages within the acceptable operating specifications has merged in operating and planning power systems throughout the world. The systemwide voltage coordination problem is viewed by many as the specialized OPF (page 13) problem. There are some drawbacks for the OPF technique. First of all, they do not offer much engineering insight for interpreting the numerical solutions. As a consequence, when the OPF technique experiences convergence problems, it cannot explain if the cause is the nonexistence of solutions, or the particular numerical method involved. Also the OPF technique does not offer much opportunity for handling specific problems of different individual regions. Another problem with the OPF technique is that a large amount of data for almost all variables of the entire system is needed in order to carry out the optimization. Therefore, state estimations are necessary for those unmeasured states. Errors in the state estimations can cause problems for the algorithm.

The main purpose of the tertiary level voltage controls is to update set values for reactive power tie-line flows $F[K]$, $K = 0, 1, \cdots$ on the tertiary level time scale in order to optimize system-wide performance for the anticipated base load $Q_L[K]$, $K = 0, 1, \cdots$. This could be done on hourly basis, if not more often in accordance with the statistical information on base load. The actual setting of tie-line flows is achieved by changing settings of secondary voltage controllers $V_G^{set}[K]$. Because this is done so infrequently, it could involve recomputing of basic matrices around a new operating point for the anticipated load over the time horizon T_t.

The idea behind the coordination of regional controllers is to establish feasible schemes for maintaining voltages throughout the interconnected system within the prespecified limits, subject to available reactive power resources. Although in this project only reactive power reserves of generators are of direct interest, the coordination under the development is directly applicable to all other sources of reactive energy which have primary controls responding to local voltages, such as static VAR compensators and on-load tap changing transformers, etc.

The determination of the optimal set values for the pilot voltages are formulated as an optimization problem. However, the notion of *optimal* voltage profiles remains as an open research question. The question has not yet been answered even for the simplest possible network with one generator supplying power to one single load. This is because the notion of optimal operation of the network has not yet been rigorously defined. The main performance candidates are concerned with:

- System reactive reserves;
- Transmission losses;
- Voltage proximity to the prespecified limits; and
- Flow scheduling.

We recognize that some of the performance criteria may be more relevant for normal operating conditions and the others for emergency conditions. Therefore, the coordination strategies under the development may be dependent on the system operating mode. In this sense there will be certain degree of adaptation to the operating mode.

Conventional thinking is that under the normal operation one wishes to minimize transmission loss, assuming that the system is well within the reactive reserve and voltage limits.

The optimization problem for the optimal set values of the pilot voltages can be formulated in three basic topologies:

- Fully centralized: The coordination tasks are performed by a global coordination center which has available the information for all the interconnected region. The entire interconnected system is modeled as a single region. One single performance criterion is optimized, and the optimal set values of the pilot voltages for all regions are obtained.

- Fully decentralized: The determination of set values of the pilot voltages is done by each individual region itself. Each region optimizes its own performance criterion. Each region does not assume any information about the rest of the system. In the optimization process of each region, the tie-line flows into the region are measured and used to determine the optimal pilot voltage set values for the region.

- Partially centralized/decentralized: In this scheme, each region assumes limited information about the rest of the system, and, with the limited information, tries to optimize its own performance criterion. The natural choice for the limited information about the rest of the system is simply the aggregate model developed previously. We model this scenario as a game theoretical setting.

The systemwide performance criterion for the fully centralized method is in general

quite difficulty to establish, and the computational effort for the solution is enormous, as the power system is very large. Therefore the coordination scheme cannot be implemented quite often. The fully centralized method also require global communication over far distances. The fully decentralized or partially centralized/decentralized schemes, on the other hand, have obvious advantages. There is an extensive degree of handling specific problems of different regions with different performance criteria. This is particularly suitable for a multi-utility environment. The performance criteria for smaller regions are easier to obtain, and the computational work is significantly reduced. As a result, no global communication is required, and the coordination schemes can be implemented relatively more frequently. The major disadvantage of the schemes with competition nature is that instability can occur.

Due to the large size of the system and complexity of the system operation, any practical on-line coordination schemes must be based on a reduced-information structure in order to be efficiently applied. In this thesis, we develop a tertiary coordination scheme based on a reduced-information structure using the interaction variables defined in the previous chapters. The defined interaction variables represent the inter-area tie-line power flows, and serve as a basis for the inter-area coordination. We shall derive an important relationship between the inter-area tie-line flows and the set values for the pilot voltages, which are the actual controls on the tertiary level. To establish some basic concepts for the notion of optimal voltage, we first study the simplest power system with only one generator and one load. The results obtained for the simple power system are then generalized to the more realistic power transmission systems.

7.2.2 A Simple Power System

In this section the basic notion of optimality with respect to voltage dynamics is studied by viewing the problem in light of known network theoretic results. New definitions of the *local maximum* and *global maximum* are proposed. The new results are interpreted in context of their potential use in operating the power system in a optimal fashion.

Consider an electric power network consisting one generator and one load [32], shown in Figure 7.3.

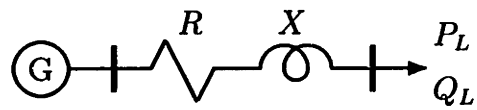

Figure 7.3: A Simple Example

The generator is connected to the load via a transmission line with impedance $\hat{Z} = R + jX$. The power balance equations at the load end are

$$P_L = G(V_L V_G \cos\theta - V_L^2) + BV_L V_G \sin\theta \tag{7.17}$$

$$Q_L = B(V_L V_G \cos\theta - V_L^2) - GV_L V_G \sin\theta \tag{7.18}$$

where $G = R/(X^2+R^2)$, $B = X/(X^2+R^2)$, V_G and V_L are the voltages of the generator terminal and the load, $\theta = \theta_G - \theta_L$ is the angle difference between V_G and V_L. Solution for the load voltage can be found as

$$2V_L^2 = V_G^2 - 2a \pm \sqrt{V_G^4 - 4(aV_G^2 + b^2)} \tag{7.19}$$

where

$$a = RP_L + XQ_L \tag{7.20}$$

$$b = XP_L - RQ_L \tag{7.21}$$

It is clear that in order for the solutions to exist, one must require

$$V_G^4 \geq 4(aV_G^2 + b^2) \tag{7.22}$$

It can be further shown that when (7.22) is satisfied, the right hand side of (7.19) is always positive, leading to no further constraint on the system as far as existence of solutions is concerned. The inequality (7.22) is the fundamental requirement to the system, and forms the basis for load limits and maximum power transfer for this simple system.

If the transmission line is lossless, i.e. $R = X = 0$, then $a = b = 0$, (7.22) is always satisfied. Mathematically, there always exists a solution to the load flow. When losses are present, however, only a limited amount of power can, due to the constraint of (7.22), be delivered to the load, with a given terminal voltage of the generator.

7.2.3 Global Maximum

For a given generator voltage V_G, there is a maximum point for the load real power P_L. This absolute maximum real power is called a *global maximum.* This is the maximum real power the system can deliver to a load under the given terminal voltage of the generator. This global maximum can be found by holding (7.22) as an equality and taking

$$\frac{dP_L}{dQ_L} = 0 \tag{7.23}$$

Differentiating (7.22), for a fixed V_G, leads to

$$V_G^2 \frac{da}{dQ_L} + 2b\frac{db}{dQ_L} = 0 \tag{7.24}$$

Differentiating (7.20) and (7.21) yields

$$\frac{da}{dQ_L} = R\frac{dP_L}{dQ_L} + X = X \tag{7.25}$$

$$\frac{db}{dQ_L} = X\frac{dP_L}{dQ_L} - R = -R \tag{7.26}$$

using the maximum condition (7.23). Substituting the above into (7.24), we can find

$$b = \frac{X}{2R}V_G^2 \tag{7.27}$$

and, with this and the equality (7.22),

$$a = (1 - \frac{X^2}{R^2})\frac{V_G^2}{4} \tag{7.28}$$

Having obtained a and b, the global maximum P_L can be easily found by (7.20) and (7.21) as

$$P_L = \frac{aR + bX}{R^2 + X^2} = \frac{V_G^2}{4R} \tag{7.29}$$

The corresponding Q_L can also be solved

$$Q_L = \frac{aX - bR}{R^2 + X^2} = -\frac{XV_G^2}{4R^2} \tag{7.30}$$

It should be noted that the global maximum is realized when, if the impedance model, $\hat{Z}_L = R_L + jX_L$, for the load is adopted, $R_L = R$ and $X_L = -X$. This agrees with the classical circuit theory.

7.2.4 Local Maximum

To understand the fundamental characteristics of the power system, and to make analysis more universal, we use dimensionless quantities. Let us define

$$r \triangleq \frac{R}{X}, \quad v \triangleq \frac{V_L}{V_G}, \quad p \triangleq \frac{XP_L}{V_G^2}, \quad q \triangleq \frac{Q_L}{P_L} \tag{7.31}$$

It can be shown that the load power factor α is related to q by

$$\alpha = \frac{P_L}{\sqrt{P_L^2 + Q_L^2}} = \frac{1}{\sqrt{1+q^2}}$$

Constant load power factor implies constant q, and high power factor means small absolute value of q.

Using these dimensionless quantities, we can rewrite the load flow solution (7.19) as

$$2v^2 = 1 - 2p(r+q) \pm \sqrt{1 - 4[(r+q)p + (1-rq)^2p^2]} \tag{7.32}$$

The inequality (7.22) becomes

$$(r+q)p + (1-rq)^2p^2 \leq \frac{1}{4} \tag{7.33}$$

Solving this we get

$$p_m \leq p \leq p_M \tag{7.34}$$

where the two limits are

$$p_M = \frac{1/2}{\sqrt{(1+r^2)(1+q^2)} + (r+q)} > 0 \tag{7.35}$$

$$p_m = \frac{-1/2}{\sqrt{(1+r^2)(1+q^2)} - (r+q)} < 0 \tag{7.36}$$

Equation (7.34) clearly indicates that, for a given r and q, there are a minimum and a maximum value for the power p. p_M is the maximum power that can be delivered to a load for a given q. To distinguish this maximum from the global maximum we refer to this as the *local maximum.* Note that p_m is the maximum power a "load" can deliver to the network – when the "load" is actually another generator.

The load voltages corresponding to the local maximum can be obtained as

$$v_M = \sqrt{\frac{1}{2} - (r+q)p_M} \tag{7.37}$$

$$v_m = \sqrt{\frac{1}{2} - (r+q)p_m} \tag{7.38}$$

Global maximum can also be re-discovered using the local maximum by setting

$$\frac{dp_M}{dq} = 0 \tag{7.39}$$

After differentiating (7.35) and some algebraic manipulation, we get the global maximum condition

$$rq = -1 \tag{7.40}$$

This condition is equivalent to the condition found in classical maximum power theory for circuits, as will be further discussed next.

It is interesting to note that at the global maximum, the real power loss on the transmission line is equal to the real power on the load, and the reactive power loss is equal to the negative of reactive power of the load. Losses are given by

$$P_{loss} = G(V_G^2 + V_L^2 - 2V_G V_L \cos\theta) \tag{7.41}$$

$$Q_{loss} = B(V_G^2 + V_L^2 - 2V_G V_L \cos\theta) \tag{7.42}$$

Using load flow solutions we can show that at the global maximum

$$P_{loss} = P_{load} \tag{7.43}$$

$$Q_{loss} = -Q_{load} \tag{7.44}$$

7.2.5 Load Impedance Model

We can apply the general results to the case of an impedance model for the load. Let the complex load impedance be

$$\hat{Z}_L = R_L + jX_L = Z_L e^{j\phi_L} \tag{7.45}$$

and the complex line impedance be

$$\hat{Z} = R + jX = Ze^{j\phi} \tag{7.46}$$

With the impedance model we can easily find

$$p_{load} = \frac{z}{(1+z^2)\sqrt{(1+r^2)(1+q^2)} + 2z(r+q)} \tag{7.47}$$

$$v_{load} = \frac{z\sqrt{(1+r^2)(1+q^2)}}{(1+z^2)\sqrt{(1+r^2)(1+q^2)} + 2z(r+q)} \tag{7.48}$$

where $z = Z_L/Z$ is the ratio of the two magnitudes.

Using these results and equations (7.32) and (7.37), we prove the following conclusion:

Proposition 7.1 (Local Maximum) *The local maximum occurs if and only if $Z_L = Z$ (magnitude matching).*

Proposition 7.2 (Global Maximum) *The global maximum occurs if and only if $Z_L = Z$ (magnitude matching) and $\phi_L = -\phi$ (phase matching), i.e. $\hat{Z}_L = \hat{Z}^*$.*

7.2.6 Performance Criteria

Assuming the secondary level control is carried out properly, the tertiary level control is to determine the set values for the pilot voltages, or equivalently the set values for the generator voltages, over the tertiary level time scale T_t, so that the global system as a whole operates optimally according to a certain performance criterion. In this section, we discuss some general aspects of the performance criteria to be used for the optimization process.

Since the system is composed of three major components, the generators, transmission network, and the loads, the overall performance criterion can be written in general as

$$J = J_{gen} + J_{net} + J_{lod} \tag{7.49}$$

where J_{gen}, J_{net} and J_{lod} are the performance criteria corresponding to each of the three major components of the power system. Specifically, using the above performance criterion, we can achieve the following:

- **Generation alignment** to nearly equalize the ratios of actual generation to the maximum capacity of all or part of the generators;
- **Flow scheduling** to schedule tie-line flows among the interconnected regions so that the global system operates in a coordinated fashion;
- **Security enhancement** to ensure the generators stay within their limits as much as possible;
- **Loss minimization** to reduce the losses on the transmission network.

For the generators, we need to deal with both the reactive generations and the terminal voltages. Therefore the choice for the generator performance criterion can be further decomposed as

$$J_{gen} = J_Q + J_V \tag{7.50}$$

with the first term J_Q dealing with reactive generations, and the second term J_V with the voltage limit problem. The term J_Q is to ensure that the reactive generations are within the physically permittable limits. One simple quadratic form, for example, can be

$$J_Q = (Q_G[K] - Q_G^{nom})^T W_Q (Q_G[K] - Q_G^{nom}) \tag{7.51}$$

where Q_G^{nom} is the desired nominal point inside the limit band of the reactive generations, and the weighting matrix $W_Q = W_Q^T \geq 0$. The term J_V is primarily to ensure that the generator terminal voltages stay within the allowable bounds. The simple quadratic form for J_V is expressed as

$$J_V = (V_G[K] - V_G^{nom})^T W_V (V_G[K] - V_G^{nom}) \tag{7.52}$$

where V_G^{nom} is the desired nominal point inside the limit band of the generator terminal voltages, and also the weighting matrix $W_V = W_V^T \geq 0$. This kind of performance criteria tends to keep the generator generations and terminal voltages close to their desired nominal values, if heavy weights are given to these terms. The justification for this type of performance criteria is that it can eliminate the situation of some generators hitting their physical operating limits under heavy loading conditions.

Similarly, for the transmission network, we can decompose the performance criterion into a term involving the total losses on the transmission network, and a term involving rescheduling the tie-line flows. For the loads, the primary concern is also for the critical

pilot node load voltages to stay within the acceptable bound. A similar expression to (7.52) can be written for the load voltages.

$$J_{lod} = (V_c[K] - V_c^{nom})^T W_c (V_c[K] - V_c^{nom}) \tag{7.53}$$

where V_c^{nom} is the desired point inside the limit band of the load voltages, and the weighting matrix $W_c = W_c^T > 0$. This performance criterion tends to keep the load voltages close to the desired point V_c^{nom}.

In the process of solving the optimal control problem given in (7.49), constraints among the tie-line flows, unit generations, losses, and the set values for the pilot voltages on the tertiary level time scale are needed. These constraints for the time K involve the values of these quantities at the previous time $(K-1)$. As a consequence, the optimal solution for the time K involves quantities at the previous time $(K-1)$. Therefore, the pilot voltage settings as a result of the optimal control problem form another discrete-time sequence on the very slow time scale T_t. The basic requirement for the optimization process is that it must guarantee the stability of this discrete-event process.

It is emphasized that this process of tertiary control involves only the information about the generators participating in the secondary control and the pilot points, plus the tie-line flows if they are to be re-scheduled. The amount of data and computation involved is drastically less than that needed for the full scale optimal power flow calculation, where information about all loads is necessary. As an example, two regions of the French network have 259 buses, while the number of pilot points for the two regions is only 9. As a result of the significantly limited amount of information needed, it is visualizable that this tertiary control scheme can be implemented on-line as a

closed-loop control.

7.3 New Tertiary Level Aggregate Models

Using the structural modeling approach discussed above, one can derive the relationship between the critical pilot voltages and the generator voltages, the relationship between the critical pilot voltages and the generator reactive outputs, the relationship between the flows and the interaction variables, and the relationship between the flows and the output variables, on the tertiary level time scale T_t. These relationships serve as constraints to the optimization problem to determine the optimal set values for the output variables – the critical pilot voltages. Since these relationships are derived for an administrative region, they explicitly involve the tie-line flows into the region from the rest of the system.

Pilot And Generator Voltages

Let us consider a single region within an interconnected system. The relationship between the load and generator voltages was introduced in (6.19) as

$$\dot{V}_L = C_V \dot{V}_G + J_{LL}^{-1}(\dot{F}_L - \dot{Q}_L) \tag{7.54}$$

To derive the relationship between the critical pilot voltages and generator voltages on the tertiary level time scale T_t, let us integrate this equation from KT_t to $(K+1)T_t$. This simply leads to

$$V_L[K+1] - V_L[K] = C_V(V_G[K+1] - V_G[K]) + D(F_L[K+1] - F_L[K]) - Dd_t[K] \tag{7.55}$$

where $D \triangleq J_{LL}^{-1}$, and $d_t[K] \triangleq Q_L[K+1] - Q_L[K]$. The critical pilot load voltages are defined as

$$V_c \triangleq C_s V_L \tag{7.56}$$

Multiplying (7.55) by C_s yields

$$V_c[K+1] - V_c[K] = C_c(V_G[K+1] - V_G[K]) + D_c(F_L[K+1] - F_L[K]) - D_c d_t[K] \tag{7.57}$$

where $C_c \triangleq C_s C_V$ is the sensitivity matrix of the critical pilot voltages relative to the control, and $D_c = C_s D$. Following the discussions in Chapter 3, one should note that C_c is chosen to be a square matrix and nonsingular. Otherwise, not all pilot voltages can be fully controlled. Under this condition, one obtains from (7.57)

$$V_G[K+1] - V_G[K] = L_V(V_c[K+1] - V_c[K]) - L_{Vd}(F_L[K+1] - F_L[K]) + L_{Vd} d_t[K] \tag{7.58}$$

where $L_V \triangleq C_c^{-1}$ and $L_{Vd} \triangleq L_V D_c$. This relationship determines the change in generator voltages for any change in the pilot voltages and the tie-line flows under the given loading condition. Let us rewrite this in a more compact form as

$$V_G[K+1] = L_V V_c[K+1] - L_{Vd} F_L[K+1] + R_V[K] \tag{7.59}$$

where

$$R_V[K] = V_G[K] - L_V V_c[K] + L_{Vd} F_L[K] + L_{Vd} d_t[K] \tag{7.60}$$

Or equivalently , with a time delay,

$$V_G[K] = L_V V_c[K] - L_{Vd} F_L[K] + R_V[K-1] \tag{7.61}$$

This relationship will be used by the decentralized regional tertiary control to determine the regional pilot voltages.

Pilot Voltages And Reactive Generations

Another important quantity for the concern of tertiary control is the reactive generations of the generating units, because, after all, the reactive generations must match the reactive loads and the losses on the transmission lines. In this subsection, we derive the relationship between the change in generator reactive outputs and the change in pilot voltages. This relationship is important because one needs to be concerned with the reactive generations when deciding on the desired pilot voltages. The fundamental relation between the reactive generations and the generator voltages was derived in (6.23) as

$$\dot{Q}_G = K_Q \dot{V}_G - \dot{F}_e + D_Q \dot{Q}_L \tag{7.62}$$

where $K_Q = J_{GG} + J_{GL}C_V$ and $D_Q = -J_{GL}J_{LL}^{-1}$. With the same derivations as in the previous subsection, by integrating this on the tertiary level time scale T_t, we have

$$Q_G[K+1] - Q_G[K] = K_Q(V_G[K+1] - V_G[K]) - (F_e[K+1] - F_e[K]) + D_Q d_t[K] \tag{7.63}$$

This, combined with (7.58), gives us

$$Q_G[K+1] - Q_G[K] = L_Q(V_c[K+1] - V_c[K]) - (F_Q[K+1] - F_Q[K]) + L_{Qd} d_t[K] \tag{7.64}$$

where $L_Q \triangleq K_Q L_V$, $F_Q \triangleq F_e + K_Q L_{Vd} F_L$, and $L_{Qd} \triangleq D_Q + K_Q L_{Vd}$. Equation (7.64) defines the relationship between the change in reactive generations and the change in pilot voltages, given the tie-line flow and load changes. Again, we can rewrite this into

$$Q_G[K+1] = L_Q V_c[K+1] - F_Q[K+1] + R_Q[K] \tag{7.65}$$

for

$$R_Q[K] = Q_G[K] - L_Q V_c[K] + F_Q[K] + L_{Qd} d_t[K] \tag{7.66}$$

Or equivalently

$$Q_G[K] = L_Q V_c[K] - F_Q[K] + R_Q[K-1] \tag{7.67}$$

This equation will also serve as the constraint for the regional tertiary optimization process.

Flows And the Interaction Variables

We have derived the secondary level interaction dynamical model in (6.41) as

$$z[k+1] - z[k] = TD_s(F_s[k] - d_s[k]) \tag{7.68}$$

or

$$z[k+1] - z[k] = S(F_s[k] - d_s[k]) \tag{7.69}$$

for

$$S \triangleq TD_s \tag{7.70}$$

Evaluating this on the tertiary level time scale T_t yields

$$z[K+1] - z[K] = S(F_L[K+1] - F_L[K]) - S(d[K+1] - d[K]) \tag{7.71}$$

Define $d_t[K] \triangleq d[K+1] - d[K]$ as the tertiary level disturbance. Equation (7.71) becomes

$$z[K+1] - z[K] = S(F_L[K+1] - F_L[K]) - Sd_t[K] \tag{7.72}$$

Matrix S as defined in (7.70) has a special structure, and can be easily constructed using inspection. Recall the definition of $C_V = -J_{LL}^{-1} J_{LG} = -D_s J_{LG}$ and the condition of $TC_V = 0$ in (6.40). One simply has

$$SJ_{LG} = TD_s J_{LG} = -TC_V \tag{7.73}$$

Therefore we derive the important equation for the S matrix as

$$SJ_{LG} = 0 \tag{7.74}$$

This gives a simple method to construct the S matrix. Let us discuss this as follows: Suppose that there are n load buses and m generator buses in the region under consideration, and assume that $n > m$. Then there are $n - m$ independent solutions for S, or S has $n - m$ independent rows. If load bus i is not connected to a generator bus, then the corresponding ith row of J_{LG} is all zero, because J_{LG} is the connection matrix between the load buses and the generator buses. In this case, vector

$$v = \begin{bmatrix} 0 & \cdots & 0 & 1 & 0 & \cdots & 0 \end{bmatrix} \tag{7.75}$$
$$\uparrow \; i^{th} element$$

will satisfy $vJ_{LG} = 0$ because the ith row of J_{LG} is all zero. In other words, matrix S will have v as one of its rows. Therefore, for all load buses not connected to generator buses, we construct S by selecting 1 at the corresponding locations, and 0 elsewhere. If the number of the load buses not connected to generator buses is equal to $n - m$, then we have found all $n - m$ independent solutions for S. If this number is less than $n - m$, then there are more independent solutions to be determined. In this case, one needs to solve (7.74) to get all the independent solutions.

Because of the special structure of the S matrix, we see from (7.72) that the interaction variables are just the tie-line flows into all the load buses that are not connected to generator buses. This is extremely important for tertiary level coordination.

7.3.1 Centralized Aggregate Models

In this subsection, the global interconnected system is considered as one single region. Since this big single region is an isolated system, there are no tie line flows into the system. All the previous derivations carry over to the global interconnected system, except all tie-line flow terms drop out. This is because there is no restriction on how to choose the region, and all results apply to the global interconnected system as one single region.

Pilot And Generator Voltages

We use the bold face script letters to represent any variable associated with the global interconnected system. For example, let us define $\boldsymbol{V}_G$, $\boldsymbol{Q}_G$ to represent the generator voltages and reactive generations of the global system, define further $\boldsymbol{V}_c$ to represent the critical pilot load voltages of the global system. The relationship between the pilot load voltages and the generator voltages is in the same form as (7.61)

$$\boldsymbol{V}_G[K] = \boldsymbol{L}_V \boldsymbol{V}_c[K] + \boldsymbol{R}_V[K-1] \tag{7.76}$$

where $\boldsymbol{L}_V \triangleq \boldsymbol{C}_c^{-1}$ and $\boldsymbol{L}_{Vd} \triangleq \boldsymbol{L}_V \boldsymbol{D}_c$. Matrices $\boldsymbol{C}_c$ is the pilot voltage sensitivity matrix for the global system, and

$$\boldsymbol{R}_V[K-1] = \boldsymbol{V}_G[K-1] - \boldsymbol{L}_V \boldsymbol{V}_c[K-1] + \boldsymbol{L}_{Vd} \mathbf{d}_t[K-1] \tag{7.77}$$

Comparing with Equation (7.61), we see that all the flow term disappeared here, because the global system is assumed to be an isolated one, and there is no flow for the isolated system.

Pilot Voltages And Reactive Generations

Similar to the generator voltage case, we can derive the tertiary level aggregate model for the reactive generations of the global system. Again, we carry the results for a single region case. The final relationship needed for tertiary level control is, derived from (7.67) without all the flow terms,

$$\boldsymbol{Q}_G[K] = \boldsymbol{L}_Q \boldsymbol{V}_c[K] + \boldsymbol{R}_Q[K-1] \tag{7.78}$$

where $\boldsymbol{L}_Q \triangleq \boldsymbol{K}_Q \boldsymbol{L}_V$ and

$$\boldsymbol{R}_Q[K-1] = \boldsymbol{Q}_G[K-1] - \boldsymbol{L}_Q \boldsymbol{V}_c[K-1] + \boldsymbol{L}_{Qd} \boldsymbol{d}_t[K-1] \tag{7.79}$$

All other matrices are defined in a similar way as in the decentralized case, except they are now defined for the global system.

Flows And the Pilot Voltages

Here we study the relationship between the internal flows among the regions within the global system and the pilot voltages. This relationship can be easily obtained from secondary quasi-static models as

$$\boldsymbol{S}(\boldsymbol{F}[K+1] - \boldsymbol{F}[K]) = \boldsymbol{L}(\boldsymbol{y}_s[K+1] - \boldsymbol{y}_s[K]) + \boldsymbol{L}_d \boldsymbol{d}_t[K] \tag{7.80}$$

where $\boldsymbol{S} = \boldsymbol{T}\boldsymbol{D}_{LL}$ and $\boldsymbol{L} = \boldsymbol{T}\boldsymbol{C}_V(\boldsymbol{T}\boldsymbol{C}_c)^{-1}$.

It is intriguing to recognize that $z[k]$ can be interpreted as the area load excess (ALE) introduced in [33] as a better alternative to the area control error (ACE) signal. This simply follows from the Kirchikoff's current law for each cutset separating an

area from its neighboring subsystems. While the ALE concept was introduced in [33] as a heuristic measure of the most meaningful signal for preserving the famous area control principle, we provide in this thesis its accurate derivation which also accounts for transmission losses. The basic difference from the previous literature including [20] and [33] is that it is not necessary to experiment with the best weighting coefficients when designing secondary and tertiary level controllers. They are simply result of general optimization methods for chosen performance criteria.

7.3.2 The 9-Bus Example

Let us illustrate the general model by considering the small 9-bus example given in Figure 6.3. For the numerical numbers given in Table 6.1, we can calculate

$$\boldsymbol{C_c} = \begin{bmatrix} 1 & 0 & 0 \\ 0 & .55 & .45 \\ 0 & .37 & .63 \end{bmatrix} \tag{7.81}$$

$$\boldsymbol{L_V} = \boldsymbol{C_c^{-1}} = \begin{bmatrix} 1 & 0 & 0 \\ 0 & 3.43 & -2.43 \\ 0 & -2.02 & 3.02 \end{bmatrix} \tag{7.82}$$

Matrix $\boldsymbol{K_Q}$ is given by

$$\boldsymbol{K_Q} = \begin{bmatrix} 0 & 0 & 0 \\ 0 & 3.71 & -3.71 \\ 0 & -3.71 & 3.71 \end{bmatrix} \tag{7.83}$$

It is easy to calculate

$$\boldsymbol{L_Q} = \boldsymbol{K_Q L_V} = \begin{bmatrix} 0 & 0 & 0 \\ 0 & 20.24 & -20.24 \\ 0 & -20.24 & 20.24 \end{bmatrix} \tag{7.84}$$

Also the $\boldsymbol{D_{LL}}$ matrix is

$$\boldsymbol{D_{LL}} = \begin{bmatrix} -7.69 & 0 & 0 & 1 & 0 & 0 \\ 0 & -52.75 & 15.67 & 21.55 & 0 & 7.19 \\ 0 & 15.67 & -38.16 & 0 & 0 & 12.49 \\ 0 & 21.55 & 0 & -21.55 & 0 & 0 \\ 0 & 0 & 0 & 0 & -9.89.8 & \\ 0 & 7.19 & 12.49 & 0 & 9.8 & -29.48 \end{bmatrix} \tag{7.85}$$

With the T matrix given in (6.45), we obtain

$$S = TD_{LL} = \begin{bmatrix} 0 & 0 & 0 & 1 & 0 & 0 \\ 0 & 0 & 0 & 0 & 1 & 0 \\ 0 & 0 & 0 & 0 & 0 & 1 \end{bmatrix} \tag{7.86}$$

$$L = \begin{bmatrix} -4.06 & 4.06 & 0 \\ -3.38 & 1.23 & 2.15 \\ 0 & 0 & 0 \end{bmatrix} \tag{7.87}$$

and also

$$L_d = (T - LC)D_s = \begin{bmatrix} -.53 & .27 & .18 & 1.27 & .21 & .21 \\ -.44 & .18 & .19 & .18 & 1.19 & .19 \\ 0 & 0 & 0 & 0 & 0 & 1 \end{bmatrix} \tag{7.88}$$

The physical meaning of the matrix S is that only the tie-line flows going into the load buses are the interaction variables. The fact that all elements of the last row of matrix L is that the third interaction variable $z_3 = 7.19(x_2 - x_6) + 12.49(x_3 - x_6) + 9.8(x_5 - x_6)$ as calculated in (6.46) will remain constant even when the tie-line are connected, if there are no load variations. This physically makes sense because this interaction variable is always equal to the load at bus #6, as can be seen from Figure 6.3, no matter what the generator voltages and/or the pilot voltages are. This is clearly demonstrated by the last row of the matrix L_d.

7.3.3 Fully Centralized Optimization

In this section, we formulate the tertiary level optimization in a fully centralized fashion, i.e. the coordination tasks are carried out by a tertiary control center. This tertiary control center is assumed to have all information about the interconnected regions needed to solve the optimization problem.

Consider an interconnected system consisting of R regions. Let V_G, Q_G and V_c represent the generator voltages, the reactive generations and critical pilot node voltages of the global system. Let the performance criterion for the global system in the

interval $[KT_t, (K+1)T_t]$ be given by

$$\boldsymbol{J}[K] = \boldsymbol{J}(\boldsymbol{V}_G[K], \boldsymbol{Q}_G[K], \boldsymbol{V}_c[K]) \tag{7.89}$$

Let us take, as an example, the quadratic form

$$\begin{aligned} \boldsymbol{J}[K] \;=\; & (\boldsymbol{V}_G[K] - \boldsymbol{V}_G^{nom})^T \, \boldsymbol{W}_V \, (\boldsymbol{V}_G[K] - \boldsymbol{V}_G^{nom}) \\ & + (\boldsymbol{Q}_G[K] - \boldsymbol{Q}_G^{nom})^T \, \boldsymbol{W}_Q \, (\boldsymbol{Q}_G[K] - \boldsymbol{Q}_G^{nom}) \\ & + (\boldsymbol{V}_c[K] - \boldsymbol{V}_c^{nom})^T \, \boldsymbol{W}_c \, (\boldsymbol{V}_c[K] - \boldsymbol{V}_c^{nom}) \end{aligned} \tag{7.90}$$

where $\boldsymbol{V}_G^{nom}$, $\boldsymbol{Q}_G^{nom}$ and $\boldsymbol{V}_c^{nom}$ are the desired nominal values for the generator voltages, reactive generations and pilot load voltages, $\boldsymbol{W}_V$, $\boldsymbol{W}_Q$ and $\boldsymbol{W}_c$ are the relative weighing matrices for the corresponding terms. The purpose of the optimization process is to determine the optimal setting for the pilot voltages $\boldsymbol{V}_c[K]$.

Note that the generator voltages $\boldsymbol{V}_G$ and reactive generations $\boldsymbol{Q}_G$ are related to the pilot voltage settings through the aggregate models presented in the previous section. These relationships serve as equality constraints for the optimization process proposed in (7.90). This optimization problem, together with these constraints, can be explicitly solved and the analytic solution can be obtained. For that purpose, let us first prove the following optimization result:

Proposition 7.3 (Optimal Solution) *The analytic solution to the constrained optimization problem:*

$$\begin{cases} J = (x - x^{nom})^T Q (x - x^{nom}) + (y - y^{nom})^T R (y - y^{nom}) \\ x = Ly + x_0 \end{cases} \tag{7.91}$$

is explicitly given by

$$\begin{cases} x = x^{nom} + X(x^{nom} - Ly^{nom} - x_0) \\ y = y^{nom} + Y(x^{nom} - Ly^{nom} - x_0) \end{cases} \tag{7.92}$$

where

$$\begin{cases} X = LY - I \\ Y = (L^T Q L + R)^{-1} L^T Q \end{cases} \tag{7.93}$$

with I being the identity matrix of the same dimension as Q.

Notice that if $x^{nom} = Ly^{nom} + x_0$, i.e. the nominal values satisfy the constraint between x and y, then the optimal solution is given by $x = x^{nom}$ and $y = y^{nom}$. This is straightforward. In this case, the optimal cost is calculated to be $J = 0$. Let us give a brief proof of the proposition.

Proof Let us convert the constrained optimization problem into an unconstrained one by constituting a Lagrangian

$$\mathcal{L} = (x - x^{nom})^T Q (x - x^{nom}) + (y - y^{nom})^T R (y - y^{nom}) - \lambda^T (x - Ly - x_0) \tag{7.94}$$

Using vector differentiation results, we derive

$$\frac{\partial \mathcal{L}}{\partial x} = 2Q(x - x^{nom}) - \lambda \tag{7.95}$$

$$\frac{\partial \mathcal{L}}{\partial y} = 2R(y - y^{nom}) + L^T \lambda \tag{7.96}$$

By setting the two partial derivatives to zero, we obtain

$$R(y - y^{nom}) + L^T Q (x - x^{nom}) = 0 \tag{7.97}$$

Using the constraint $x = Ly + x_0$, we get

$$R(y - y^{nom}) + L^T Q (Ly + x_0 - x^{nom}) = 0 \tag{7.98}$$

or

$$(L^T Q L + R)(y - y^{nom}) = L^T Q (x^{nom} - Ly^{nom} - x_0) \tag{7.99}$$

which leads to the conclusion in the proposition. Having obtained the optimal solution for y, one can calculate the corresponding optimal solution for x from the constraint $x = Ly + x_0$. That simply yields the result stated in the proposition.

Now we can use the proposition to solve the optimization problem posed in (7.90). To put the performance criterion into the form in Proposition 7.3, let us define the vector of generator quantities as

$$x \triangleq \begin{bmatrix} \boldsymbol{V}_G \\ \boldsymbol{Q}_G \end{bmatrix} \tag{7.100}$$

and the weighting matrix for the generator quantities

$$\mathcal{Q} \triangleq \text{BlockDiag}(\boldsymbol{W}_V, \boldsymbol{W}_Q) \tag{7.101}$$

The performance criterion in (7.90) can be rewritten as

$$\boldsymbol{J}[K] = (x[K] - x^{nom})^T \mathcal{Q}(x[K] - x^{nom}) + (\boldsymbol{V}_c[K] - \boldsymbol{V}_c^{nom})^T \boldsymbol{W}_c(\boldsymbol{V}_c[K] - \boldsymbol{V}_c^{nom}) \tag{7.102}$$

The generator voltages and pilot voltages satisfy the constraint as derived in (7.76):

$$\boldsymbol{V}_G[K] = \boldsymbol{L}_V \boldsymbol{V}_c[K] + \boldsymbol{R}_V[K-1] \tag{7.103}$$

The reactive generations and pilot voltages satisfy the constraint as given in (7.78):

$$\boldsymbol{Q}_G[K] = \boldsymbol{L}_Q \boldsymbol{V}_c[K] + \boldsymbol{R}_Q[K-1] \tag{7.104}$$

Let us further rewrite these constraints as one single constraint in the form

$$x[K] = \mathcal{L}\boldsymbol{V}_c[K] + \mathcal{R}[K-1] \tag{7.105}$$

where

$$\mathcal{L} \triangleq \begin{bmatrix} \boldsymbol{L}_V \\ \boldsymbol{L}_Q \end{bmatrix} \quad \text{and} \quad \mathcal{R} \triangleq \begin{bmatrix} \boldsymbol{R}_V \\ \boldsymbol{R}_Q \end{bmatrix} \tag{7.106}$$

Now the problem is in exactly the same format as Proposition 7.3, with x corresponding to x and $\mathbf{V}_c[K]$ corresponding to y of the Proposition. The optimal solution for the pilot voltage settings are simply given by

$$\mathbf{V}_c[K] = \mathbf{V}_c^{nom} + \mathcal{Y}(x^{nom} - \mathcal{L}\mathbf{V}_c^{nom} - \mathcal{R}[K-1]) \tag{7.107}$$

for

$$\mathcal{Y} = (\mathcal{L}^T Q \mathcal{L} + \mathbf{W}_c)^{-1} \mathcal{L}^T Q \tag{7.108}$$

Corresponding to this optimal solution for the pilot voltage settings, the generator voltages and the reactive generations are given by

$$x[K] = x^{nom} + \mathcal{X}(x^{nom} - \mathcal{L}\mathbf{V}_c^{nom} - \mathcal{R}[K-1]) \tag{7.109}$$

with

$$\mathcal{X} = \mathcal{L}\mathcal{Y} - \mathcal{I} \tag{7.110}$$

Note that in the process of solving the optimality problem, inequality constraints such as voltage or reactive generation limits are not explicitly taken in to account, for the purpose of simplicity. In real situations, these physical limits must be checked to ensure that all generators operate in admissible ranges.

The obtained optimal solution forms a control-driven discrete-event process on the tertiary level time scale, driven by the load variations $\boldsymbol{d}_t[K]$ through $\mathcal{R}[K-1]$. As a result, the optimal solution will be a function of the load variations so that the global system is kept optimal as loading varies.

7.3.4 Fully Decentralized Optimization

As opposed to the fully centralized optimization discussed in the previous section, here we study the the tertiary level control in a fully decentralized fashion, i.e. each region within the interconnected system optimizes its own performance criterion, while assuming no structural information about the rest of the system. In the regional optimization process, each region measures the tie-line flows, and uses the measurement to determine its optimal settings.

Consider a single region within an interconnected system consisting of R regions. Let V_G, Q_G and V_c represent the generator voltages, reactive generations and critical pilot node voltages of the region under consideration. Similar to the fully centralized optimization, the performance criterion for the region in the interval $[KT_t, (K+1)T_t]$ can be written in the form

$$J[K] = J(V_G[K], Q_G[K], V_c[K]) \tag{7.111}$$

Let us also take the quadratic form

$$\begin{aligned} J[K] \;=\; & (V_G[K] - V_G^{nom})^T W_V (V_G[K] - V_G^{nom}) \\ & + (Q_G[K] - Q_G^{nom})^T W_Q (Q_G[K] - Q_G^{nom}) \\ & + (V_c[K] - V_c^{nom})^T W_c (V_c[K] - V_c^{nom}) \end{aligned} \tag{7.112}$$

Again, V_G^{nom}, Q_G^{nom} and V_c^{nom} are the desired nominal values for the generator voltages, reactive generations and pilot load voltages of the particular region, W_V, W_Q and W_c are the relative weighing matrices for the corresponding terms. The purpose of the optimization process is also to determine the optimal setting for the pilot voltages $V_c[K]$, as in the fully centralized optimization case.

The constraints between $V_G[K]$ and $V_c[K]$, $Q_G[K]$ and $V_c[K]$ are derived in Section 7.3 as given in (7.61) and (7.67). For convenience, let us repeat them

$$V_G[K] = L_V V_c[K] - L_{Vd} F_L[K] + R_V[K-1] \tag{7.113}$$

$$Q_G[K] = L_Q V_c[K] - F_Q[K] + R_Q[K-1] \tag{7.114}$$

where $R_V[K-1]$ and $R_Q[K-1]$ are defined as

$$R_V[K-1] = V_G[K-1] - L_V V_c[K-1] + L_{Vd} F_L[K-1] + L_{Vd} d_t[K-1] \tag{7.115}$$

$$R_Q[K-1] = Q_G[K-1] - L_Q V_c[K-1] + F_Q[K-1] + L_{Qd} d_t[K-1] \tag{7.116}$$

Similar to the fully centralized optimization case, let us convert the problem into the form in Proposition 7.3 in order to utilize the proposition. Define again the vector of generator quantities for the particular region under study

$$x \triangleq \begin{bmatrix} V_G \\ Q_G \end{bmatrix} \tag{7.117}$$

and its weighting matrix

$$\mathcal{Q} \triangleq \text{BlockDiag}(W_V, W_Q) \tag{7.118}$$

The performance criterion in (7.90) can now be rewritten as

$$J[K] = (x[K] - x^{nom})^T \mathcal{Q} (x[K] - x^{nom}) + (V_c[K] - V_c^{nom})^T W_c (V_c[K] - V_c^{nom}) \tag{7.119}$$

The two constraints (7.113) and (7.114) can be put together into

$$x[K] = \mathcal{L} V_c[K] - \mathcal{F}[K] + \mathcal{R}[K-1] \tag{7.120}$$

where

$$\mathcal{L} \triangleq \begin{bmatrix} L_V \\ L_Q \end{bmatrix}, \quad \mathcal{F} \triangleq \begin{bmatrix} L_{Vd} F_L \\ F_Q \end{bmatrix}, \quad \text{and} \quad \mathcal{R} \triangleq \begin{bmatrix} R_V \\ R_Q \end{bmatrix} \tag{7.121}$$

In the optimization process, the tie-line flows $\mathcal{F}[K]$ will be taken as a measured constant. By Proposition 7.3, the resulting optimal solution is given as

$$V_c[K] = V_c^{nom} + \mathcal{Y}(x^{nom} - \mathcal{L}V_c^{nom} + \mathcal{F}[K] - \mathcal{R}[K-1]) \tag{7.122}$$

for

$$\mathcal{Y} = (\mathcal{L}^T Q \mathcal{L} + W_c)^{-1} \mathcal{L}^T Q \tag{7.123}$$

Corresponding to this optimal solution for the pilot voltage settings, the generator voltages and the reactive generations are given by

$$x[K] = x^{nom} + \mathcal{X}(x^{nom} - \mathcal{L}V_c^{nom} + \mathcal{F}[K] - \mathcal{R}[K-1]) \tag{7.124}$$

with

$$\mathcal{X} = \mathcal{L}\mathcal{Y} - \mathcal{I} \tag{7.125}$$

All individual regions measure the tie-line flows, and use equation (7.122) to determine their optimal pilot voltage settings.

7.3.5 Partially Centralized/Decentralized Optimization

Fully centralized and fully decentralized approaches discussed above represent two extremes, one takes the full information about the global system and one neglects the structural properties of the rest of the system. One approach that lies in between the two is the partially centralized/decentralized optimization method, in which one assumes partial information about the rest of the system. The partial information is simply the aggregate models discussed before. This approach falls into the category of game theory. We first give a brief review of the game theory.

Review of Basic Game Theory

This subsection gives a brief review of the basic Nash game theory. Details can be found in [34] [35] [36]. We believe that the Nash strategy is more relevant for the voltage control problem than other game settings such as leader-follower game theory.

Consider a game setting consisting of R persons. Assume that each person has the equal role in the game. Each person tries to optimize its own performance criterion which is coupled to other persons' performance criteria. The standard setting for this problem is given by

$$\begin{cases} \min_{u_1} J_1 = J_1(u_1, u_2, \cdots, u_R) \\ \cdots \\ \min_{u_R} J_R = J_R(u_1, u_2, \cdots, u_R) \end{cases} \tag{7.126}$$

where the vector u_i is the decision variables of person i. Notice that the hidden assumption with this setting is that each person knows explicitly how the other persons' decisions affect its performance criterion. This is in general not the case for power system, where the interactions among subsystems are only through the tie-line flows. More details will be discussed on this later.

The optimal solution for each person is obtained by optimizing each person's performance criterion assuming a given set of other persons' decisions. This is often called the *reaction* of the person. The reaction curves are defined as

$$\frac{\partial J_i}{\partial u_i} = 0, \quad i = 1, 2, \cdots, R \tag{7.127}$$

The solution $(u_1, u_2, \cdots, u_R)$ obtained from this set of equations are often called the *Nash* strategy.

As an example, let us consider a symmetric 2-person game defined by

$$J_1 = u_1^2 + 2u_2 + 1 \tag{7.128}$$

$$J_2 = u_2^2 + 2u_1 + 1 \tag{7.129}$$

The reaction curves are obtained from (7.127) as

$$\frac{\partial J_1}{\partial u_1} = 2u_1 = 0, \quad \text{for player 1} \tag{7.130}$$

$$\frac{\partial J_2}{\partial u_2} = 2u_2 = 0, \quad \text{for player 2} \tag{7.131}$$

The Nash strategy is simply obtained as

$$u_1 = u_2 = 0 \tag{7.132}$$

The costs under the Nash strategy can be calculated as

$$J_1 = J_2 = 1 \tag{7.133}$$

Notice that the Nash strategy is in general not the "best" solution for the players. For the above simple example, we can easily show that for

$$u_1 = u_2 = -1 \tag{7.134}$$

the cost for each person is given by

$$J_1 = J_2 = 0 \tag{7.135}$$

i.e. both will have smaller costs if they take the solution $u_1 = u_2 = -1$, which is the centralized global optimal solution. Although the Nash strategy is not the real optimal solution for the system, it is proven to be a stable one, in the sense that if any

players give up the Nash strategy and select other solutions, they will have a higher cost than the one when they stay at the Nash strategy. For the same example given above, assume that both players are at the Nash solution $u_1 = u_2 = 0$ with the cost $J_1 = J_2 = 1$. If player 1, for example, changes to the real optimal solution $u_1 = -1$, while player 2 stays at the Nash solution $u_2 = 0$, the costs for the two players will be $J_1 = 2$ and $J_1 = -1$. Clearly player 1, who moved away from the Nash solution, has a higher cost, while player 2, who stayed at the Nash solution, receives a lower cost. As a result, both players will try to stay at the Nash strategy.

Game Formulation for Voltage Control

In power systems, the decision variables are the generator or equivalently critical pilot point voltage settings. For a specific region, the performance criterion usually involves quantities like the transmission losses, reactive generations, the generator voltages, and the critical pilot point voltages. The decision variables of other regions do not directly enter the expression of the performance criterion for this region. In other words, the competition is not in a standard game theoretical setting.

To see this, we consider again an interconnected system consisting of R regions. Let the performance criterion of any single region be given by

$$J[K] = J(V_G[K], Q_G[K], V_c[K]) \tag{7.136}$$

Note that all variables in this expression are associated with this particular region only, no variables associated with other regions directly enter the cost function. The coupling among the regions occurs only when the constraints among $V_G[K]$, $Q_G[K]$, and $V_c[K]$ are introduced. These constraints involve the inter-regional tie-line flows,

which couple all interconnected regions together.

To see this, let us rewrite (7.136) as

$$J[K] = J(x[K], V_c[K]) \tag{7.137}$$

with x as being defined in (7.117). The constraint between x and V_c was derived in (7.120) as

$$x[K] = \mathcal{L}V_c[K] - \mathcal{F}[K] + \mathcal{R}[K-1] \tag{7.138}$$

where all quantities were defined in the previous subsection. In this equation, the tie-line flow $\mathcal{F}[K]$ acts to couple different regions together, because it is a function of the generator and/or load voltages of all the involved regions. This function can be expressed as

$$\begin{aligned}\mathcal{F}[K] = \mathcal{N}_G \boldsymbol{V}_G[K] + \mathcal{N}_c \boldsymbol{V}_c[K] \;=\; & \mathcal{N}_G^I V_G^I[K] + \cdots + \mathcal{N}_G^R V_G^R[K] \\ & + \mathcal{N}_c^I V_c^I[K] + \cdots + \mathcal{N}_c^R V_c^R[K]\end{aligned} \tag{7.139}$$

where $\boldsymbol{V}_G$ and $\boldsymbol{V}_c$ are the generator voltages and critical pilot voltages of the global system consisting of all regions involved, matrices $\mathcal{N}_G$ and $\mathcal{N}_c$ are related to the strength of interconnections. When all interconnections are removed, they both are zero.

In light of this constraint, the performance criterion in (7.137) becomes a function of the pilot load voltages, generator voltages of all the regions within the interconnected global system. In other words, Eq. (7.137) can be represented in the form of

$$J[K] = J(\boldsymbol{V}_G[K], \boldsymbol{V}_c[K]) \tag{7.140}$$

With this performance criterion, we define the reaction curves for this particular region under study as

$$\frac{\partial J}{\partial V_c} = 0 \tag{7.141}$$

The solution corresponding to the intersection of these reaction curves is called the *Nash* strategy for the power system. This definition is a natural extension of the standard Nash reaction curves.

Let us explicitly find the Nash solution for a quadratic performance criterion

$$J[K] = (x[K] - x^{nom})^T Q(x[K] - x^{nom}) + (V_c[K] - V_c^{nom})^T W_c(V_c[K] - V_c^{nom}) \quad (7.142)$$

To do this, we need the following vector differentiation results:

Vector Differentiation *Let x and y, $y = y(x)$, be column vectors, and let A be a matrix (independent of x) of appropriate dimension such that all operations are meaningful. The following is true:*

$$\frac{\partial}{\partial x}\left[\, x^T A\, y \,\right] = A\, y + \left[A\, \frac{\partial y}{\partial x}\right]^T x \quad (7.143)$$

$$\frac{\partial}{\partial x}\left[\, y^T A\, y \,\right] = \left[\frac{\partial y}{\partial x}\right]^T (A + A^T)\, y \quad (7.144)$$

where the matrix

$$\frac{\partial y}{\partial x} \triangleq \left[\frac{\partial y_i}{\partial x_j}\right]_{i,j} \quad (7.145)$$

One can easily verify these two equations by simply expanding the expressions and doing element-by-element differentiation. Details are left to the reader.

Now we are ready to derive the analytic Nash solution for the posed problem. From Eq. (7.142), using the above vector differentiation results, one has

$$\frac{\partial J}{\partial V_c} = 2\left[\frac{\partial x}{\partial V_c}\right]^T Q(x[K] - x^{nom}) + 2W_c(V_c[K] - V_c^{nom}) = 0 \quad (7.146)$$

Matrix $\frac{\partial x}{\partial V_c}$ can be found from (7.138) as

$$\frac{\partial x}{\partial V_c} = \mathcal{L} - \frac{\partial \mathcal{F}}{\partial V_c} \tag{7.147}$$

Using further Equation (7.139), one obtains

$$\frac{\partial \mathcal{F}}{\partial V_c} = \mathcal{N}_c + \mathcal{N}_G \frac{\partial V_G}{\partial V_c} = \mathcal{N}_c + \mathcal{N}_G L_V \tag{7.148}$$

Therefore

$$\frac{\partial x}{\partial V_c} = \mathcal{L} - \mathcal{N}_c - \mathcal{N}_G L_V \tag{7.149}$$

From this equation, we can rewrite (7.146) as

$$(\mathcal{L} - N_c - \mathcal{N}_G L_V)^T \mathcal{Q}(x[K] - x^{nom}) + W_c(V_c[K] - V_c^{nom}) = 0 \tag{7.150}$$

Together with the constraint relationship (7.138), we obtain

$$V_c[K] = V_c^{nom} + \mathcal{Y}(x^{nom} - \mathcal{L}V_c^{nom} + \mathcal{F}[K] - \mathcal{R}[K-1]) \tag{7.151}$$

where $\mathcal{Y}$ is defined by

$$\mathcal{Y} = [(\mathcal{L} - \mathcal{N}_c - \mathcal{N}_G L_V)^T \mathcal{Q}\mathcal{L} + W_c]^{-1}(\mathcal{L} - \mathcal{N}_c - \mathcal{N}_G L_V)^T \mathcal{Q} \tag{7.152}$$

In this optimization result, the optimal pilot voltage settings are expressed explicitly in terms of the tie-line flows, which are measured by each individual region. Similar to the previous cases, we can find the generator voltages and the reactive generations, corresponding to this optimal solution for the pilot voltage settings, as

$$x[K] = x^{nom} + \mathcal{X}(x^{nom} - \mathcal{L}V_c^{nom} + \mathcal{F}[K] - \mathcal{R}[K-1]) \tag{7.153}$$

with

$$\mathcal{X} = \mathcal{L}\mathcal{Y} - \mathcal{I} \tag{7.154}$$

Again, if $x^{nom} = \mathcal{L}V_c^{nom} - \mathcal{F}[K] + \mathcal{R}[K-1]$, i.e. the two nominal values also satisfy the constraint, then the optimal solution is simply the nominal values.

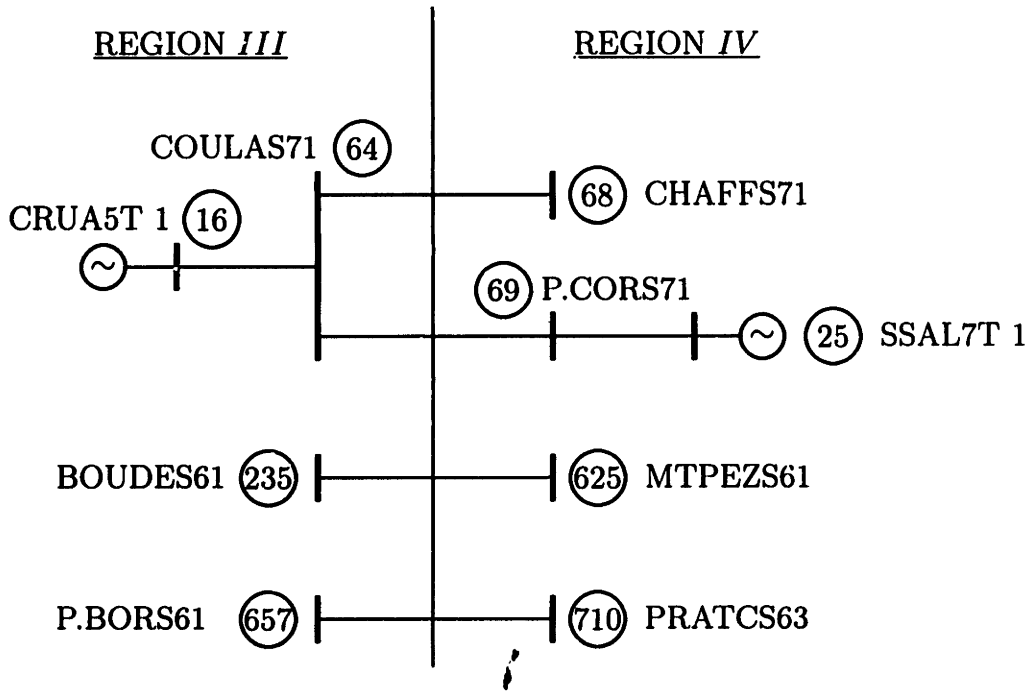

Figure 7.4: Tie Line Interconnections on the French Network

7.3.6 French Power Network Simulations

In this section, we describe the French Power Network as an example to illustrate the concepts and results developed in the previous sections. The most serious coordination problems are described to us by the EDF personels as occurring for two regions on the EDF Network. The entire French Power Network consists of more than 1000 nodes, and is divided into 7 regions. The two most important regions for the study of coordination are the eastern part and south eastern part of France. To be consistent with the French division, we also name the two regions as region III and IV. The boundary interconnections are depicted in Figure 7.4.

These two regions are highly interconnected through two strong tie-lines COULAS71 to CHAFFS71, and COULAS71 to P.CORS71. There are also two weak tie-lines con-

Regions	Pilot Nodes	Control Units
III	COULAS71	CRUA5T 1
III	TRI.PS61	TRICAT 1
III	TAVELS71	ARAMOT 1
III	SEPTES61	M.PONT 1
IV	CHAFFS71	BUGEYT 2
IV	P.CORS71	SSAL7T 1
IV	GIVORS61	LOIRET 3
IV	CPNIES61	VAUJH 7
IV	ALBERS71	S.BIH 4

Table 7.1: Pilot Nodes and Control Units of the EDF Network

necting the two regions, BOUDES61 to MTPEZS61, and P.BORS61 to PRATCS63. There are totally 205 nodes in these two regions. Region *III* has 4 pilot nodes and Region *IV* has 5 pilot nodes. The pilot voltages and the generating units participating in the secondary control are listed in Table 7.1.

The practical problems that may arise when the regional secondary voltage controls are not appropriately coordinated can be classified into the dynamical problems and static problems. The dynamical problems are seen, for example, as the overshooting of pilot voltages, due to coupling among the pilot voltages, or reactive generation outputs of units moving in opposition directions during the transient process. The static problems arise when each region chooses its set points for the pilot voltages without taking into account the neighboring region. Such scenarios may result in excessive and useless reactive power exchanges on the tie lines or large unbalance of the reactive generations on the system. In such cases, the ability of the network to handle rapid cascades of endangering events can be greatly reduced.

Here we use the coordination schemes described in the previous sections to address

Regions	Control Units	Maximum	Before Control	After Control
III	CRUA5T 1	2111	455	844
III	TRICAT 1	488	198	258
III	ARAMOT 1	674	386	312
III	M.PONT 1	619	283	281
IV	BUGEYT 2	976	965	936
IV	SSAL7T 1	1438	1166	681
IV	LOIRET 3	309	−83	94
IV	VAUJH 7	889	296	425
IV	S.BIH 4	371	249	191

Table 7.2: Maximum & Actual Generations of the EDF Network, MVAR

these problems. It will be shc vn that the developed theory for tertiary level coordination successfully solves the mentioned problems. The simulation results show that it is feasible and efficient to achieve the coordination purposes by directly controlling a few selected pilot voltages at the subsystem level.

Generation Alignment Control

First we show the fully centralized tertiary control results of aligning the generations of the generating units participating in the secondary control. The performance objective is chosen as the alignment of all generation ratios, defined as the ratio of reactive generation to the maximum capacity of each generator. The idea is that the generation limit is the least possible to be reached when the generators are kept aligned with their generations, because all generators reach their limits at the same time. The maximum generation capacities and actual generations of the 9 generators in Regions *III* and *IV*, before and after the tertiary control, are given in Table 7.2.

Before the tertiary control, the reactive generations are quite uneven, with one

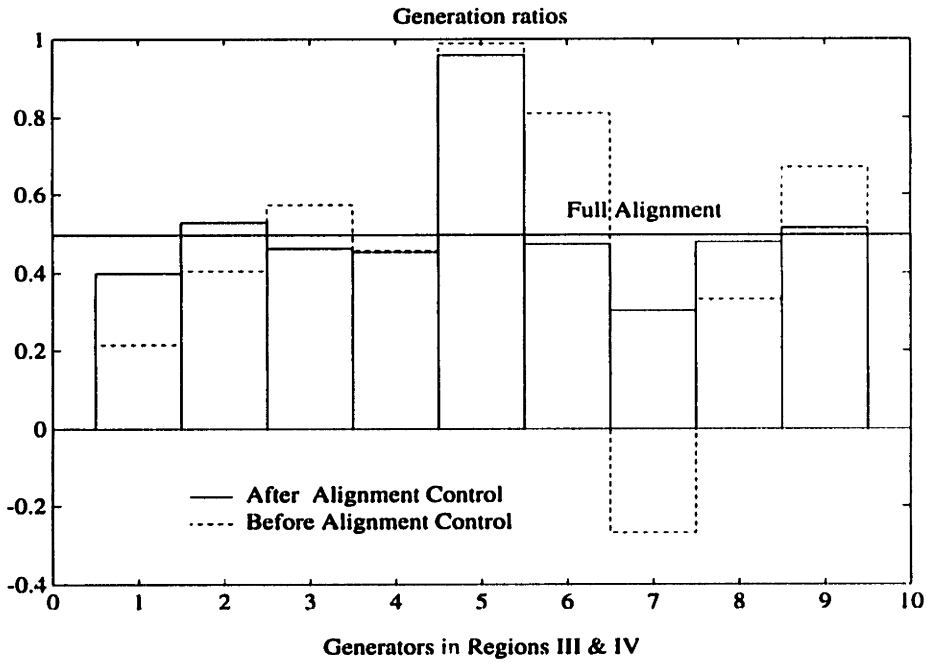

Figure 7.5: Generation Ratio Alignment

generator named LOIRET 3 absorbing reactive power of 83 MVAR. Let us plot the generation ratios for the 9 generators in Region *III* and Region *IV* of the French system before and after the tertiary control, in Figure 7.5.

It is seen that the tertiary control scheme simply eliminates the situation of generator absorbing reactive power as an actual load to the network. The generator LOIRET 3 is generating reactive power of 94 MVAR after the tertiary control. The generation ratios are uniformly made more even towards the complete alignment line. It is also noted that the units do not reach the full alignment. The reason is that some units are already operating at their limits, and thus no further adjustments on their terminal voltages can be done. However, all units go towards the alignment line after the tertiary control, even when some units are operating at the limits.

Tie-Line Flow Control

The tertiary control can reset the tie-line flows by adjusting the pilot voltage set-points in each region. This can be easily done by imposing additional equality constraint

$$\mathcal{F}[K] = \mathcal{F}^{set} \tag{7.155}$$

where $\mathcal{F}^{set}$ is the desired scheduling value. Using Equation (7.139), one has

$$\mathcal{N}_G \mathbf{V}_G[K] + \mathcal{N}_c \mathbf{V}_c[K] = \mathcal{F}^{set} \tag{7.156}$$

This is already in the form of (7.105) or (7.138), and can be readily incorporated into (7.105) or (7.138). The optimal solutions have thus exactly the same form as the ones given before.

We study the scenario in which the reactive load at bus BOUDES61 in Region III increases by 160 MVAR at time t=500 seconds. The goal of the tertiary control is to increase the reactive tie-line flow from CHAFFS71 in Region IV to COULAS71 in Region III by 20 MVAR to account for the load increase in region III. Figure 7.6 shows the reactive tie-line flow on this line. The tertiary control is activated at time t=800 seconds. Clearly we see that the flow is successfully controlled to the desired given new steady state value.

Generator Voltage Control

In this section, we present the case of adjusting pilot voltages so that generator voltages, which were at their limits before the tertiary control, move away from the limits and stay within the desired bounds. The Nominal Voltages for the generators and Pilot nodes in Region III and IV are given in Table 7.3.

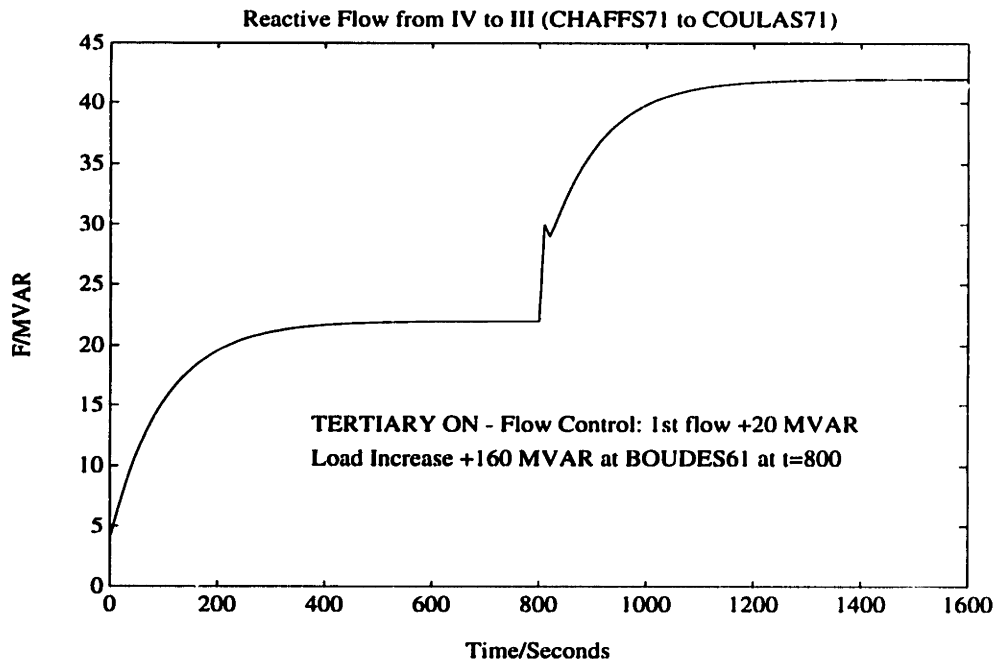

Figure 7.6: Tie-Line Flow Control

Regions	Control Units	Nominal	Pilot Nodes	Nominal
III	CRUA5T 1	418	COULAS71	415
III	TRICAT 1	238	TRI.PS61	234
III	ARAMOT 1	420	TAVELS71	410
III	M.PONT 1	245	SEPTES61	241
IV	BUGEYT 2	425	CHAFFS71	411
IV	SSAL7T 1	425	P.CORS71	415
IV	LOIRET 3	225	GIVORS61	235
IV	VAUJH 7	415	CPNIES61	410
IV	S.BIH 4	415	ALBERS71	410

Table 7.3: Nominal Voltages of Generators and Pilots of the EDF Network, KV

The weighting coefficients are chosen as the reciprocal of the corresponding nominal voltages, i.e.,

$$\boldsymbol{W}_G = \text{Diag}(1/V_{G1}^{nom}, \cdots, 1/V_{G9}^{nom}) \tag{7.157}$$

$$\boldsymbol{W}_c = \text{Diag}(1/V_{c1}^{nom}, \cdots, 1/V_{c9}^{nom}) \tag{7.158}$$

The generator and pilot voltages before and after the tertiary control are shown in Figures 7.7-7.12. It is seen that Generators BUGEYT 2, SSAL7T 1 and S.BIH hit their upper limits, and LOIRET 3 operates at its lower limit. It is noted that all of these generators are in Region IV. As a result of these generators operating already at their limits, some pilots cannot reach their set values. This is clearly seen from Figures 7.10-7.12. There are small steady state offsets in the responses of pilots GIVORS61, CPNIES61, and ALBERS71. More seriously, CHAFFS71 moves away from its setting from the beginning.

The tertiary control adjusts the set values of the pilot nodes in a way such that the voltages of the generators at upper limits will be lowered, and the voltages of the generators at lower limits will be increased. This adjustment ensures that all generators stay within their voltage bounds, and that all pilot voltages, as a consequence, will reach their new settings. Figures 7.7-7.12 show that all generators operate within the desired bounds, and all pilot voltages reach their settings after the tertiary control.

Tue Jan 25 12:10:41 1994

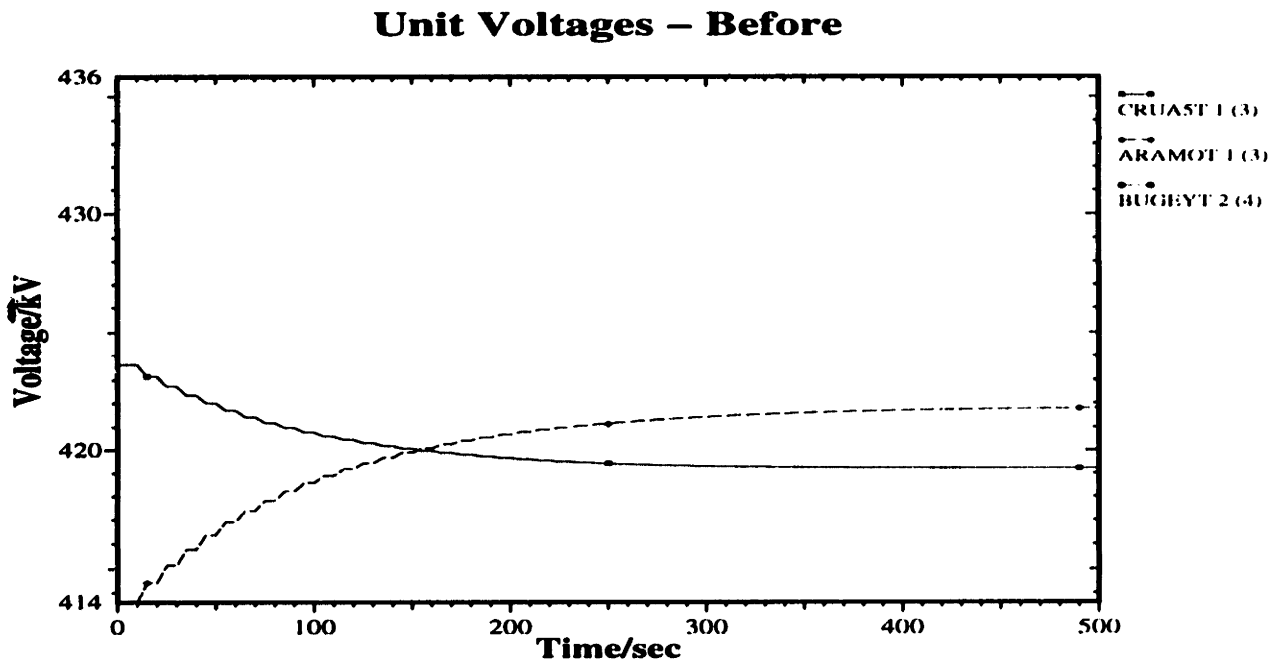

Tue Jan 25 12:08:28 1994

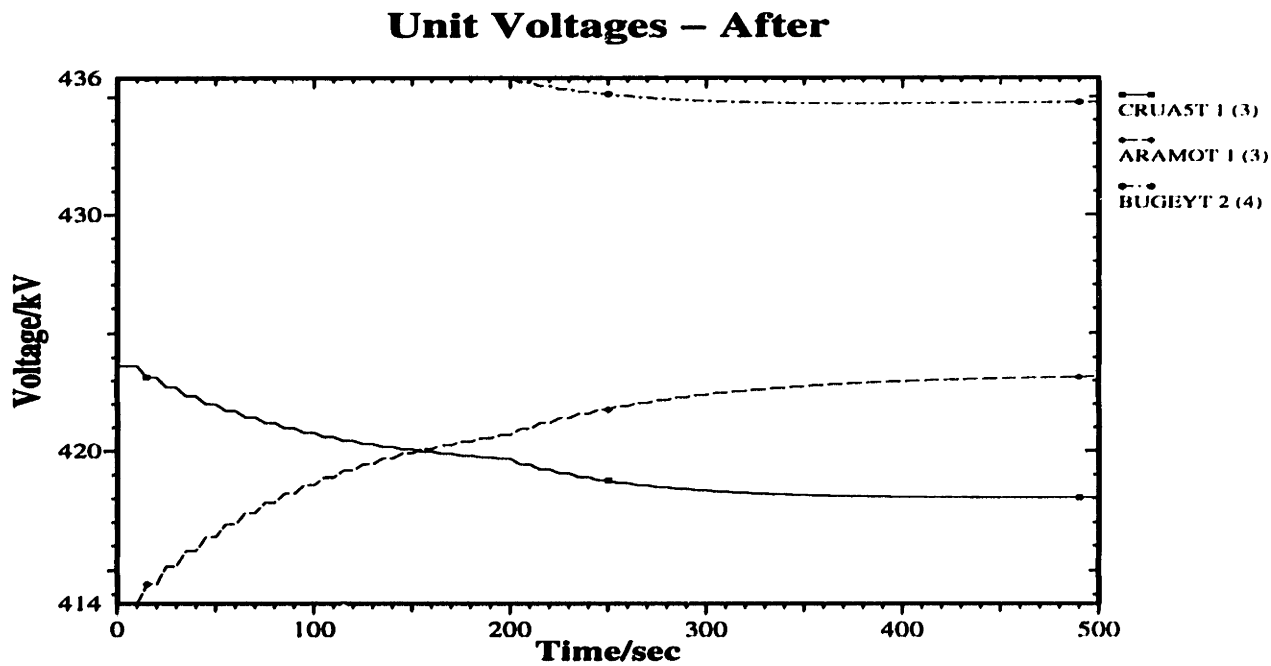

Figure 7.7: Generator Voltages: Before and After Tertiary Control

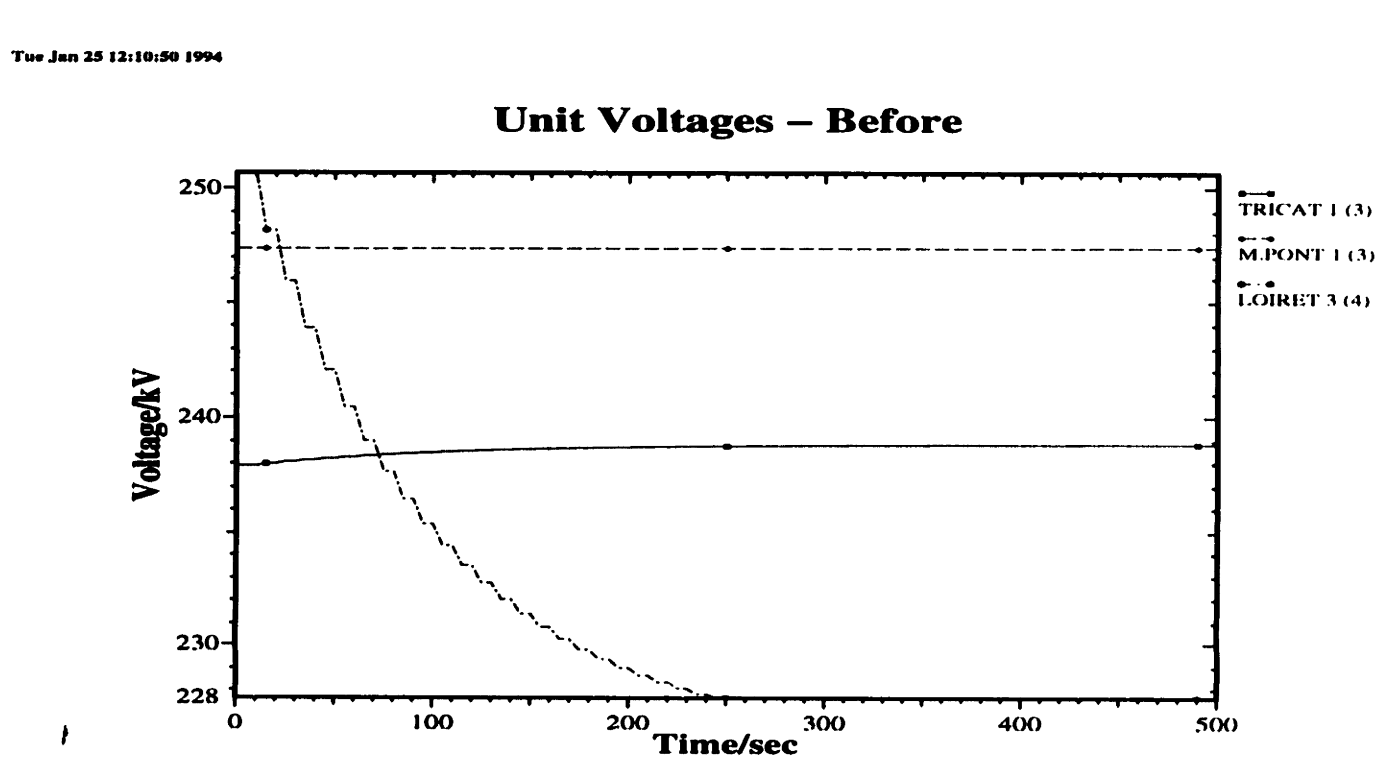

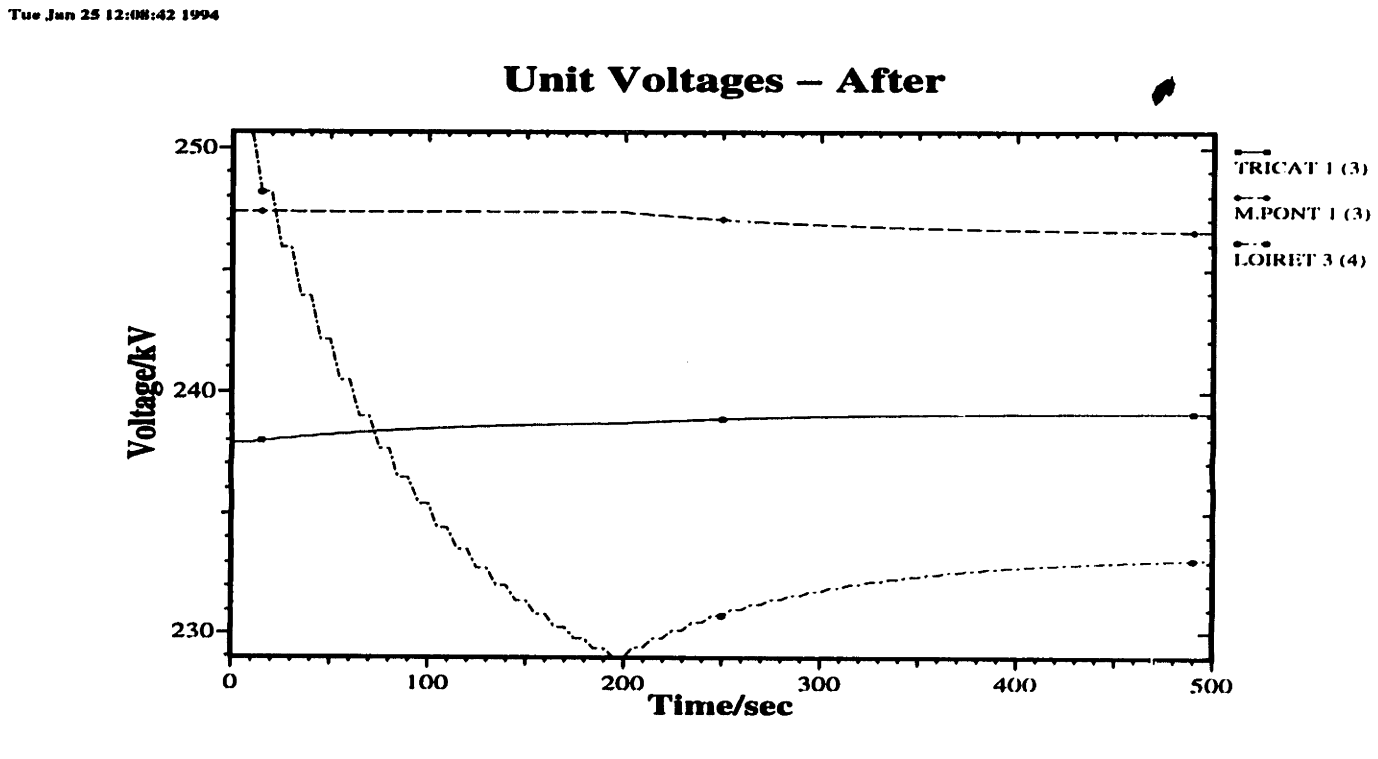

Figure 7.8: Generator Voltages: Before and After Tertiary Control

Tue Jan 25 12:10:56 1994

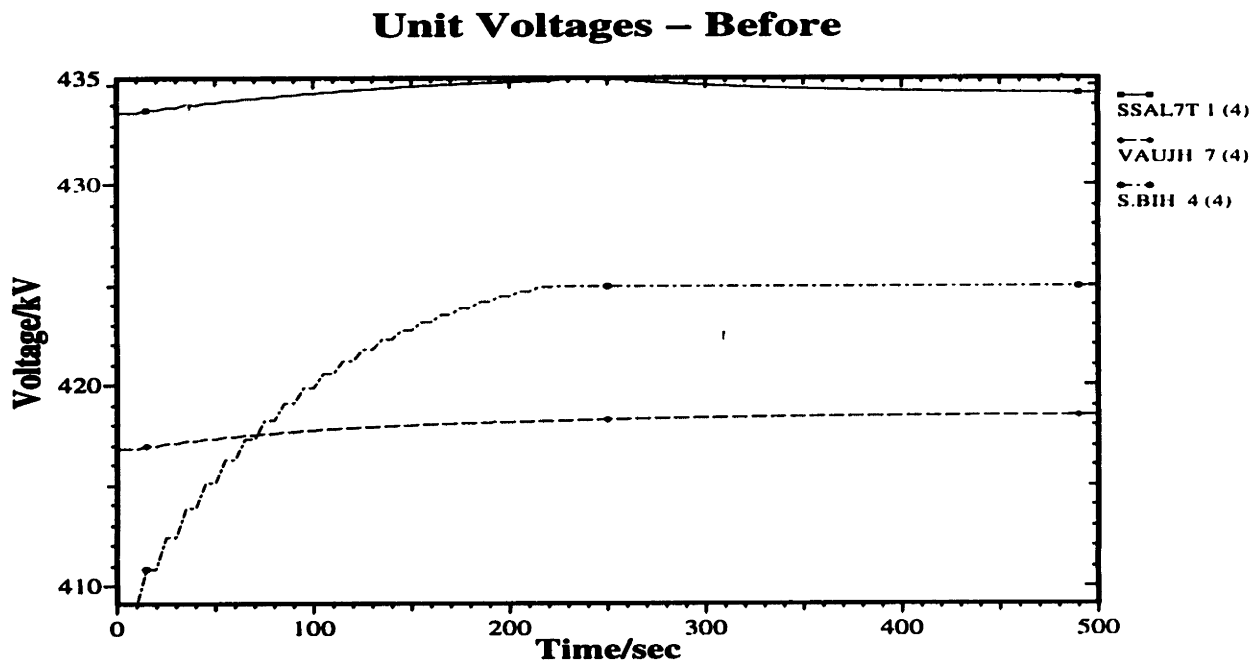

Tue Jan 25 12:08:51 1994

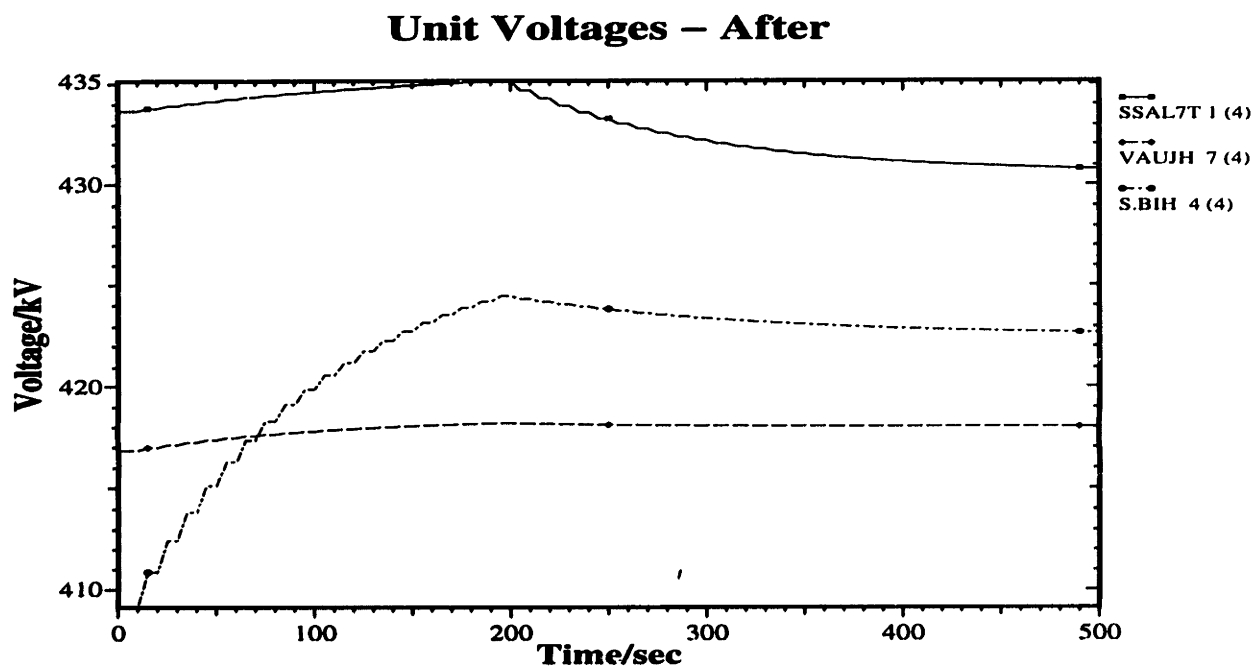

Figure 7.9: Generator Voltages: Before and After Tertiary Control

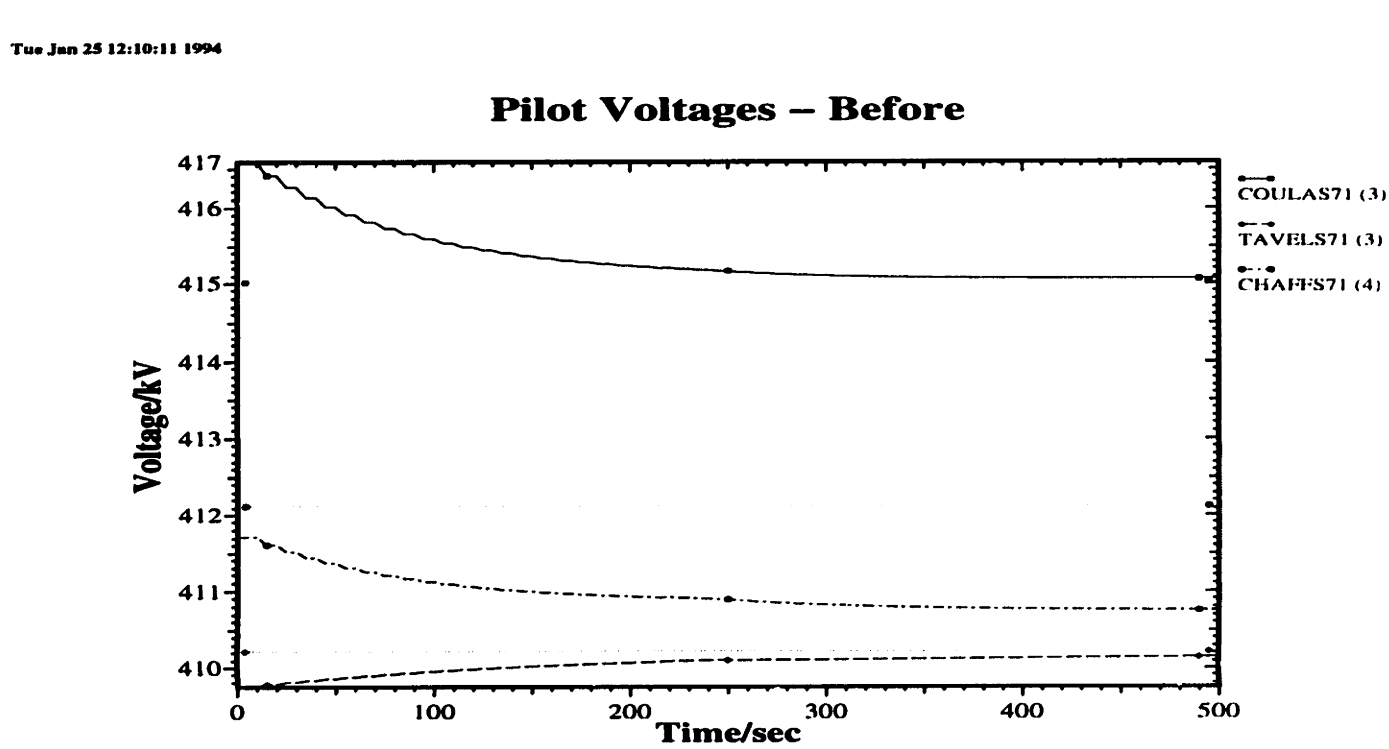

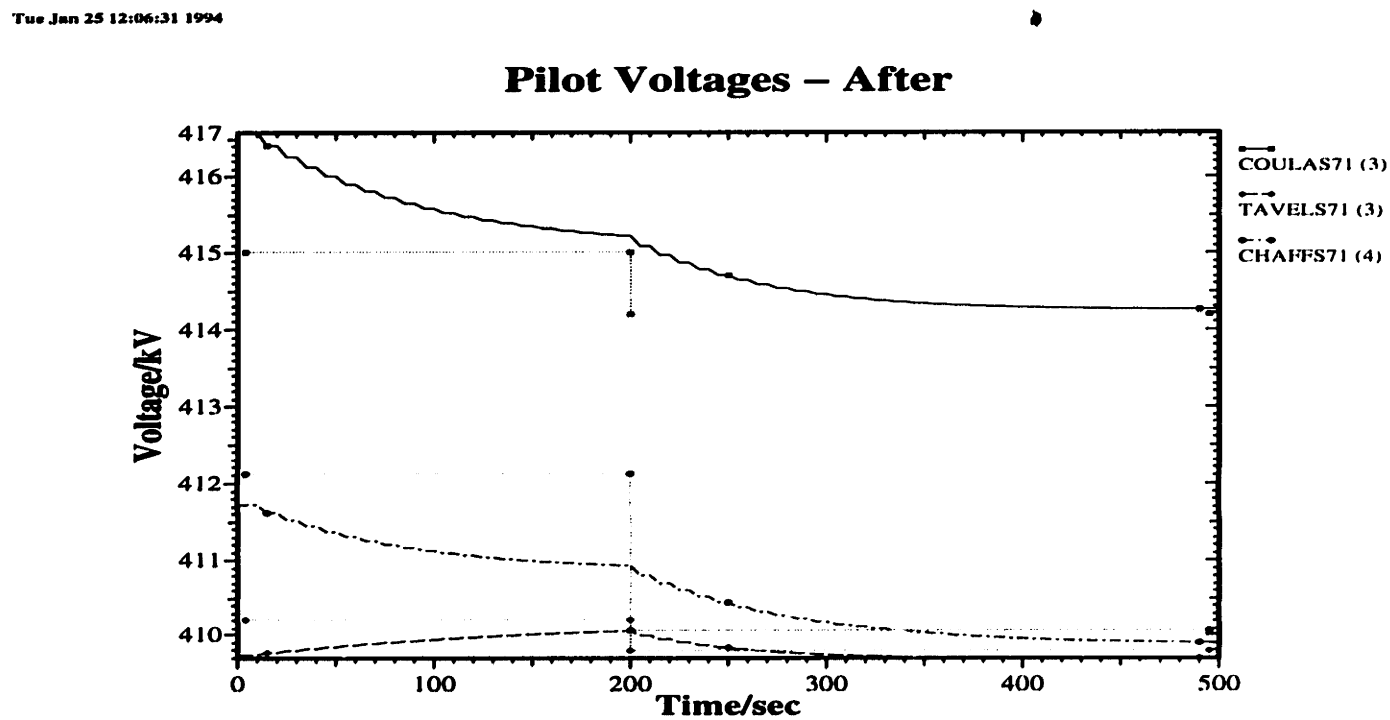

Figure 7.10: Pilot Voltages: Before and After Tertiary Control

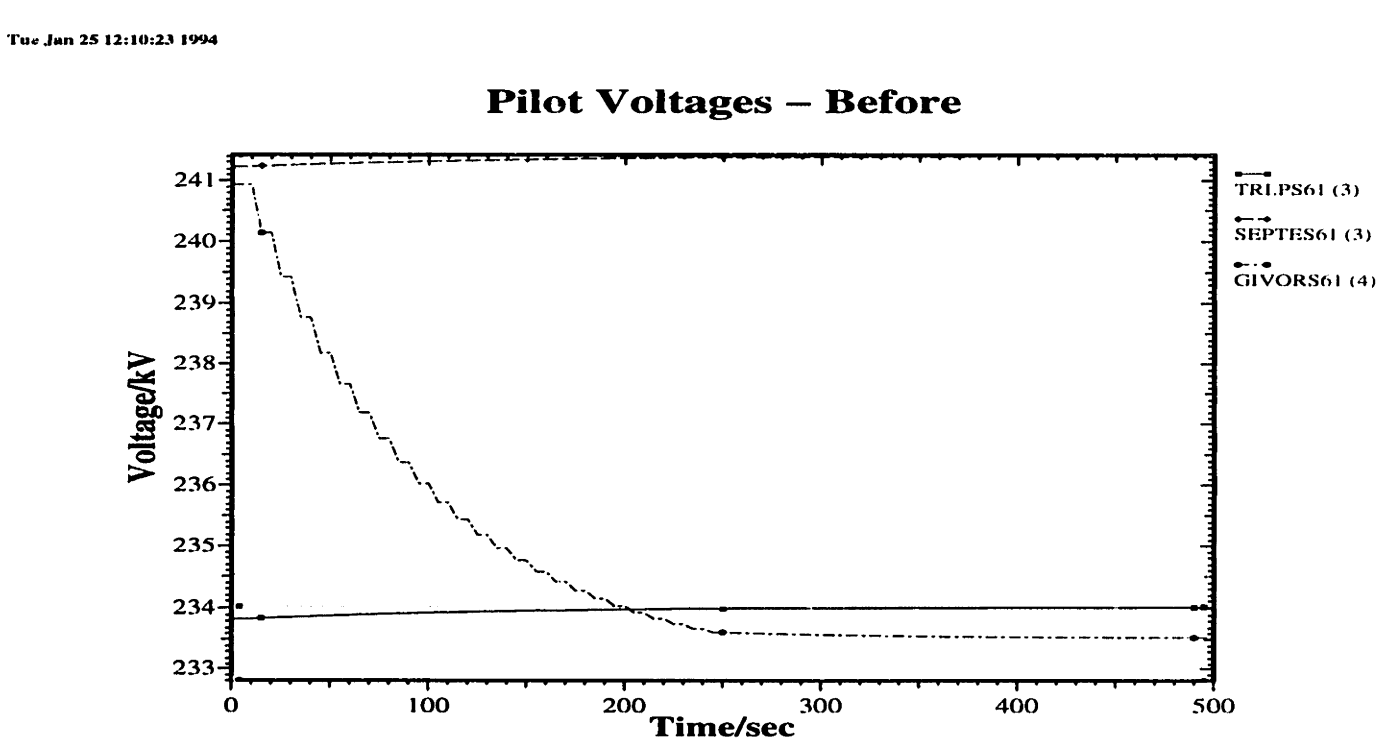

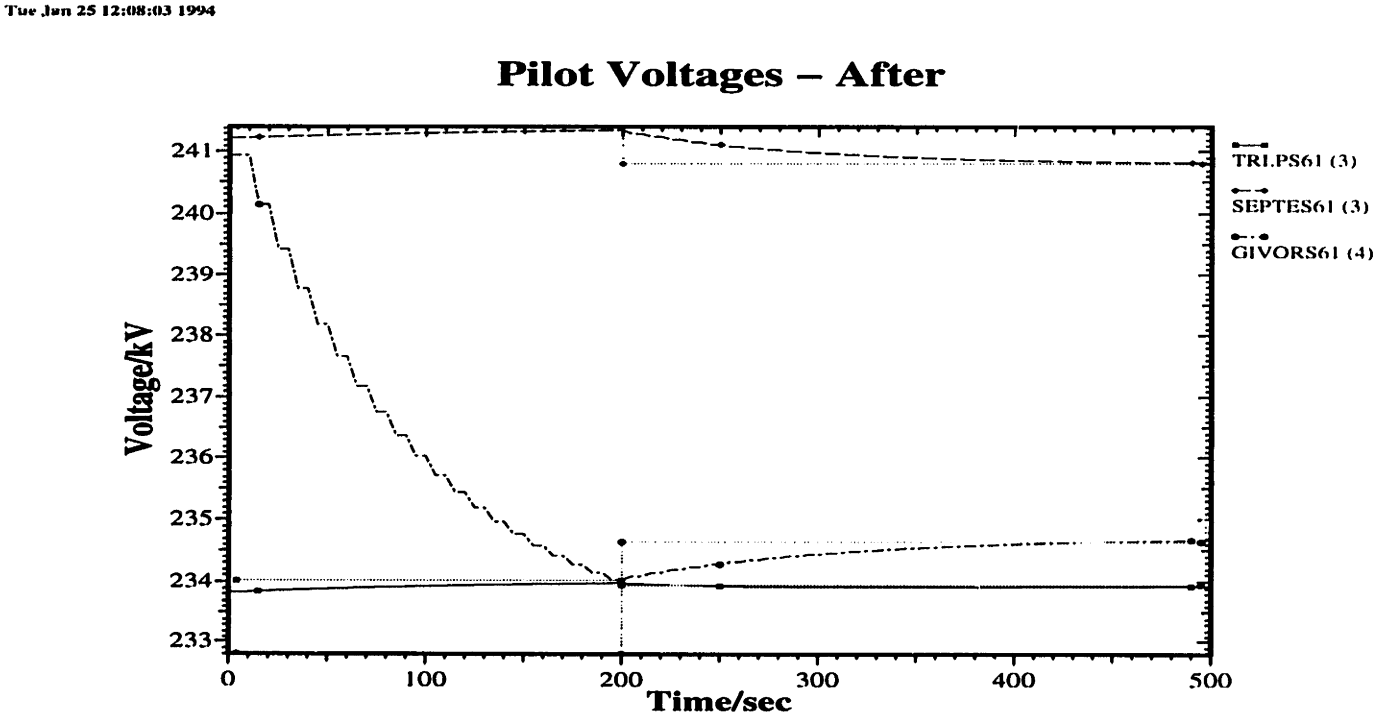

Figure 7.11: Pilot Voltages: Before and After Tertiary Control

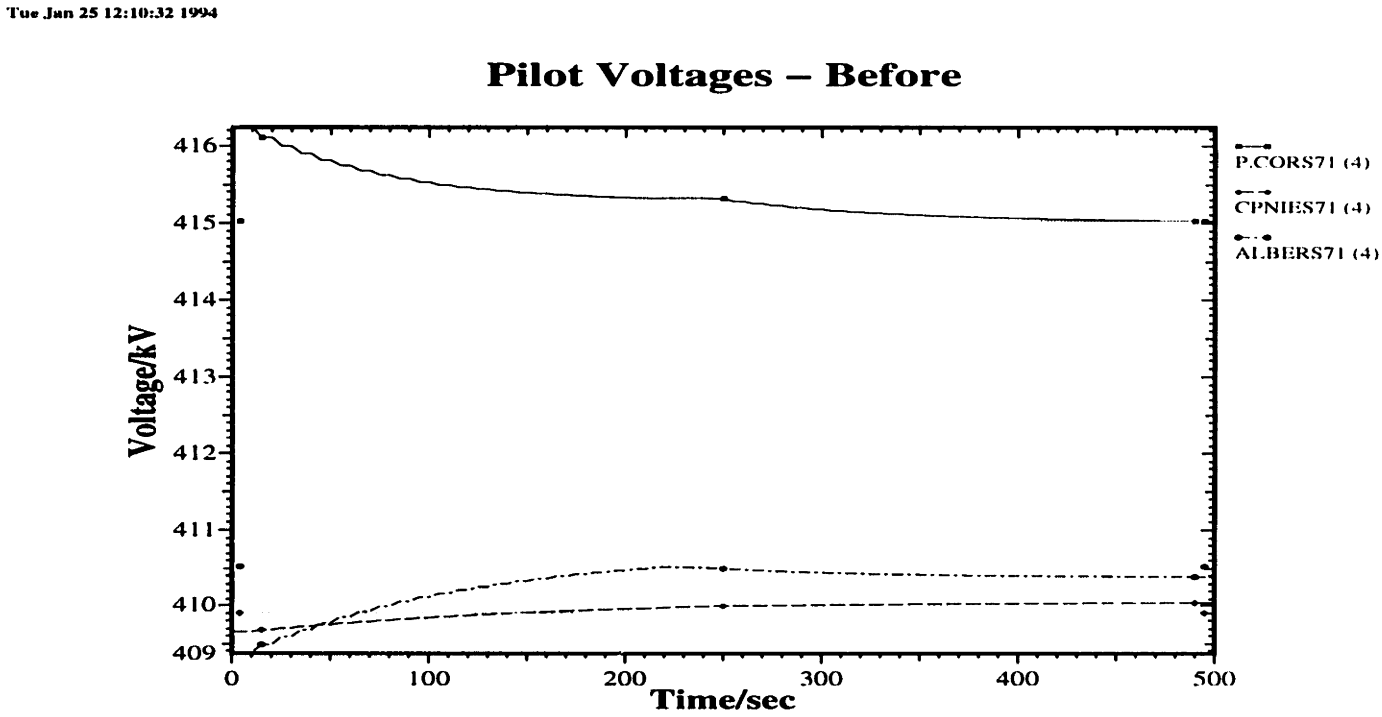

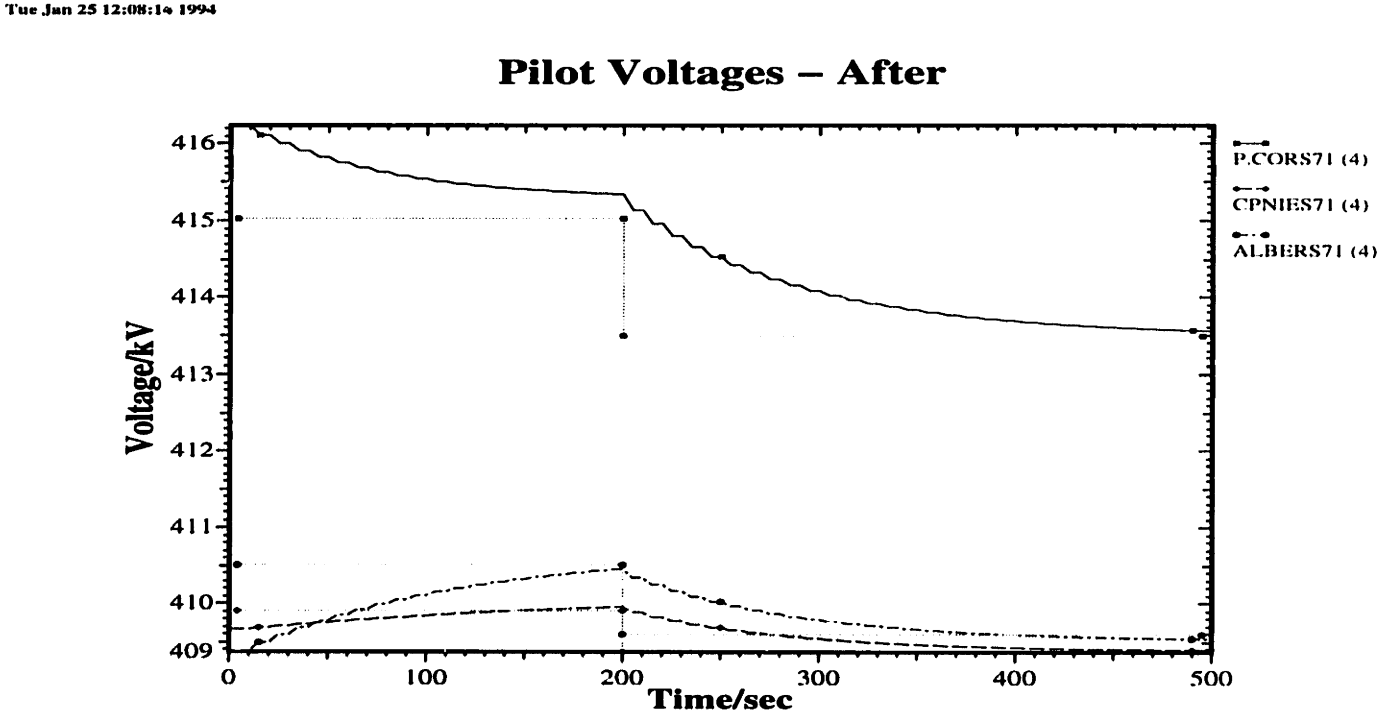

Figure 7.12: Pilot Voltages: Before and After Tertiary Control

7.4 Summary

In this part of the thesis, a hierarchical structure of voltage control for large-scale power systems is presented. Dynamics of an interconnected system are formulated by combining the local dynamics of individual generators and the network couplings. Under the assumption of stable primary voltage control design, the discrete-time voltage dynamics on slower time scales are derived. Improved secondary control is introduced and compared with the conventional control. Simulations show a significant improvement over the conventional control. The concept of tertiary level coordination is introduced. Simulations are done for both a small power system and the large-scale French Network to illustrate the proposed tertiary control schemes.

Conclusions

A structurally-based modeling and hierarchical control approach for large-scale electric power systems is proposed in this thesis. The interconnected system is decomposed according to the natural administrative boundaries. Dynamical models of each region are obtained by first deriving the local dynamics of individual components and then recognizing the coupling variables that interrelate local dynamics of all components in the system. The complete dynamical models in the standard ODE form in an extended state space are proposed by differentiating algebraic constraints imposed by the transmission network.

In contrast to the present state-of-the-art methods in large-scale system modeling, which typically require the weak interconnection assumption, the structurally-based approach proposed in this thesis does not require any typical assumptions on interactions among the subsystems. Avoiding the weak interconnection assumption offers an essential basis for modeling and analysis of power systems under extensive inter-regional wheeling, since strong interconnections are typically needed for this operating mode.

Based on the structural properties of the system, interaction variables on different control levels are defined and the corresponding interaction dynamical models are derived. These interaction variables reflect structural singularities of the system on different time scales and account for interactions among interconnected regions. It is important to note that interaction variables defined here have a simple physical interpretation in terms of real and reactive power flows on the tie-lines connecting subsystems. Tertiary level controllers are proposed for a systematic scheduling of tie-line

flows in response to load variations. They serve the functions of the automatic generation control and optimal coordination of the secondary voltage controllers. It is further shown that the newly proposed formulation lends itself to simple ways of entirely decentralized controls at the secondary level. This formulation naturally represents the DEP's evolving from interactions among the subsystems of large-scale electric power systems.

The approach is particularly suited for establishing different levels of model complexity directly associated with specific hierarchical levels of control design. Quasi-static control-driven models on slow time scales are derived, which are straightforward for control design at the secondary and tertiary levels: At the secondary level an optimal design is possible in which a performance criterion is regional. The main function of the secondary level is to assign set values to primary controllers to reach desired set values at selected outputs of each subsystem in a manner that guarantees subsystem level optimality, without neglecting interactions with the neighboring subsystems.

A much simplified relevant model formulation is derived at a secondary level which captures only changes in set values at primary controllers at each subsystem level needed to regulate changes in relevant output variables to within the feasible, and possibly most desired range of operation. In the earlier literature, even in the most frequently studied examples of the secondary level control problems the assumption of stable primary control has not been used for establishing simpler models. In this thesis this assumption is taken as the starting point in formulating the model directly relevant for the secondary level frequency and voltage controls. The model is also interpreted as representing a discrete-event process of controlling a moving equilibrium

[8] to an a priori defined region of acceptable operation in response to the slow system disturbances.

The tertiary level, on the other hand, employs the derived aggregate models for assigning desired output set values to achieve the coordination purposes. Interactions among the interconnected regions are essential in establishing game-theoretic trade-offs between the subsystem performance criteria and the single performance criterion of the interconnected system. The use of aggregate models proposed is essential for defining an explicit, closed form relationship between output settings at subsystem levels and the desired interaction settings which lead to the optimal system performance. This is needed to implement the desired interactions among the subsystems. From a physical viewpoint these flows are still direct consequences of states and controls in all subsystems, and are controlled to certain values by directly changing control settings at subsystem levels.

Bibliography

[1] D. N. Ewart, "Automatic Generation Control: Performance Under Normal Conditions", Proc. of the Systems Engineering for Power: Status and Prospects, Henniker, NH, August 1975.

[2] M. Ilic, X. Liu, "Direct Control of Inter-Area Dynamics in Large Power Systems Using Flexible AC Transmission Systems (FACTS) Technology", 1993, pending.

[3] M. Ilic, J. Zaborszky, *Fundamentals of Voltage Analysis, and Control*, Springer-Verlag, to appear.

[4] NYPP-OH TSWG Report, Phase V, Planning Studies, Vol I, August 1992.

[5] B. Avramovic, P. Kokotovic, J. Winkelman, J. Chow, "Area Decomposition for Electro-mechanical Models of Power Systems", *Automatica*, Vol. 16, 1980.

[6] M. Calovic, "Recent Developments in Decentralized Control of Generation and Power Flows", *Proc. 25th IEEE Conference on Decision and Control*, Athens, Greece, 1986.

[7] "Definitions for Terminology for Automatic Generation Control on Electric Power Systems", IEEE Standard 94, *IEEE Transactions on Power Apparatus and Systems*, Vol. PAS-89, July/August 1970.

[8] D. Siljak, *Large-Scale Dynamic Systems*, Elsevier North-Holland, New York, 1978.

[9] G. Quazza, "Noninteracting Controls of Interconnected Electric Power Systems", *IEEE Transactions on Power Apparatus and Systems*, Vol. PAS-85, No. 7, July, 1986.

[10] H. Kwatny, T. Bechert, "On the Structure of Optimal Area Controls in Electric Power Networks", *IEEE Trans. on Automatic Control*, AC-18, 1973.

[11] M. Ilic, F. Mak, "Mid-range Voltage Dynamics Modeling With the Load Controls Present", *Proc. 26th IEEE Conference on Decision and Control*, Los Angeles, CA December 1987.

[12] P. Sauer, M. Pai, *Power System Dynamics and Stability*, Course Notes EE476, University of Illinoise at Urbana-Champaign.

[13] P. M. Anderson and A. A. Fouad, *Power System Control and Stability*, Iowa State University Press.

[14] J. Paul et al., "Survey of the Secondary Voltage Control in France: Present Realization and Investigation", *IEEE Trans. on Circuits and Systems*, CAS-33, No. 3, 1986.

[15] G. Blanchon, "A New Aspect of Studies of Reactive Energy and Voltage of the Networks", *Proc. Power Systems Computer Conference*, 1972.

[16] J. Paul and J. Leost, "Improvements of the Secondary Voltage Control in France", *IFAC Symposium on Power Systems and Power Plants Control*, Beijing, 1986.

[17] D. Hill, I. Marcels, "Stability Theory for Differential/Algebraic Systems with Applications to Power Systems", *IEEE Trans. on Circuits and Systems*, vol. CAS-37, no. 11, pp. 1416-1423, November 1990.

[18] P. Kokotovic, H. Khalil, (Editors), *Singular Perturbations in Systems and Control*, IEEE Press, 1986.

[19] J. Chow, *Time-Scale Modeling of Dynamic Networks with Applications to Power Systems*, Springer-Verlag, 1982.

[20] M. Calovic, "Linear Regulator Design for a Load and Frequency Control", *IEEE Transactions on Power Apparatus and Systems*, Vol. PAS-91, pp. 2271-2285, 1972.

[21] P. Sauer, M. Pai, "Power system steady-state stability and the load-flow Jacobian", *IEEE Transactions on Power Apparatus and Systems*, Vol. 5, No. 4, Nov. 1990.

[22] C. Desoer, E. Kuh, Basic Circuit Theory, McGraw-Hill Book Co., 1969.

[23] A. R. Bergen, *Power Systems Analysis*, Prentice-Hall, 1986.

[24] M. Klein, G. Rogers, P. Kundur, "A Fundamental Study of Inter-area Oscillations in Power Systems", *IEEE Trans. on Power System*, Vol. 6, No. 3, August 1991.

[25] Proceedings: FACTS Conference I: The Future of High-voltage Transmission, EPRI TR-100504, March 1992.

[26] Proceedings: FACTS Conference II, EPRI TR-101784, Dec. 1992.

[27] J. C. Doyle, K. Glover, P. P. Khargonekar, and B. A. Francis, "State space solutions to standard $\mathcal{H}_2$ and $\mathcal{H}_\infty$ control problems", *IEEE Transactions on Automatic Control*, Vol. 34, No. 8, pp. 831-847, 1989.

[28] N. Cohn, "Research Opportunities in the Control of Bulk Power and Energy Transfers on Interconnected Systems", EPRI EL-377-SR, Special Report on Power System Planning and Operations: Future Problems and Research Needs, February 1977.

[29] Proceedings: Automatic Generation Control-Research Priorities, EPRI TR-100451, April 1992.

[30] J. Carpentier, "'To be or not to be modern' that is the question for automatic generation control (point of view of a utility engineer)", International Journal on Electric Power & Energy Systems, Vol. 7, No. 2, April, 1985.

[31] M.L. Crenshaw, et. al., "Excitation system models for power system stability studies", *IEEE Transactions on Power Apparatus and Systems*, Vol. PAS-100, No. 2, February, 1981.

[32] C. Barbier and J. Barret, "An analysis of phenomena of the voltage collapse on a transmission system", RGE - Tome 89 - no 10 - Octobre 1980.

[33] J. Zaborszky, T.Y. Chiang, "Economic Areawise Load Frequency Control", Report No. SSM 7402 Parts I and II, Dept. of Systems Science and Mathematics, Washington University, St Louis, MO 63130.

[34] J. F. Nash, Jr., "Equilibrium points in N-person games", *Proc. Nat. Acad. Sci. U. S.*, vol. 36, pp48-49, 1950.

[35] J. B. Cruz, Jr., " Survey of Nash and Stackelberg equilibrium strategies in dynamic games", *Ann. Econ. Soc. Meas.*, vol. 4, pp 339-344, 1975.

[36] T. Basar, "On the uniqueness of the Nash solution in linear quadratic differential games", *Int. J. Game Theory*, vol. 5, pp 65-90, 1976.